AD-A149 535 ELECTRON PRODUCTION ELECTRON ATTACHMENT AND CHARGE RECOMBINATION PROCESS I..(U) SAN DIEGO STATE UNIV CA DEPT OF ELECTRICAL AND COMPUTER ENGIN.. L C LEE 1/2

UNCLASSIFIED 17 SEP 84 AFOSR-82-0314 F/G 7/4 NL

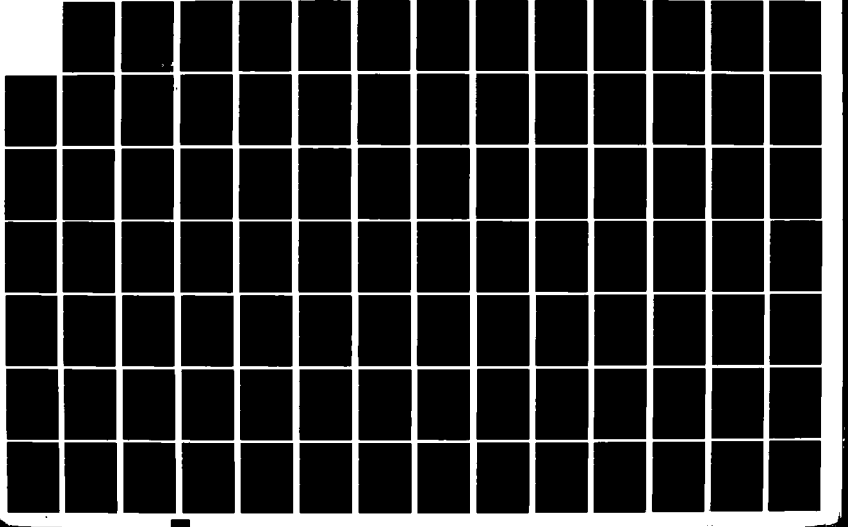

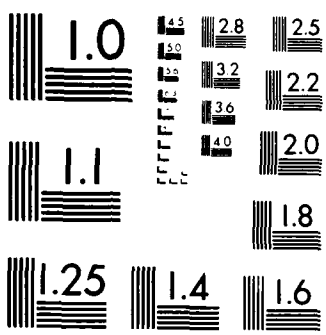

September 17, 1984

Annual Scientific Report for Grant No. AFOSR-82-0314
Covering the Period from 1 August 1983 to 31 July 1984

ELECTRON PRODUCTION, ELECTRON ATTACHMENT, AND CHARGE RECOMBINATION PROCESS IN HIGH PRESSURE GAS DISCHARGES

By: Long C. Lee
Department of Electrical and Computer Engineering
San Diego State University
San Diego, California 92182-0190
Telephone: (619) 265-3701

Prepared For:

U. S. Air Force Office of Scientific Research
Bolling Air Force Base
Washington, D. C. 20332
Attention: Major Henry L. Pugh, Jr.
Directorate of Physics

SECURITY CLASSIFICATION OF TH' AGE (When Data Entered)

REPORT DOCUMENTATION PAGE

READ INSTRUCTIONS BEFORE COMPLETING FORM

1. REPORT NUMBER AFOSR-TR- 1295	2. GOVT ACCESSION NO.
3. RECIPIENT'S CATALOG NUMBER	
4. TITLE (and Subtitle) Electron Production, Electron Attachment, and Charge Recombination Process in High Pressure Gas Discharges	5. TYPE OF REPORT & PERIOD COVERED Annual Report 1 August 1983 - 31 July 1984
	6. PERFORMING ORG. REPORT NUMBER
7. AUTHOR(s) Long C. Lee	8. CONTRACT OR GRANT NUMBER(s) AFOSR-82-0314
9. PERFORMING ORGANIZATION NAME AND ADDRESS San Diego State University San Diego, California 92182	10. PROGRAM ELEMENT, PROJECT, TASK AREA & WORK UNIT NUMBERS 61102F 2301 /A7
11. CONTROLLING OFFICE NAME AND ADDRESS U. S. Air Force of Scientific Research Bolling Air Force Base Washington, D. C. 20332	12. REPORT DATE 17 September 1984
	13. NUMBER OF PAGES
14. MONITORING AGENCY NAME & ADDRESS(if different from Controlling Office)	15. SECURITY CLASS. (of this report) Unclassified
	15a. DECLASSIFICATION DOWNGRADING SCHEDULE

16. DISTRIBUTION STATEMENT (of this Report)

Approved for public release; distribution unlimited

17. DISTRIBUTION STATEMENT (of the abstract entered in Block 20, if different from Report)

18. SUPPLEMENTARY NOTES

The findings in this report are not to be construed as an official position of the Department of the Air Force, unless so designated by other authorized documents.

19. KEY WORDS (Continue on reverse side if necessary and identify by block number)

Electron production; electron attachment, electron diffusion, charge recombination; electron conduction current; temporary negative ion; space charge effect; plasma decay; electron leakage from plasma, electron attaching gas; excimer laser; parallel-plate drift-tube apparatus; computer modeling

20. ABSTRACT (Continue on reverse side if necessary and identify by block number)

A parallel-plate drift-tube apparatus was used to investigate the electron transport parameters in high gas pressure. The initial electrons were produced either by irradiation of the cathode with excimer laser photons or by two-photon-ionization of a trace of trimethylamine in high pressure gas. The transient voltage pulses due to electron motion between the electrodes were observed. The plasma decay time and the probability for electron leakage from plasma were measured as a function of the ratio of the initial charge density to the applied field. The shortening of electron conduction pulses by adding electron (over)

DD FORM 1 JAN 73 1473 EDITION OF 1 NOV 65 IS OBSOLETE

SECURITY CLASSIFICATION OF THIS PAGE (When Data Entered)

block 20 continued

attaching gases to various buffer gases were investigated. The electron attachment rate constants of O_2, N_2O, and CF_4 in N_2 as well as H_2O in Ar, N_2 and CH_4 were measured at various gas concentrations and E/N. It is observed that temporary negative ions due to electron attachment to H_2O and CF_4 are formed. The diffusion coefficients of electrons in Ar were measured in the E/N = 30 - 300 Td region.

I. INTRODUCTION

This annual report describes the research results covering from August 1, 1983 to July 31, 1984 for a research project currently supported by AFOSR under Grant No. AFOSR-82-0314. In this research program, we investigate the processes for electron production, electron attachment and charge recombination in high gas pressure discharges. The information obtained from this research project is currently needed for developing various electrical switching devices and for understanding the phenomena occurring in plasma physics as well.

Various electrical switching devices, such as high energy and high repet tion-rate discharge switches, opening switches, radiation or e-beam controlled switches, are needed for the development of high power lasers, fusion experiment, magnetic energy storage system, as well as particle beam experiment. High pressure gas discharges are used in these switching devices. For a specific application, a discharge switch may require some special characteristics pertinent to the rise and decay times of discharge pulse, discharge stability, discharge uniformity, high conduction current, etc. These characteristics depend strongly on electron transport parameters, such as electron drift velocity, electron attachment, detachment and ionization coefficients, and charge recombination rates. Therefore, the electron transport parameters for some electron-attaching gases in various high pressure buffer gases are needed for designing various discharge switches. This research program is aimed to provide the basic information for such development.

In addition to providing data for practical applications, this research program also studies basic phenomena in plasma physics. For example, the intense excimer laser pulse can produce a plasma of high charge density, which gives a new experimental approach for examining the probability of electron leakage from plasma and the decay time of plasma in various high gas pressure

environments. Another example, because the initial electrons are produced by the laser pulse of short duration (~10 ns), we can examine the formation process of short-lived negative ions in this experiment. The temporary negative ions of CF_4^- and H_2O^- are observed in this funding period. The physical properties of temporary negative ions were not well investigated before, although it is likely that temporary negative ions may play some important roles in determining discharge characteristics, such as slowing down electron drift velocity and inducing charge recombination and ion reactions in discharge media.

II. RESEARCH ACCOMPLISHMENTS

In this funding period, a parallel-plate drift-tube apparatus has been used to investigate electron transport parameters in high pressure buffer gases. The initial electrons are produced either by irradiation of the cathode with an intense excimer laser pulse or by two-photon-ionization of a trace of trimethylamine in buffer gas. The electrons drift in an electric field by applying a high negative voltage on the cathode. The transient voltage pulses induced by electron motion between the electrodes are observed. The electron attachment rates are obtained from the ratio of the amplitudes of transient pulses with and without a gas attacher in a buffer gas. The electron drift velocity and the electron diffusion coefficient are obtained by analyzing the time dependence of the transient pulse. The plasma decay time and the probability for electron leakage from plasma are measured, and the mechanism for plasma decay is investigated in accord with the time behavior of transient pulse. The subjects we studied are described more specifically below.

A. Electron Attachment of H_2O in Ar, N_2 and CH_4

The electron attachment due to H_2O in a buffer gas of Ar, N_2 or CH_4 at pressure in the 100 - 400 torr range is studied at various applied E/N. The rate constants for the dissociative attachment process of H_2O in Ar are measured in the E/N = 2 - 15 Td region. The onset for the dissociative attachment process is observed to be in the E/N = 1 - 2 Td range, for which the mean electron energy in Ar is about 5 eV. The attachment rate constants increase with increasing E/N. This is an ideal characteristic for designing an opening switch.

For the N_2 buffer gas, the mean electron energy is limited to 1 eV even at relatively high E/N. This energy is too low for the dissociative attachment

process of H_2O. Instead, a temporal attachment appears in the earlier time of the transient pulse. This attachment is attributed to the formation of a temporary negative ion H_2O^-.

The formation of the temporary negative ion is further studied using CH_4 as a buffer gas. The drift velocity of electron in CH_4 is about one order of magnitude higher than that of Ar or N_2, so the duration of transient pulse in CH_4 is greatly shortened (from 4 μs in Ar or N_2 to about 0.4 μs in CH_4). Thus, the temporal electron attachment due to H_2O in CH_4 is observable. The observed lifetime of H_2O^- is estimated to be about 0.2 μs. The electron attachment rate constants for the formation of H_2O^- in CH_4 are measured in E/N = 1 - 18 Td region, which decrease monotonically with increasing E/N. The data suggest that the potential energy of H_2O^- is only slightly higher than that of H_2O + e and the potential surface of H_2O^- is similar to that of H_2O.

The electron drift velocities for various gas mixtures are measured. It is observed that the electron drift velocity increases when H_2O is added to Ar or N_2, but it decreases when H_2O is added to CH_4. The increase of electron drift velocity by adding an electron-attaching gas to a buffer gas is a desirable characteristic for the design of opening switches.

The results for the electron attachment due to H_2O in Ar, N_2 or CH_4 are described in more detail in a paper attached as Appendix A, which will be submitted to a scientific journal for publication.

B. Electron Attachment of O_2, N_2O and CF_4 in N_2

The pulse duration of electron conduction current is shortened when O_2, N_2O and CF_4 are added to the buffer gas N_2. The shortening is caused by attachment of electrons by the electron-attaching gas added. For O_2, the

attachment is due to a three-body process $e + O_2 + M \rightarrow O_2^- + M$. The electron attachment rate constants for O_2 in N_2 are measured at various applied E/N and gas pressures. The results are consistent with the data measured by other previous methods.

For N_2O in N_2, the attachment is due to the dissociative attachment process, $e + N_2O \rightarrow O^- + N_2$. The electron attachment rate constants are measured in the E/N = 0 - 10 Td region in 400 torr of N_2. The attachment rate constants increase with increasing E/N and reach a plateau at E/N > 5 Td. This characteristic is good for the design of opening switch.

The mean electron energy in N_2 is never high enough to make the dissociative attachment process of CF_4 occur. Thus, the electron attachment observed in the $CF_4 - N_2$ mixture is likely due to the non-dissociative attachment process. However, no stable CF_4^- ion is known, implying that the CF_4^- ion is a temporary one, similar to H_2O^- that is short-lived.

The results for the shortening of electron conduction pulses by electron attachers O_2, N_2O and CF_4 are described in more detail in a paper attached as Appendix B, which has been accepted by the Journal of Applied Physics for publication.

C. Electron Kinetics in Plasma

High densities of electrons and positive ions are produced by two-photon-ionization of a trace of trimethylamine in N_2 by ArF laser photons. The electrons drifted by the applied electric field move initially toward the anode. As soon as the electrons slightly separate from the ions, the electrons moved to the plasma front (toward the anode) and the ions left in the plasma tail (toward the cathode) will induce an electric field to cancel out the applied field. The space-charge-induced field could be so large that it suppresses the applied

field. For this case, the electrons inside the plasma could be forced to move toward the anode, and the direction of electron conduction current is reversed as observed in our experiment. This phenomenon is not well understood and is subject to further study.

The decay time of the electron conduction pulse is a measure for the decay time of plasma. And, the amplitude of the electron conduction current is a measure for the probability of electron leakage from plasma. It is found that the ratio of the initial charge density to the applied field, n_e/E, is a good parameter for the characterization of the plasma decay time and the probability of electron leakage from plasma. We have measured these plasma parameters as a function of n_e/E, and found that the experimental data are consistent with theoretical calculations.

The results for the electron kinetics in plasma are described in more detail in a paper attached as Appendix C which has been submitted to the IEEE Transactions on Plasma Science for publication.

D. Electron Diffusion Coefficients in Ar

The transient pulses induced by electron motion between the electrodes are observed for the Ar pressure in the 0 - 10 torr range. The electron drift velocity, the electron ionization coefficient, and the electron diffusion coefficient are obtained from fitting transient voltage pulses with Boltzman transport equation. The electron diffusion coefficients measured in the E/N = 30 - 300 Td range are consistent with theoretical calculations. At E/N = 100 Td, the product of the longitudinal electron diffusion coefficient and the Ar density is 3×10^{22} $cm^{-1}s^{-1}$.

The dependencies of the measured longitudinal diffusion coefficients on the Ar pressure and the laser power are investigated. The results for the study are described in more detial in a paper attached as Appendix D, which has been submitted to J. of Phys. D: Applied Physics for publication.

III. CUMULATIVE PUBLICATIONS AND PRESENTATIONS

1. "Two-Photon-Ionization Coefficients of Propane, 1-Butene, Methylamines", L. C. Lee and W. K. Bischel, presented at the 12th International Conference on the Physics of Electronic and Atomic Collisions, Gatlinburg, TN., July 15 - 21, 1981.

2. "Electron Attachment and Charge Recombination Following Two-Photon-Ionization of Methylamines", L. C. Lee and W. K. Bischel, presented at the 34th Gaseous Electronics Conference, Boston, MA., October 20-23, 1981.

3. "Two-Photon-Ionization Coefficients of Propane, 1-Butene, and Methylamines", L. C. Lee and W. K. Bischel, J. Appl. Phys. 53, 203 (1982).

4. "Electron Ionization and Attachment Processes in Diffuse Discharges", L. C. Lee, presented to the Workshop on Optical Control of Diffuse Discharges, Eugene, OR., December 2 - 3, 1982.

5. "Diffusion of Electrons in Gases Under Electric Field", F. Li and L. C. Lee, presented at the 1983 Annual Meeting, APS Division of Electronic and Atomic Physics, Boulder, CO., May 23 - 25, 1983.

6. "Electron Longitudinal Diffusion Coefficients in Ar", F. Li and L. C. Lee, presented at the 36th Gaseous Electronics Conference, Albany, N. Y., October 10 - 14, 1983.

7. "Space Charge Effect on the Electron Kinetics Occurring in Atmospheric Gas Pressure", L. C. Lee and F. Li, presented at the 1984 IEEE International Conference on Plasma Science, St. Louis, Missouri, May 14 - 16, 1984.

8. "Shortening of Electron Conduction Pulses by Electron Attachers O_2, N_2O and CF_4", L. C. Lee and F. Li, paper accepted for publication in J. Appl. Phys., 1984.

9. "Space Charge Effect on Electron Conduction Current", L. C. Lee and F. Li, paper submitted to IEEE Transactions on Plasma Science, 1984.

10. "Longitudinal Diffusion Coefficients of Electrons in Ar at High E/N", F. Li and L. C. Lee, paper submitted to J. Phys. D: Appl. Phys. 1984.

11. "Electron Attachment of H_2O in Ar, N_2 and CH_4 in Electric Fields", W. C. Wang and L. C. Lee, paper to be submitted to J. Appl. Phys. for publication.

IV. PERSONNEL INVOLVED IN THIS RESEARCH

1. Principal Investigator:

   Dr. Long C. Lee, Professor of Electrical and Computer Engineering

2. Research Associates:

   Dr. F. Li
   Dr. J. B. Nee
   Dr. W. C. Wang

3. Students:

   Mr. F. C. Clark
   Mr. J. S. Lai
   Mr. J. A. Marcrum
   Ms. M. Waxman

V. INTERACTIONS

1. The results obtained in the current funding period had been presented at the 36th Gaseous Electronics Conference and at the 1984 IEEE International Conference on Plasma Science (See Section III).

2. Dr. Lee made a trip to the Texas Tech. University, Lubbock, Texas on May 21-22, 1984 to discuss with Professors G. Schaefer, K. Schoenbach, and F. Williams for the application of our basic data to their opening switch development.

3. We have constantly sent our papers to Dr. A. H. Guenther at the Air Force Weapons Laboratory, Dr. M. Gundersen at the University of Southern California, Dr. J. T. Moseley at the University of Oregon, Dr. Bob Reinovsky at the Air Force Weapons Laborator, Dr. S. K. Srivastava at the Jet Propulsion Laboratory, and Dr. G. Schaefer, Dr. K. Schoenbach, and Dr. F. Williams at the Texas Tech. University. We appreciate the useful comments and suggestions received from Dr. A. H. Guenther.

APPENDIX A

Electron Attachment of H_2O in Ar, N_2 and CH_4 in Electric Fields

Electron Attachment of H_2O in Ar, N_2 and CH_4 in Electric Fields

W. C. Wang and L. C. Lee
Department of Electrical and Computer Engineering
San Diego State University
San Diego, CA 92182-0190

ABSTRACT

The electron attachment due to H_2O in Ar, N_2 and CH_4 is investigated using a parallel-plate drift-tube apparatus. The initial electrons are produced either by an irradiation of the cathode with ArF laser photons or by two-photon-ionization of a trace of trimethylamine in a buffer gas. The transient voltage pulses induced by the electron motion between the electrodes are observed. The electron attachment rates are obtained from the decrease of transient voltage as H_2O is added to the buffer gas. The electron attachment rate constants for the dissociative attachment process of H_2O in Ar are measured, which increase with increasing E/N from 2 - 15 Td. Electron attachments due to the formation of temporary negative ion are observed in the H_2O - N_2 and H_2O - CH_4 mixtures. The negative ion is attributed to H_2O^- whose lifetime measured is about 200 ns. The electron attachment rate constants for the formation of H_2O^- in CH_4 are measured which decrease with increasing E/N from 1 - 20 Td, indicating that the potential energy of H_2O^- is only slightly higher than that of H_2O + e, and the potential surface for H_2O^- resembles to that of H_2O. The effects of H_2O on the electron drift velocities in various buffer gases are investigated.

I. INTRODUCTION

Recent advance in pulse-power technology indicates[1] that an opening switch is needed for developing the magnetic energy storage system. The inductive energy storage is preferable to the capacitive storage because the energy density in the inductive system is much higher (some 10^2 to 10^3 times).[2] The opening switch requires a fast decay of conduction current, which could be achieved by attaching electrons with gas attachers mixed in a buffer gas.[1] The electron attachment rates for various gas mixtures are thus needed for the development of this type of discharge switch. The electron attachment for the mixtures of small amount of H_2O in Ar, N_2, and CH_4 is reported in this paper.

The dissociative attachment of electrons in water vapor has been extensively studied by the swarm method[3-10] and the electron-beam method.[11] The predominant negative-charged species are H^- and O^- ions with the onset energies of about 5.5 and 4.9 eV, respectively.[12,13] Because these onset energies are high, the density-reduced electric field E/N in H_2O must be larger than 40 Td (1 Td = 10^{-17} V-cm^2) in order to induce electron attachment. The E/N can be low if Ar buffer gas is used, because the electron energy in Ar is high.[12] Earlier works for the electron attachment have been summarized by Gallagher et al.[14] Here we further measure the electron attachment rates for the dissociative attachment process of H_2O in Ar at varied electric fields.

Bradbury and Tatel[15] observed an electron attachment in water vapor at very low electron energy. The attachment probability increases with $[H_2O]$ and decreases with increasing E/N. A similar result was later reported by Kuffel[3]. The attachment is attributed to the nondissociative process that will lead to

the formation of H_2O^- ion. However, no long-lived H_2O^- ions were observed.[7,10,12,16] This discrepancy could be reconciled if there exists a short-lived H_2O^- ion, as suggested a long time ago by Hurst et al.[17,18] This short-lived negative ion does exist as evident from our obervation that electrons are attached by H_2O in N_2 or CH_4 at low E/N.

In this work, we apply a relatively new method[19] to investigate the electron attachment in the mixtures of water vapor in Ar, N_2, and CH_4. The mean electron energies in the buffer gases decrease in the order of Ar, N_2 and CH_4. For example, the mean electron energies at E/N = 1.2 Td are 2.53, 0.41, and 0.15 eV for Ar, N_2, and CH_4, respectively.[12] Thus, we are able to study the electron attachment processes in water vapor in a wide range of electron energy.

II. EXPERIMENTAL

In this experiment, initial electrons are produced either from an irradiation of cathode by ArF laser photons or by two-photon-ionization (TPI) of trace trimethylamine in N_2 gas when the H_2O - N_2 mixture is studied. The experimental set-up has been discussed in a previous paper.[19] Briefly, the gas cell is a 6" six-way aluminium cross. The electrodes are two parallel stainless steel plates of 5 cm in diameter at 3.7 cm apart. The energy of ArF laser pulse (Lumonics model 861S) was monitored by an energy meter (Scientech Model 365). A negative high voltage was applied to the cathode. The conduction current induced by electron motion between the electrodes was converted to a transient voltage pulse by a resistor (220 - 1000Ω) connecting the anode to the ground. The transient pulse was monitored by a 275 MHz storage oscilloscope (HP model 1727A). Each single transient pulse was

captured and stored in the oscilloscope, which was later photographed for permanent record. This experimental method is similar to that used by Verhaart and Van der Laan[20] and Christophorous et al.[21] for the electron ionization and electron attachment measurements.

The gas pressure in the cell was maintained constant by continuously supplying with fresh gas and slowly pumping out by a mechanical pump. The flow system will reduce the impurities released from walls and electrodes as well as produced from the photofragment of gases. The gas pressure was measured by an MKS Baratron manometer. All measurements were done at room temperature. The Ar, N_2, CH_4 gases (supplied by MG Scientific Gases) have minimum purities of 99.998%, 99.998%, 99.99%, respectively. To produce electrons by the TPI method, a diluted trimethylamine (0.05%) in prepurified nitrogen (supplied by Matheson) was used. All these gases were admitted to the gas cell without further purification. The water vaopr was carried by Ar, N_2 or CH_4 into the gas cell. The concentration of H_2O was determined from the ratio of water vapor pressure ($\sim$ 25 Torr at 26°C) to the pressure of carrier gases ($\geq$ 1 atom). In order to remove the oxygen dissolved in water, the water in a container was pumped periodically for several days before the water vapor was used for the experiment.

III. ANALYSIS METHOD

The method for the data analysis has been described in the previous paper.[19] In brief, the current induced by electron motion is expressed as

$$i(t) = eN_e W/d \qquad (1)$$

where N_e is the total electrons between the electrodes, W is the electron drift velocity, and d is the electrode spacing.

When water vapor is added to the gas cell, the electron conduction current becomes

$$i'(t) = eN_e'W'e^{-\eta t}/d \tag{2}$$

where η is the electron attachment rate of water vapor. Since the absorption coefficient of H_2O at 193 nm (ArF laser wavelength) is very small, N_e' is about equal to N_e if the laser power is constant. The current is converted to a transient voltage by

$$V(t) = f(t)i(t)R \tag{3}$$

where R is the resistor connecting the anode to the ground, and f(t) is the response function of the detection system.

The logarithm of the ratio of the voltages without and with water vapor is thus,

$$\ln(V'/V) = \ln(N_e'W'/N_eW) - \eta t \tag{4}$$

For an atmospheric pressure and a relative low value of E/N, W can reach equilibrium in a very short time. Thus, W and W' can be practically considered as constant except for those electrons near the electrodes (see later discussion). For $t < d/W$ (or d/W'), N_e (or N_e') is nearly a constant except for the beginning of the pulse that some electrons diffuse back to the cathode. Therefore, after a reasonable time, the first term of Eq. (4) is dependent of time. The plot of ln (V'/V) versus t thus gives the electron attachment rate η. The electron drift velocity is approximately equal to d/T, where T is the electron drift

time between the electrodes which can be determined from the transient voltage waveform.

If trimethylamine is used to produce electrons[22] as in the case of H_2O - N_2 mixture, equal amounts of electrons and ions are created by the TPI process in space. Since ions move much slower than electrons, ions can be considered as stationary in the time scale of interested, and Eq. (4) will thus be applicable in this case. Nevertheless, the charge density should be kept low to avoide the space charge effect due to the charge-induced field.[23] For this case, the electron conduction current is very sensitive to the laser power fluctuation, because N_e is proportional to I^2 (I is laser intensity), instead of I as in the case of electrons produced from an irradiation of the cathode by laser.

IV. RESULTS

A. H_2O - Ar Mixture

The electron transient waveform V(t) for electron motion in 200 Torr of Ar at E/N = 14.5 Td is shown in Figure 1a. The voltage decreases rapidly after the first peak, which is due to the loss of electrons by back diffusion to the cathode.[24] The voltage approaches an asymptotic value as the electrons escape far enough from the cathode. When electrons arrvie at the anode, V(t) drops as shown in Figure 1. This drop can in turn be used to measure the drift time T. The amplitude shows slight increase before its drop. This may be caused by the electrode effect, namely, the electrons are accelerated more by the image charges when they move close to the plate. Since the gas pressure is high (140 - 400 Torr), the effect of electron diffusion is negligible.[24] Thus, T is presumably equal to the time when V(t) starts to drop. The electron drift velocity in the H_2O - Ar mixture as a function of E/N are plotted in Figure 2. Our measured drift velocities are about 10%

1e

less than the published data.[5,25] Our data may be affected by the large electrical noise created by the laser discharge, so the uncertainty for the t = 0 point is quite large (∿ 20 ns).

When 0.073 Torr of H_2O is admitted to Ar at same E/N, the pulse duration and the amplitude at the asymptotic portion decrease as shown in Figure 1b. This is caused by the increase of electron drift velocity as well as the electron attachment by water vapor. The electron drift velocities for adding H_2O in Ar ($[H_2O]/[Ar]$ = 0.15%) are shown in Figure 2 for various E/N. The first peak in Figure 1b is higher than that in Figure 1a, which is caused by the fact that the electron drift velocity becomes higher when H_2O is added to Ar. In fact, the amplitudes of the first peaks at various water vapor concentrations are found to be linearly dependent on the electron drift velocity as expected from Eq. (4) for $t \sim 0$.

The decrease of the voltage in the asymptotic portion due to the addition of H_2O is an ideal case for the measurement of electron attachment rate. During the duration of the asymptotic portion ($1 < t < 3\mu s$ in Figure 1), the first term in Eq. (4) is independent of time. The ratios of $V'(t)/V(t)$ for with and without H_2O in Ar are plotted in Figure 3a, b, and c at E/N = 14.5 Td for 0.024, 0.048, and 0.073 Torr of H_2O, respectively. It is worth noting that the extrapolations of V'/V at t = 0 increase with increasing H_2O concentrations. This is caused by the increase of electron drift velocity when H_2O is added as stated before. As shown in Figure 3, the $\ln(V'/V)$ is linearly dependent on t, and the electron attachment rates are obtained from the slopes.

The results for $\eta/[H_2O]$ as a function of the ratio of the H_2O to Ar concentrations are shown in Figure 4. At a fixed E/N, $\eta/[H_2O]$ values decrease

with increasing $[H_2O]/[Ar]$, which is likely caused[5] by the effect of H_2O on the electron energy distribution in Ar, i.e., an increase in $[H_2O]/[Ar]$ decreases the number of electrons in the range where dissociative attachment takes place. The attachment rate constants increase with increasing E/N at a constant H_2O pressure.

The extrapolation of $\eta/[H_2O]$ at $[H_2O] = 0$, $[\eta/[H_2O]_0$, is associated with the electron energy distribution of pure Ar. The $[\eta/[H_2O]]_0$ values as a function of E/N are shown in Figure 5. The signal levels of V(t) for E/N < 2.5 Td are too low to observe the attachment certainly, so the measurements at low E/N are prohibited. The electron attachment rate constants shown in Figure 5 give the onset for the electron attachment to be at E/N $\leq$ 2 Td. An the onset, some of the electrons may gain enough energy so that the dissociative attachment process takes place. This observation is consistent with the result of Hurst et al.[5], whose measured the onset to be at E/N $\sim$ 1.2 Td. However, the data given by Hurst et al.[5] in the E/N = 1 - 2 Td region do not join smoothly with the present data, for which a comparison is made in the discussion Section. At high E/N, the attachment rate constants do not increase as fast as those at low E/N. This may be caused by the fact that the increase of the mean electron energy in Ar at high E/N is limited.[12] In addition, the ionization process will take place at high E/N so that the measurements of electron attachment rate constants at high E/N are interferred. For this reason, our measurements are limited to E/N at 15 Td.

B. $H_2O - N_2$ Mixture

For $H_2O - N_2$ mixture, there are no differences in the electron conduction waveforms with and without water vapor at E/N from 8 to 24 Td. In this E/N region, the mean electron energies are in the range of 0.8 - 1.5 eV.[12,25] These energies may be too low for the dissociative attachment process,[12,13]

but too high for the non-dissociative attachment process.[3,15] Therefore, the result of non-attachment is reasonable as expected from the earlier observations.

When E/N is reduced, the waveforms without and with H_2O in N_2 show some differences. Two waveforms at E/N = 6.3 Td, one without H_2O in 390 Torr of N_2 and the other with 2.7 Torr of H_2O in 468 Torr of N_2, are shown in Figure 6a and b, respectively. The electrodes spacing is 3.7 cm and the external resistor is 510 Ω. As shown in Figure 6b, the pulse duration is shortened when H_2O is added, indicating that the electron drift velocity increases as H_2O is added. We have measured the electron drift velocities at various $[H_2O]$ and E/N, and found them to be consistent with the published data.[18]

Since the electron drift velocity increases with the addition of H_2O, is it expected that the first peak in Figure 6b will be larger than that of Figure 6a. This expectation is different from the waveforms observed, namely, the amplitude of the first peak in Figure 6b is smaller than that of Figure 6a. This result suggests that an electron attachment occurs in this period. Furthermore, the amplitude of the second peak in Figure 6b increases more than that of Figure 6a. This could result from the electrons attached earlier are released later to enhance the electron current. In other words, a short-lived negative ion exists so that electrons are attached in the beginning of the pulse and are detached to enhance the electron current at the end of the pulse as observed. Comparing the amplitudes of Figures 6a and b, the current starts to show enhancement at a time less than 0.7μs, indicating that the negative ion is not lived longer than this value.

Because the first peak is decreased by attachment and the second peak is enhanced by detachment, the ratio of the amplitudes of these two peaks can be

counted as a measure for the attachment effect. As examples, the ratios for the amplitudes of the second peak V_2 to the first peak V_1 for the data taken at E/N = 4.2 and 6.3 Td at varied $[H_2O]$ are shown in Figure 7. The V_2/V_1 values do not depend largely on E/N at $[H_2O] = 0$, but increase with $[H_2O]$. The increase tate of the V_2/V_1 is larger at low E/N. This result suggests that the electron attachment rate for the formation of negative ion increases with decreasing E/N. This is consistent with the earlier observations[3,15] that the electron attachment rate for the non-dissociative attachment process in water increases with decreasing mean electron energy. This non-dissociative attachment process is further studied in this experiment by measuring the apparent electron attachment rate constant in the H_2O - CH_4 mixture (see next section).

We have repeated the above experiments by producing the initial electrons by two-photon-ionization of a trace of trimethylamine in N_2. The results are consistent with the experiments that produce electrons from an irradiation of the cathode with ArF laser photons as described above.

C. H_2O - CH_4 Mixture

Two transient voltage waveforms, one without H_2O in 324 Torr of CH_4 and the other with 3.6 Torr of H_2O in 420 Torr of CH_4, are shown in Figures 8a and b, respectively. These waveforms were taken at an E/N fixed at 5 Td, an electrode spacing of 3.7 cm, and an external resistor of 220 Ω. The waveform duration (∿ 350 ns) here is much shorter than that in Ar or N_2 gas. This is because the electron drift velocity in CH_4 is about one order of magnitude higher[12] than that in Ar or N_2. The drift velocities as a function of E/N at various water vapor contents in CH_4 are shown in Figure 9. It is noted that the electron drift velocity becomes smaller when H_2O is added to CH_4, instead of bigger as H_2O is added to Ar or N_2. The drift velocities we measured agree well with the published data.[18]

The second peak of Figure 6b is much smaller than the first peak as compared with Figure 6a, clearly indicating than an electron attachment due to H_2O occurs in this short pulse period. The electron attachment rate can be measured from the ratio of the voltages with and without H_2O in CH_4. The ratios of V'/V for the H_2O pressures of 0.72, 2.16, and 3.59 Torr are plotted in Figures 10a and b for E/N = 2.5 and 7.6 Td, respectively. The electron attachment rates measured from the slopes at various $[H_2O]$ are shown in Figure 11. At each E/N, the electron attachment rates η increase linearly with $[H_2O]$, from which the electron attachment rate constants $\eta/[H_2O]$ are obtained as shown in Figure 12. Note that the data were measured at several different CH_4 pressures.

The second peak shown in Figure 8a is significantly longer than the asympotic portion, indicating that in CH_4 the drift velocity for electrons near the anode is significantly affected by the electrode. For the measurements of attachment rates, the $[H_2O]$ concentrations were kept as low as possible so that the electron drift velocities were not significantly altered when H_2O was added. For E/N = 7.6 Td, the electron drift velocity is not seriously affected by $[H_2O]$ as shown in Figure 9. Thus, for the amount of H_2O (0.7 - 3.6 Torr) used in the experiment, the electron drift velocity is not significantly altered as reflected in Figure 10b that the extrapolation of V'/V at t = 0 is nearly equal to 1. (The V'/V at t = 0 is proportional to W'/W as shown in (4)). At low E/N, the electron drift velocity depends strongly on the $[H_2O]$ added (see Figure 9). When $[H_2O]$ is large, the electron drift velocity changes greatly. However, the plot of ℓn (V'/V) is still linear on t as shown in Figure 10a. The W'/W values determined from the extrapolation of V'/V at t = 0 with a correction of laser power fluctuation

are consistent with the electron drift velocities measured from the pulse duration. These results ensure that the present method is suitable for the measurements of electron attachment rate.

As indicated in the measurements of the H_2O - N_2 mixture, the negative ion is short-lived species, so that it will be detached later. Since the transient pulse in the H_2O - CH_4 mixture is short, the current induced by the released electrons may become observable after the primary electrons are absorbed by the anode. This expectation is indeed shown in the transient pulses. The after-current of V'(t) in Figure 8b after t = T' has a tail longer than that of V(t) in Figure 8a after t = T. The after-currents of V(t) and V'(t) are plotted in a logarithm scale as shown in Figures 13a and b, respectively. The decay rate in Figure 13a is mainly caused by the external RC time constant (R = 220 Ω, C $\sim 3\times10^{-10}$ farad). On the other hand, the after-current shown in Figure 13b has an additional long tail of a decay time about 210 ns, which results from the detachment of the temporary ion. The decay time of the long tail reflects the lifetime of the temporal negative ion which vary in the range of 190 - 220 ns as measured at various $[H_2O]$ and E/N.

Because the lifetime of the negative ion is short, its detachment will affect the measurement of the attachment rate, that is, the attachment rate measured will appear low. Nevertheless, the transient pulse duration in CH_4 ($\sim$ 400 ns) is not much longer than the lifetime of negative ion, also the concentration of negative is much less than that of primary electrons, so the detachment effect on the measured attachment rate may not be serious. It is estimated that the uncertainty of the attachment rate may not be larger than $\pm$ 30% of the given value.

The earlier observations[3,15] of electron attachment in H_2O at low E/N have been attributed[12,14] to be due to the presence of impurities, most likely O_2. This makes us more cautious. There are several facts to prove that the attachment observed is not due to O_2. First, the negative ion observed is short-lived, in contrast to the O_2^- ion that is very stable. Second, the attachment is a two-body process as evident from the facts that the attachment rate constant is linearly dependent on $[H_2O]$ (see Figure 11) and independent on the CH_4 pressure (see Figure 12). This is quite different from the attachment process of O_2 which is a three-body process that the attachment rate will be quadratically dependent on the gas pressure. Third, the attachment rates measured are quite high. The impurity must have very high concentration and high attachment cross section to make the attachment rates observed which is unlikely to occur. From these arguments, it is clear that the attachment is not caused by the possible impurity O_2, but is by the formation of temporary ion such as H_2O^-.

V. Discussion

The electron attachment rate constants are plotted versus the mean electron energies (D/μ) in CH_4, H_2O and Ar as shown in Figure 14. The mean electron energy in CH_4 at each E/N is calculated from the data given by Cochran and Forester.[26] The attachment rate constant for electrons in H_2O is obtained from the product of the attachment coefficient and the electron drift velocity at each E/N. The attachment coefficient is the average value given by various investigators[4,6,8,27,28] as reviewed by Gallagher et al.[14] The electron drift velocity and the mean electron energy at each E/N are also adopted from the review paper.[14] The mean electron energy for Ar at each

E/N is obtained from a review paper given by Dutton.[25] The electron attachment rate constants measured by Hurst et al.[5] for Ar at low E/N are also plotted for comparison.

The electron attachment in H_2O at low electron energy was reported[3,15] before. However, since no stable H_2O^- ions are detected, the earlier observation of attachment is subject to question.[12,14] In order to resolve the discrepancy, Hurst et al.[17] proposed that H_2O might quasi-trap low energy electrons, for which the "quasi-trap" H_2O^- may have a limited lifetime in the order of 10^{-8} - 10^{-7} sec. Later, in order to explain that the measured momentum transfer cross section for H_2O is larger than a theoretical value by a factor of 2, Hurst et al.[18] reproposed that low energy electron motion in H_2O may form a temporary negative ion. The formation of temporary negative ion can be used to explain[18] the decrease of electron drift velocity when H_2O is added to CH_4 (see Figure 9). The temporary ion (of lifetime about 200 ns) observed in this experiment fits very well with the expectation of Hurst et al.[18]

Considering the experimental fact that the electron attachment rate depends linearly on $[H_2O]$ and not on $[CH_4]$, the temporary ion formed is likely to be H_2O^- only, but not the complex ions such as $H_2O^-\cdot M$ (M = N_2, H_2O and CH_4), because the electron attachment rate for the formation of complex ions will depend on [M]. The electron attachment occurs at very low electron energy as shown in Figure 14, indicating that the potential energy of H_2O^- is not much higher than that of H_2O + e, probably within few thermal energy range. The potential energy of H_2O^- is definitely higher than that of H_2O + e, because H_2O^- is not stable. This potential energy is, however, much lower than the theoretical value that is about 2 eV.[29] For a reconciliation with the

theoretical calculation, one could consider that the attachment is due to the vibrational and rotational excited species. However, it is unlikely that the excited species will have such concentrations that the electron attachment rate is as large as observed. Thus, it is likely that the potential energy of H_2O^- is only slightly higher than that of H_2O + e.

As shown in Figure 14, the electron attachment rates decrease monotonically with increasing mean electron energy. This result indicates that the potential surface of H_2O^- should resemble with that of H_2O, because the Franck-Condon overlap integral for two similar potential surfaces will decrease with increasing transition energy. This assertion is consistent with the theoretical calculation[29] that the potential surface for H_2O^- ($^2A_1$) is similar to that of H_2O.

The observation for the attachment of low energy electrons by water could be applied to explain the phenomenon observed in daily life. It is well known that static chrages will build up on metal surface in winter in dry air, but not in humid air. The water molecules in air may pick up the low energy electrons on surface to form temporary negative ions. The electrons released from the temporary ions could be later attached by O_2 in space. Thus, H_2O may serve as an immediate for dispatching the charges on surface.

For high energy electrons, the attachment is due to the dissociative attachment process. The extrapolation of the measured attachment rate constant in Ar indicates that the attachment will start at a mean electron energy of about 4 eV. This is consistent with the thresholds[12,13] for producing O^- and H^- from dissociative attachment of H_2O as of 4.9 and 5.5 eV, respectively. The attachment rate constants given bt Hurst et al.[5] are

higher than the present values. The reason for this discrepancy is not known. The dissociative attachment process has been used to explain the observation that the addition of water vapor to dry air will increase the breakdown voltage.[3]

The magnitude of the attachment rate constant for electrons in pure water is about the same as that in Ar as shown in Figure 14, indicating that the electron attachment in H_2O is due to the dissociative attachment process. However, the mean electron energy in H_2O is less than the threshold for the dissociative attachment process to occur. This result suggests that the electron energy in H_2O may have a wide spread, or the mean electron energy is not well measured. Considering the same magnitude of the electron attachment rate constants for both Ar and H_2O, it is unlikely that the attachment in H_2O at low mean electron energy is caused by the reason of wide energy spread. Instead, it seems to require more measurements on the mean electron energies in H_2O, which are relatively less studied.[14]

VI. CONCLUDING REMARKS

A relatively new approach is applied to investigate the transient electron conduction current in the H_2O - Ar, H_2O - N_2 and H_2O - CH_4 mixtures. This method, which is different from the conventional swarm method that detects negative ions, has been demonstrated in a previous paper[19] as a useful way for measuring electron attachment rate. This method has an advantage that measures the electron attachment rate due to the short-lived species as demonstrated in the study of H_2O^- in N_2 and CH_4.

For the application of opening switch, the electron attachment rate during the opening period requires to be high, namely, the attachment rate needs to increase with increasing E/N. This experiment shows that H_2O - Ar

mixture has this characteristic. The increase of electron drift velocity, when H_2O is added to Ar, is an additional benefit, because it will increase the electron conduction current during the switching period.

ACKNOWLEDGEMENT

The authors wish to thank Professor K. Schoenbach and Professor G. Schaefer at the Texas Tech University and Dr. F. Li, Dr. E. R. Manzanares, Dr. J. B. Nee, and Dr. M. Suto in our laboratory for useful suggestions and discussion. This work is supported by the Air Force Office of Scientific Research, Air Force Systems Command, USAF, under Grant No. AFOSR-82-0314.

REFERENCES

1. K. Schoenbach, G. Schaefer, M. Kristiansen, L. L. Hatfield, and A. H. Guenther, Electrical Breakdown and Discharges in Gases, part B, Eds. E. E. Kunhardt and L. H. Luessen, (Plenum Press, New York, 1983), P. 415.

2. J. K. Burton, D. Conte, R. D. Ford, W. H. Lupton, V. E. Scherrer, and I. M. Vitkovitsky, Digest of Technical Papers, 2nd IEEE International Pulsed Power Conference, Lubbock, Texas, Eds, A. Guenther and M. Kristiansen, (1979), P. 284.

3. E. Kuffel, Proc. Phys. Soc. London, 74, 297 (1959).

4. A. N. Prasad and J. D. Craggs, Proc. Phys. Soc. London, 76, 223 (1960).

5. G. S. Hurst, L. B. O'Kelly, and T. E. Bortner, Phys. Rev., 123, 1715 (1961).

6. R. W. Crompton, J. A. Rees, and R. L. Jory, Aust. J. Phys., 18, 541 (1965).

7. J. L. Moruzzi and A. V. Phelps, J. Chem. Phys., 45, 4617 (1966); J. L. Pack and A. V. Phelps, J. Chem. Phys. 45, 4316 (1966).

8. J. E. Parr, and J. L. Moruzzi, J. Phys. D, Appl. Phys., 5, 514 (1972).

9. C. E. Klots, and R. N. Compton, J. Chem. Phys., 69 1644 (1978).

10. J. L. Pack, R. E. Voshall, and A. V. Phelps, Phys. Rev., 127, 2084 (1962).

11. I. S. Buchel'nikova, Soviet Phys. JETP, 35, 783 (1959).

12. L. G. Christophorou, Atomic and Molecular Radiation Physics, (John Wiley & Sons, New York, 1971).

13. H. Massey, Negative Ions, (Cambridge University Press, London, 1976), P. 347.

14. J. W. Gallagher, E. C. Beaty, J. Dutton, and L. C. Pitchford, J. Phys. Chem. Ref. Data, 12, 109 (1983).

15. N. E. Bradbury and H. E. Tatel, J. Chem. Phys., 2, 835 (1934).

16. J. F. Wilson, F. J. Davis, D. R. Nelson, R. N. Compton, and D. H. Crawford, J. Chem. Phys. 62, 4204 (1975).

17. G. S. Hurst, L. B. O'Kelly, and J. A. Stockdale, Nature, 195, 66 (1962).

18. G. S. Hurst, J. S. Stockdale, and L. B. O'Kelly, J. Chem. Phys., 38, 2572 (1963).

19. L. C. Lee, and F. Li, J. Appl. Phys., in press.

20. H. F. A. Verhaart and P. C. T. Van der Laan, J. Appl. Phys., 53, 1430, (1982), and ibid, 55, 3286 (1984).

21. L. G. Christophorou, J. G. Carter, and D. V. Maxey, J. Chem. Phys., 76, 2653 (1982).

22. L. C. Lee, and W. K. Bischel, J. Appl. Phys., 53, 203 (1982).

23. L. C. Lee and F. Li, unpublished.

24. L. G. H. Huxley, and R. W. Crompton, The Diffusion and Drift of Electrons in Gases, John Wiley and Sons, New York, 1974, P. 298-303.

25. J. Dutton, J. Phys. Chem. Ref. Data, 4, 577 (1975).

26. L. W. Cochran and D. W. Forester, Phys. Rev. 126, 1785 (1962).

27. H. Ryzko, Ark. Fys. 32, 1 (1966).

28. A. V. Risbud and M. S. Naidu, J. Phys. (Paris) Colloq. C7 40, 77 (1979).

29. C. R. Claydon, G. A. Segal, and H. S. Taylor, J. Chem. Phys., 54, 3799 (1971).

FIGURE CAPTIONS

FIGURE 1 The transient voltage waveforms produced from electron motion in (a) without H_2O and (b) with 0.073 Torr of H_2O in 200 Torr of Ar. The electrons are produced from an irradiation of the cathode by ArF laser photons. The E/N is fixed at 14.5 Td, the electrode spacing is 3.7 cm, and the external resistor is 510 Ω.

FIGURE 2 The electron drift velocities as a function of E/N for the gases without (●) and with 0.15% of H_2O (▲) in Ar. The electron drift velocity increases when H_2O is added to Ar.

FIGURE 3 The ratios of the transient voltages measured with and without H_2O in Ar, V'/V, as a function of the elapsed time after laser pulse. The $[H_2O]$ are: (a) 0.024 Torr, (b) 0.048 Torr, and (c) 0.073 Torr. The E/N is fixed at 14.5 Td, and [Ar] = 200 Torr.

FIGURE 4 The $\eta/[H_2O]$ values as a function of $[H_2O]/[Ar]$ for various applied E/N.

FIGURE 5 Electron attachment rate constants obtained from the extrapolation of $\eta/[H_2O]$ at $[H_2O] = 0$ in the H_2O - Ar mixture as a function of E/N.

FIGURE 6 The transient voltage waveforms produced from electron motion in (a) 390 Torr of N_2 without H_2O and (b) 2.7 Torr of H_2O in 468 Torr of N_2. The E/N is fixed at 6.3 Td. The electrode spacing is 3.7 cm, and the external resistor is 510 Ω.

FIGURE 7 The ratios for the magnitudes of the second peak to the first peak V_2/V_1 as a function of $[H_2O]$ at E/N = 4.2 Td (●) and 6.3 Td (▲).

FIGURE 8 The transient voltage waveforms produced from electron motion in (a) 324 Torr of CH_4 without H_2O and (b) 3.6 Torr of H_2O in 420 Torr of CH_4. The E/N is fixed at 5 Td, the electrode spacing is 3.7 cm, and the external resistor is 220 Ω.

FIGURE 9 The electron drift velocities in H_2O - CH_4 mixtures as a function of E/N. The $[H_2O]/[CH_4]$ are: 0(●), 0.4% (▼), 1.2% (■) and 1.7% (▲).

FIGURE 10 The ratios of transient voltages measured with and without H_2O in CH_4, V'/V, as a function of the elapsed time after the laser pulse at E/N of (a) 2.5 Td, and (b) 7.6 Td. The gas pressures for H_2O in CH_4 are: (A) 0.72 Torr in 342 Torr, (B) 2.16 Torr in 379 Torr and (C) 3.59 Torr in 417 Torr, respectively.

FIGURE 11 The electron attachment rates for various $[H_2O]$ in $[CH_4]$ at E/N of (a) 2.5 Td (●) and (b) 7.6 Td (▲). The CH_4 pressures vary from 340 to 420 Torr as increasing with $[H_2O]$.

FIGURE 12 Attachment rate constants as a function of E/N in H_2O - CH_4 mixture. The data were measured at the CH_4 pressures of 325 (●), 200 (▲), and 135 (■) Torr.

FIGURE 13 The amplitudes of after-currents in Figure 8a and b as a function of time after the primary electrons reaching the anode. The short decay times for both curves (a) and (b) are caused by the external RC circuit. The long decay time for (b) is caused by the electron detachment from the short-lived H_2O^- ion.

FIGURE 14 Electron attachment rate constants versus mean electron energies in CH_4, H_2O and Ar. The mean electron energies (D/μ) in CH_4, H_2O and Ar are converted from E/N using the data in refs. 26, 14 and 25, respectively. The data for H_2O in CH_4 (▲) and Ar (▼) are measured in this experiment. The data for pure H_2O (■) obtained from ref. 14 and for H_2O - Ar (●) from ref. 5 are plotted for comparison.

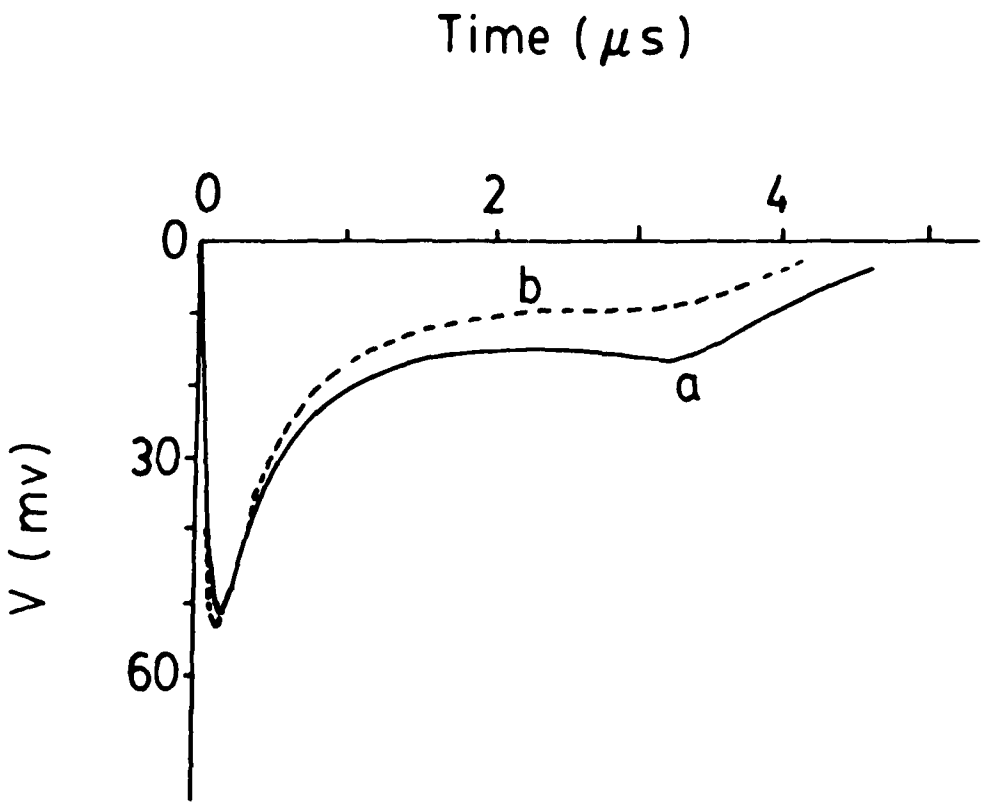

FIGURE 1

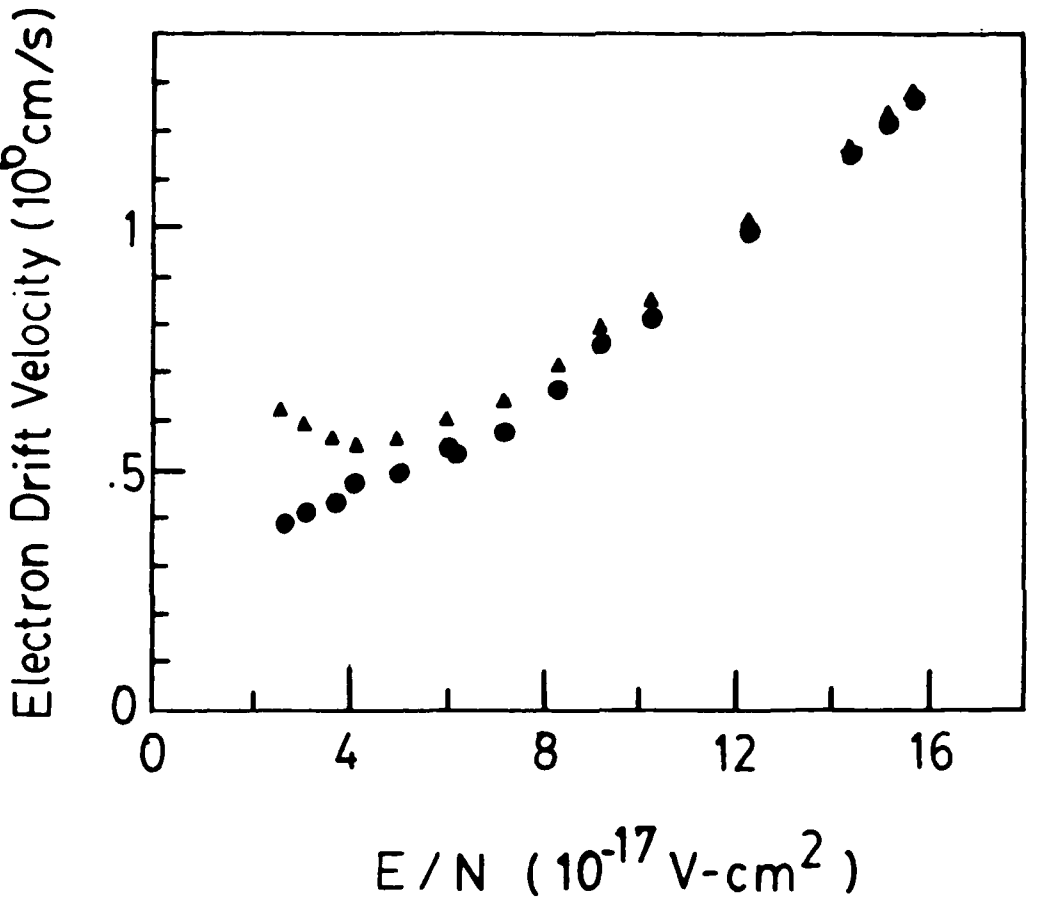

FIGURE 2

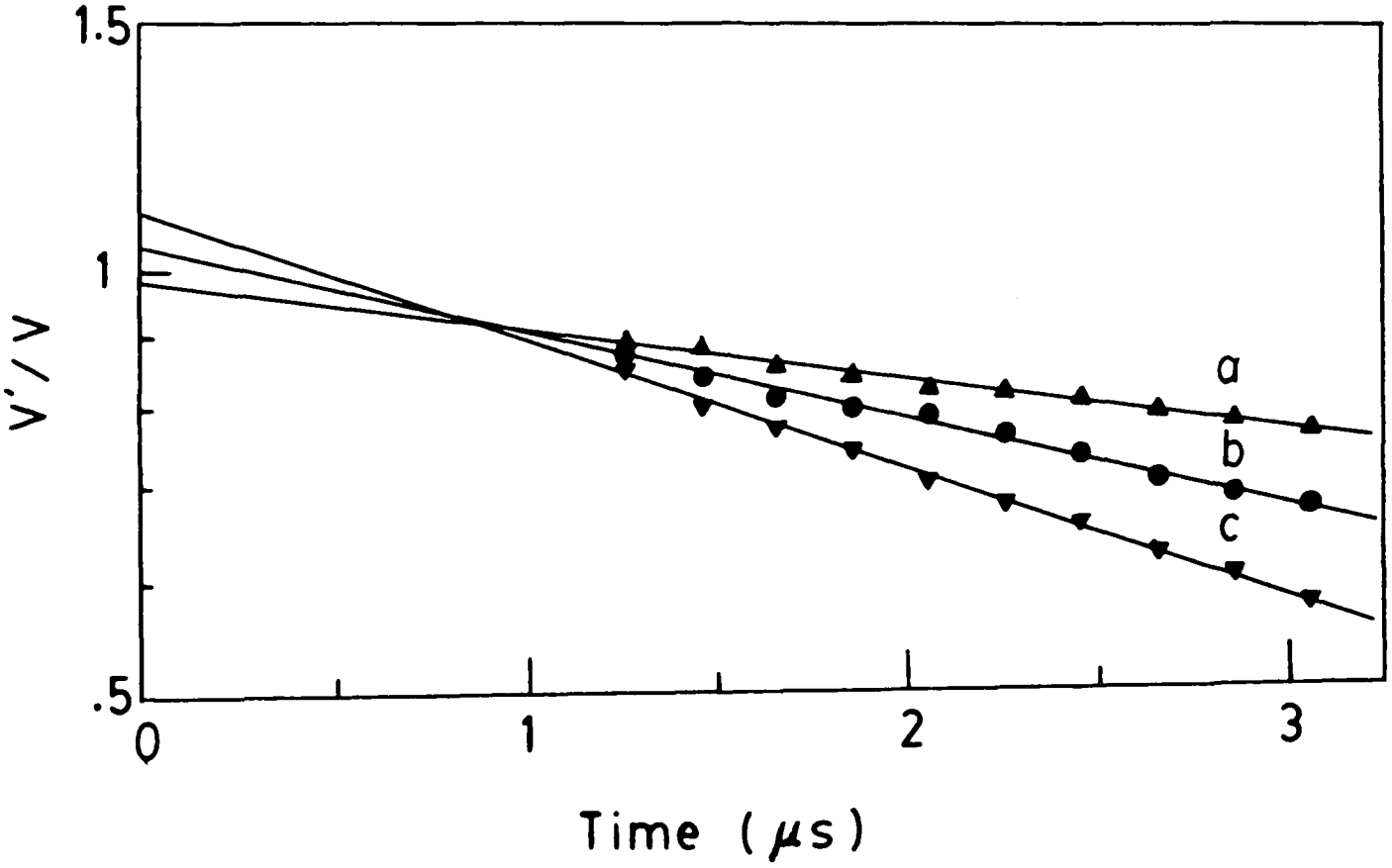

FIGURE 3

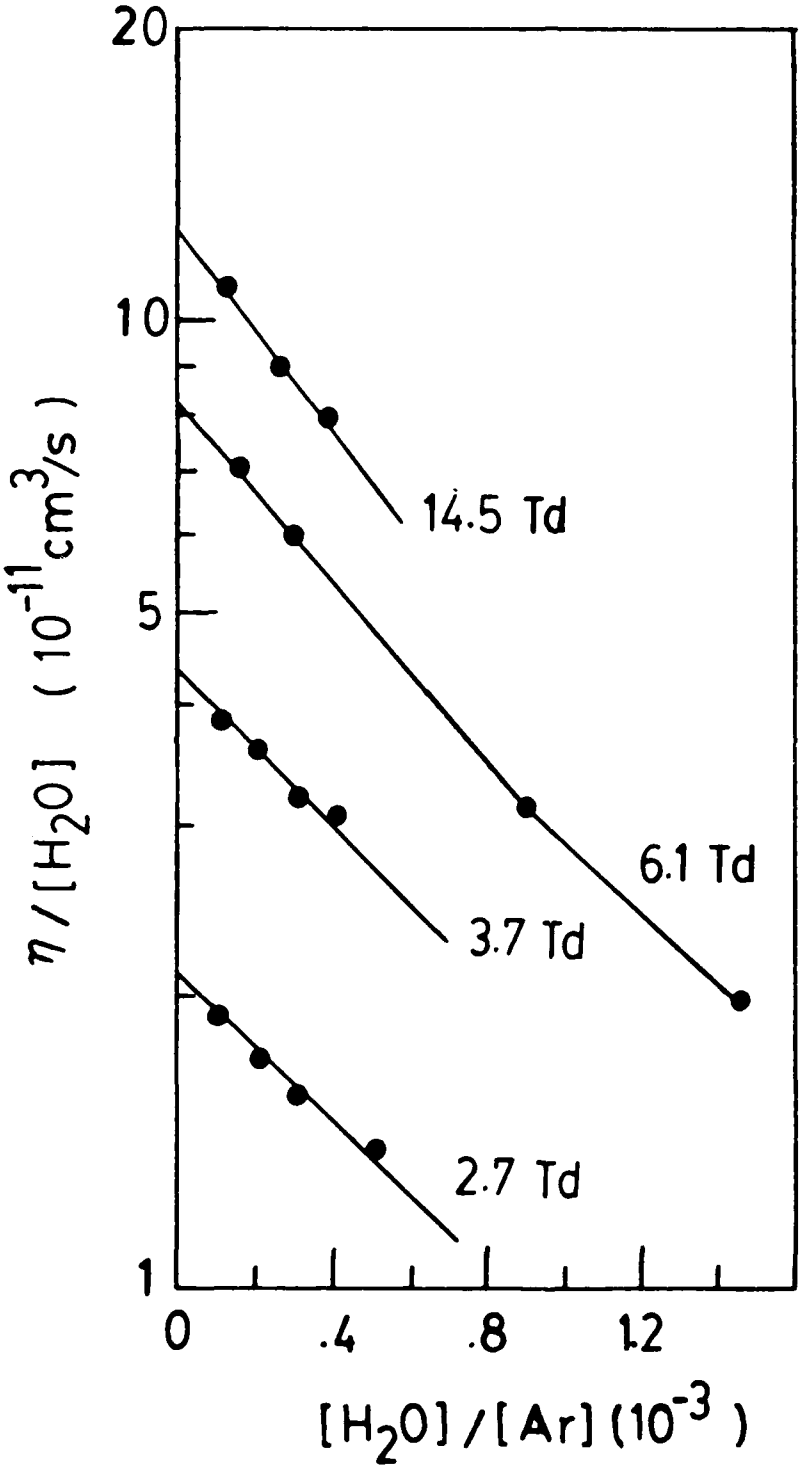
20
10
5
1
0
.4
.8
1.2
$\eta / [H_2O]$ ($10^{-11} cm^3/s$)
$[H_2O] / [Ar]$ (10^{-3})
14.5 Td
6.1 Td
3.7 Td
2.7 Td

FIGURE 4

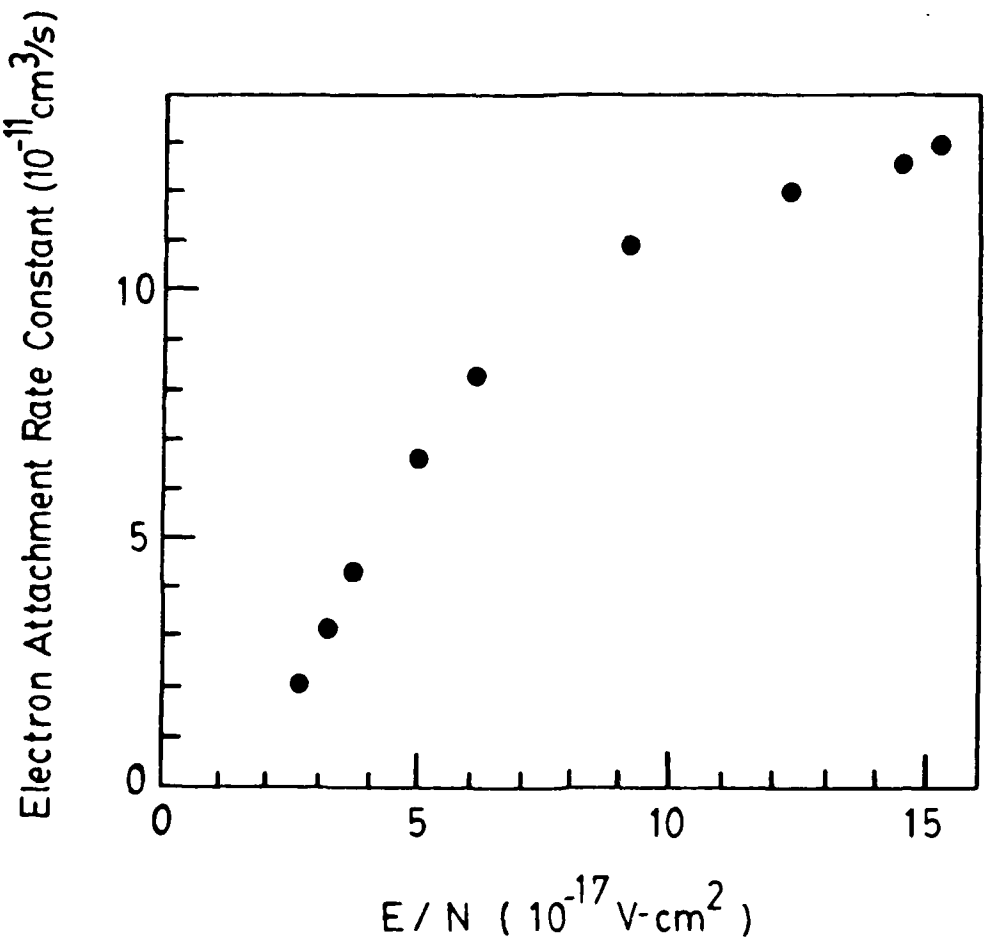
Electron Attachment Rate Constant (10^{-11} cm^3/s)
0
5
10
0
5
10
15
E / N (10^{-17} V-cm^2)

FIGURE 5

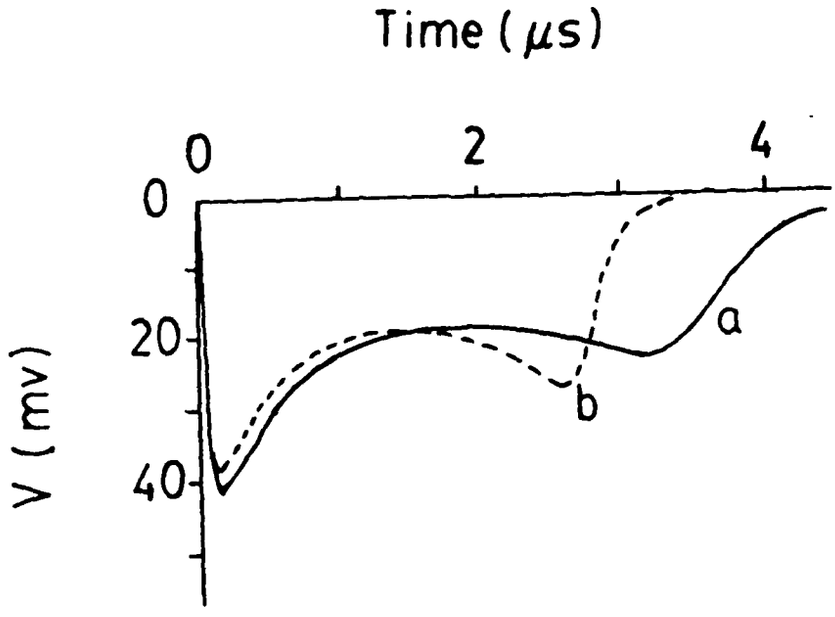

FIGURE 6

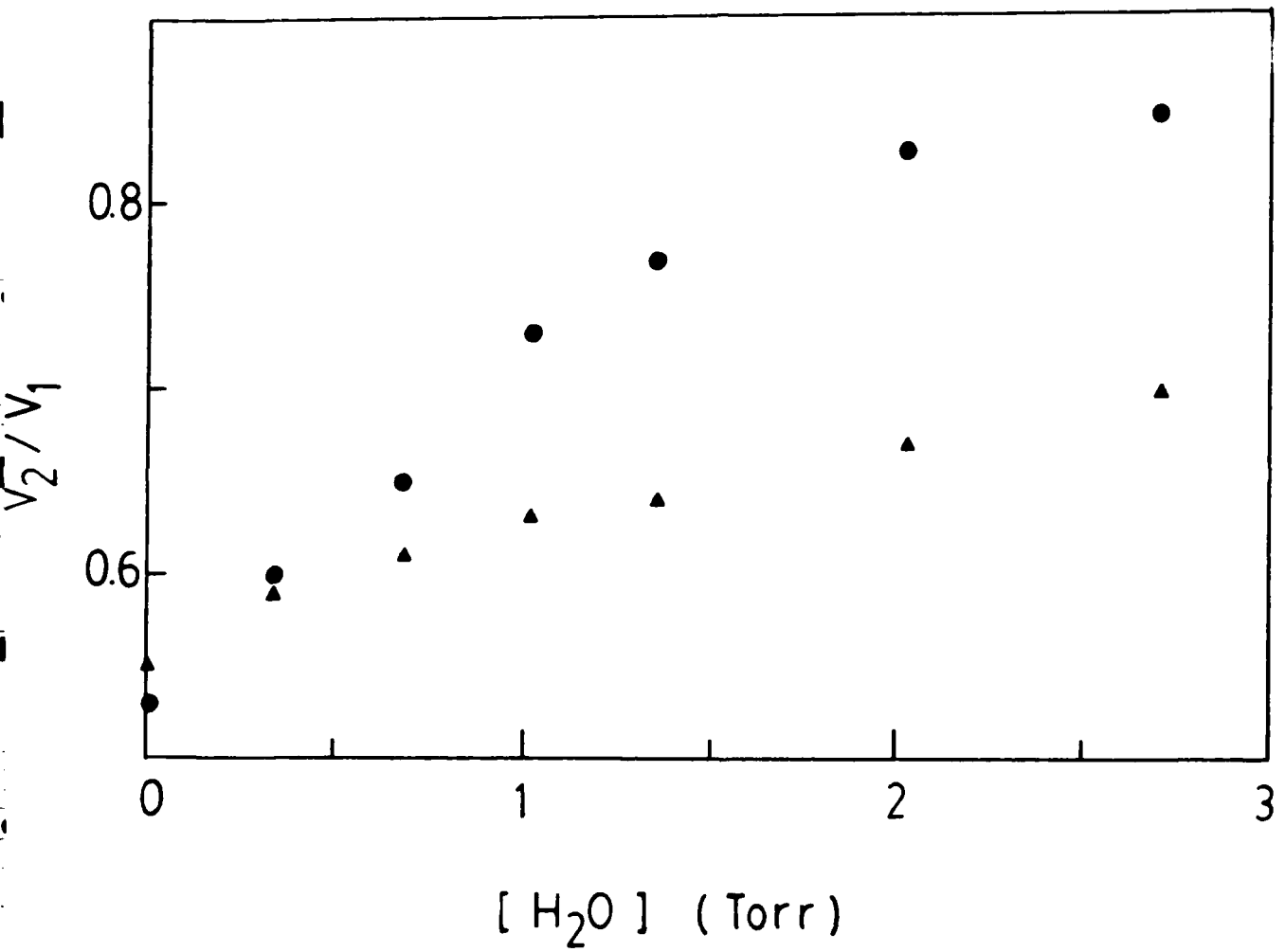

FIGURE 7

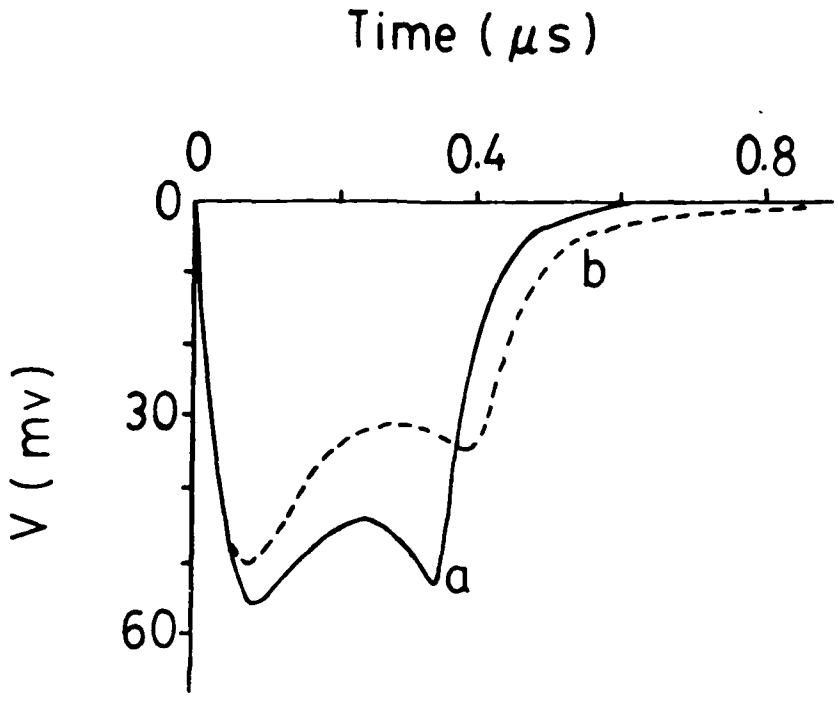

FIGURE 8

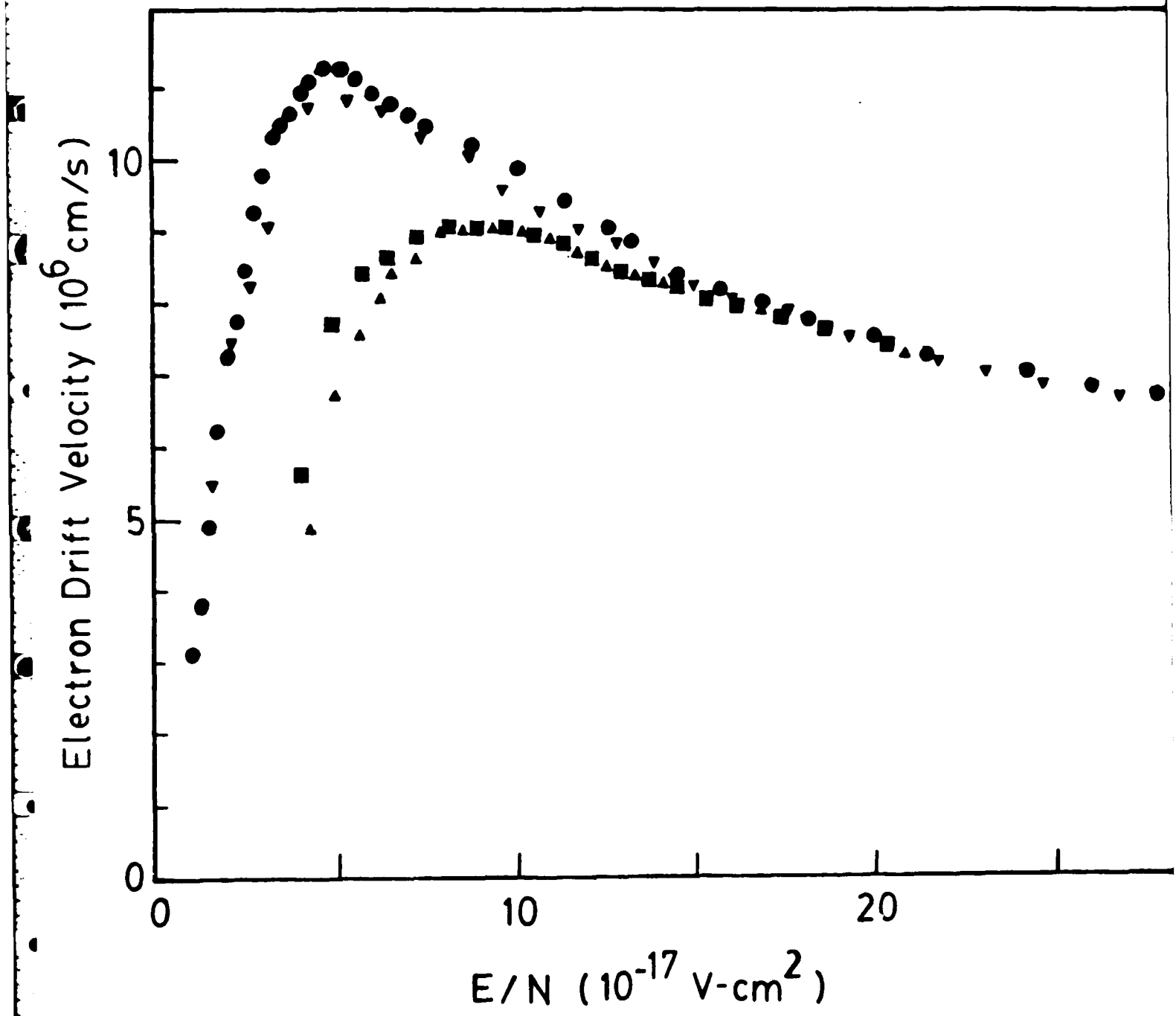

FIGURE 9

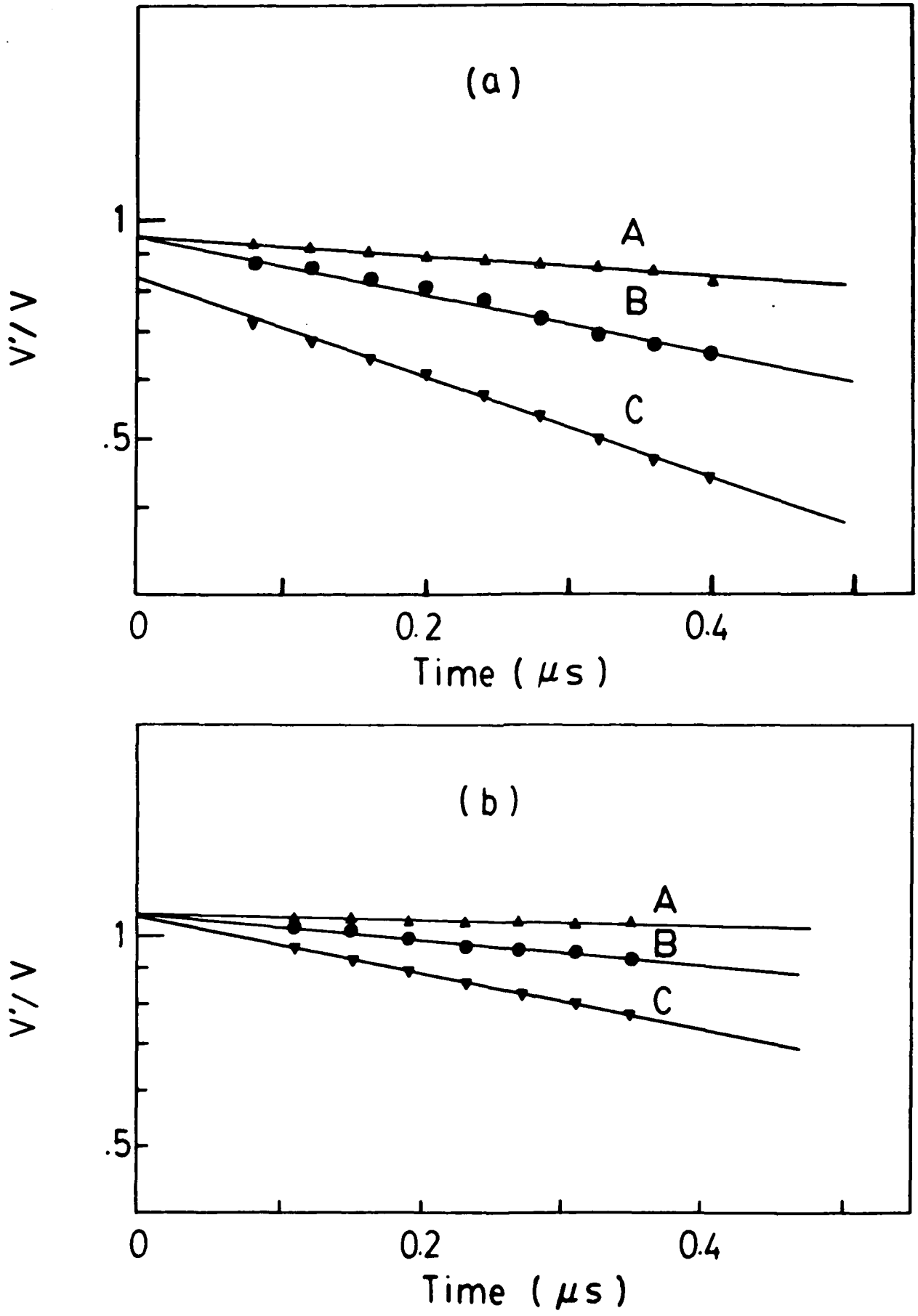

FIGURE 10

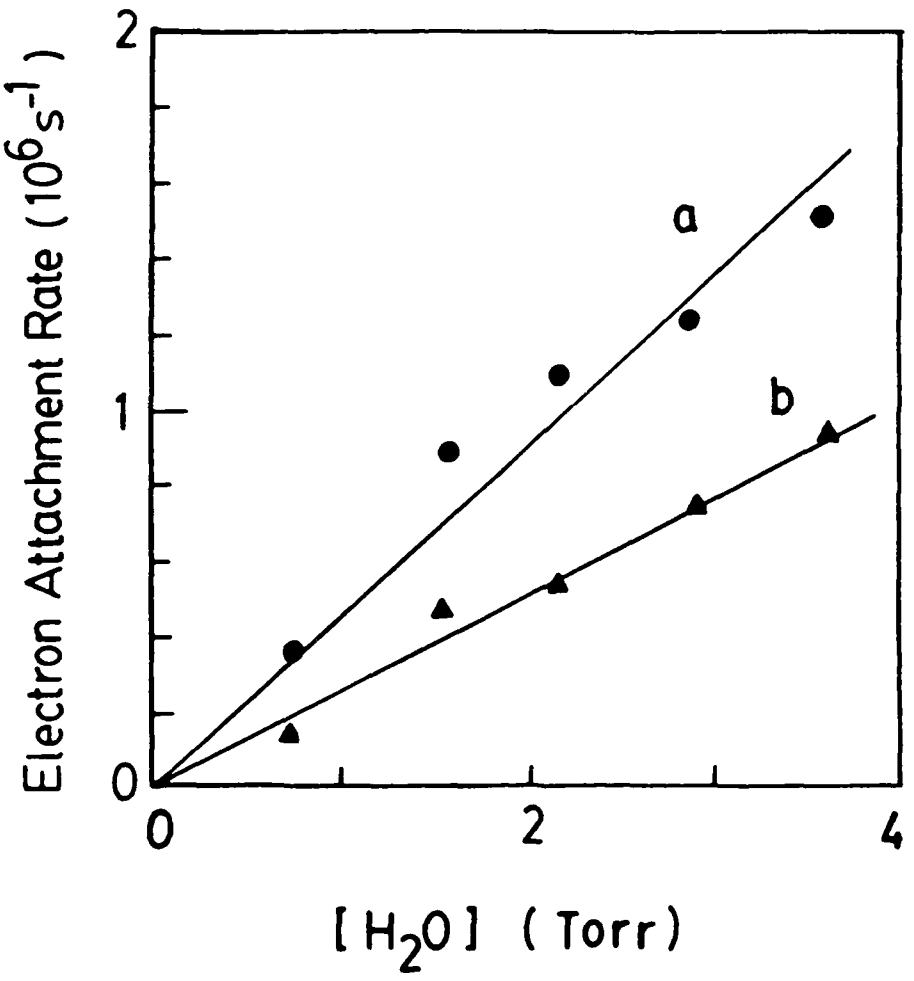

FIGURE 11

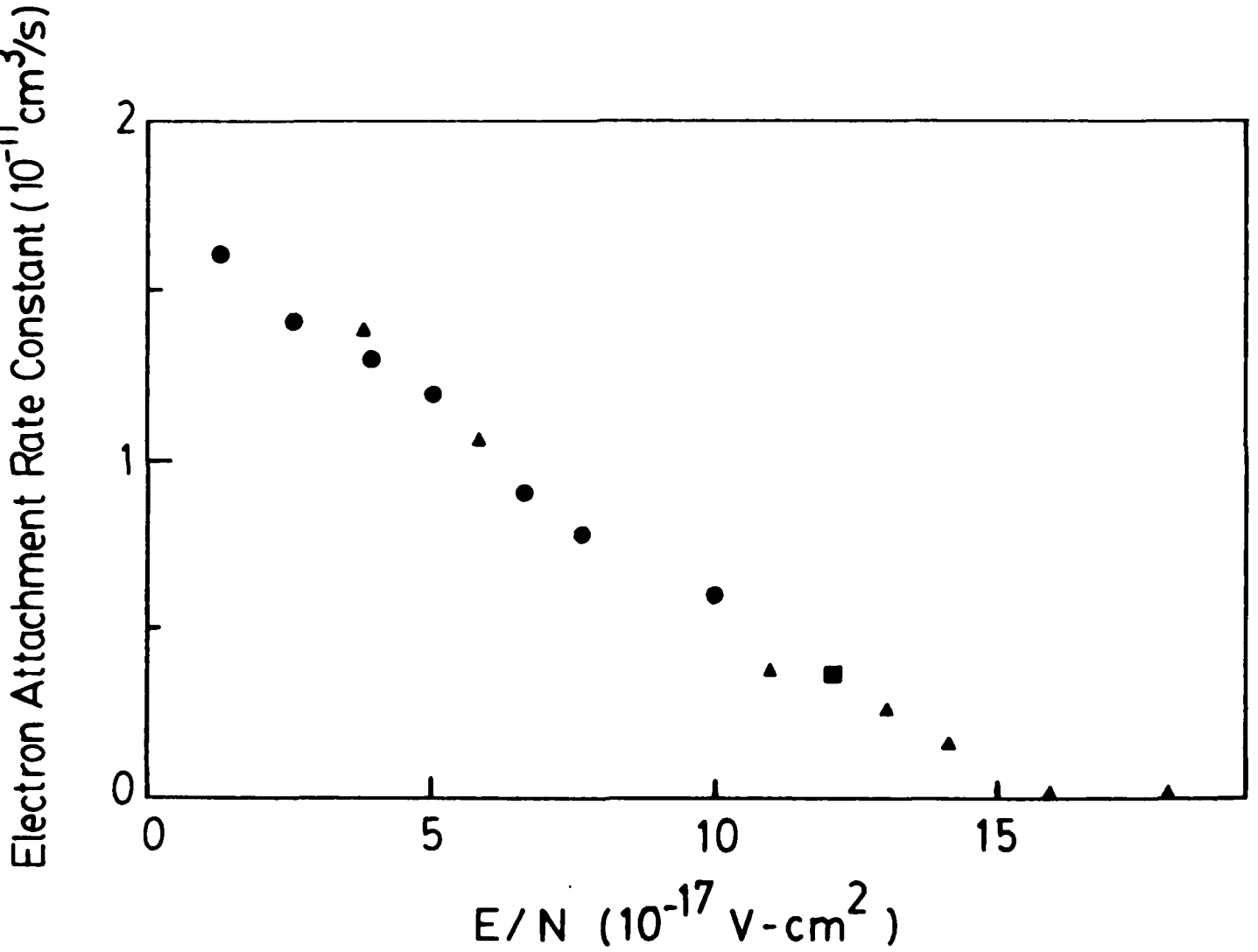
Electron Attachment Rate Constant (10^{-11} cm^3/s)
2
1
0
0
5
10
15
E/N (10^{-17} V-cm^2)

FIGURE 12

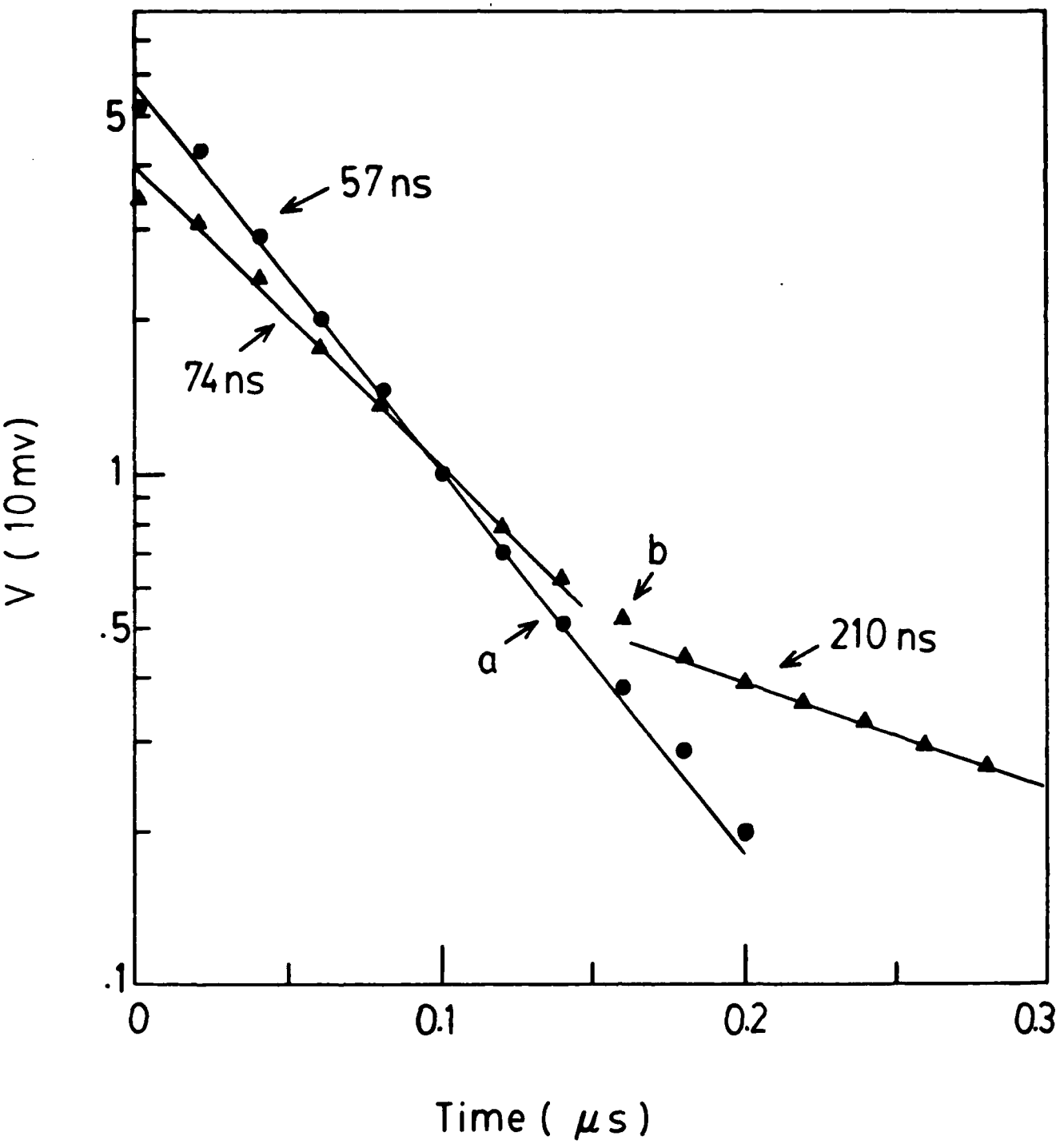

FIGURE 13

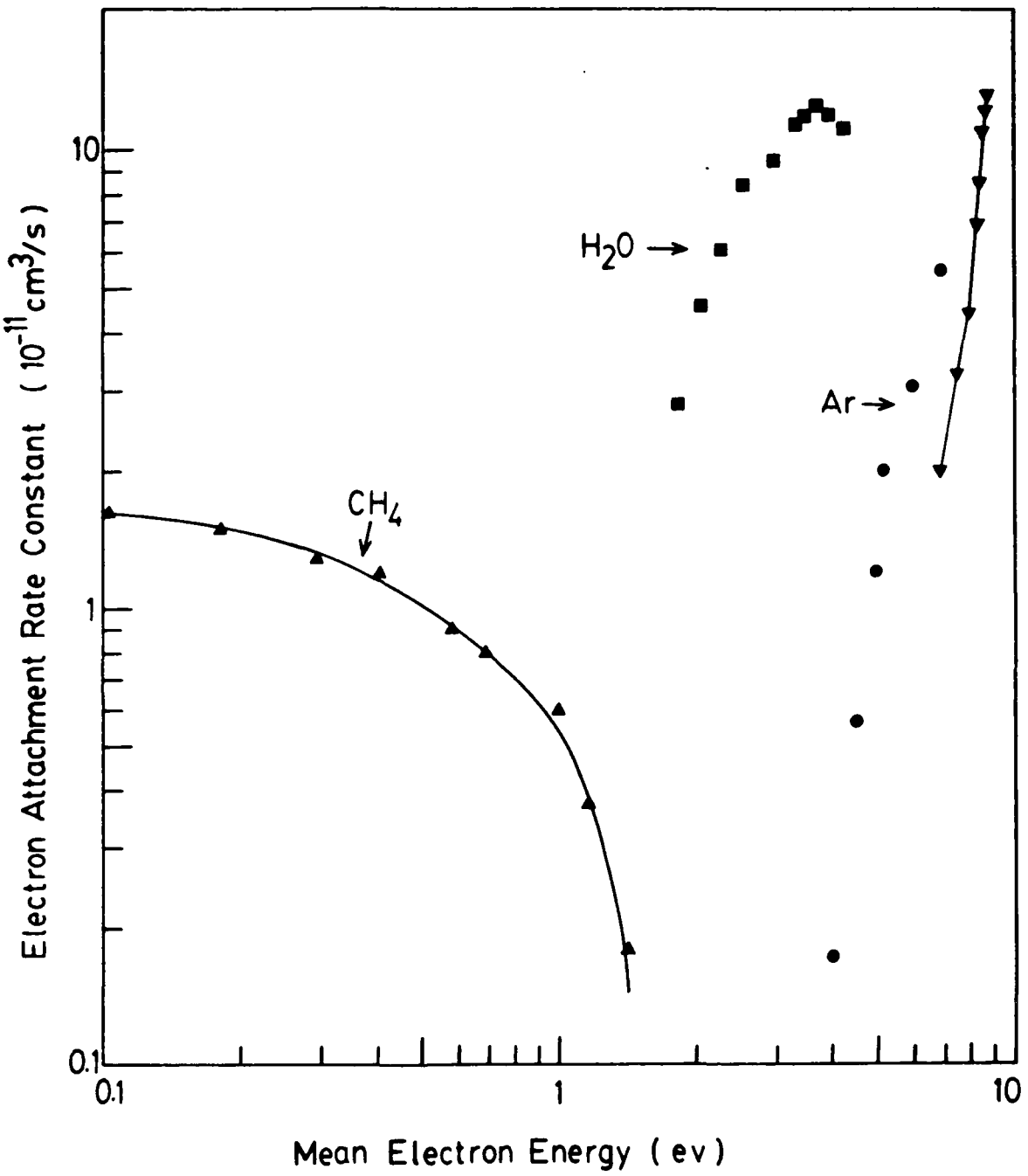
Electron Attachment Rate Constant (10^{-11} cm^3/s)
10
1
0.1
0.1
1
10
Mean Electron Energy (ev)
H_2O →
Ar →
CH_4

FIGURE 14

APPENDIX B

Shortening of Electron Conduction Pulses by Electron Attachers O_2, N_2O and CF_4

827421jap

Shortening of electron conduction pulses by electron attachers O_2, N_2O, and CF_4

L. C. Lee and F. Li

Department of Electrical and Computer Engineering, San Diego State University, San Diego, California 92182-0190

(Received 20 April 1984; accepted for publication 12 July 1984)

A uniform electron density is produced by two-photon ionization of trace trimethylamine in the N_2 buffer gas of atmospheric pressure using ArF laser photons. The transient conduction pulses induced by the electron motion between parallel electrodes under various applied electric fields are observed. The duration of the electron transient pulse is shortened when the electron attacher O_2, N_2O, or CF_4 is added to the buffer gas. Electron attachment rate constants are obtained from the ratios of the transient current with and without attachers at various times after the laser pulses. For O_2 and N_2O, the electron attachment rate constants measured in this experiment agree with previous values measured by different methods. The apparent rate constants for the attachment of low-energy electrons by CF_4 are measured. The electron drift velocity is found to increase when CF_4 is added to N_2. The present method is applicable for the measurement of the electron attachment rate associated with the production of short-lived negative ions.

INTRODUCTION

Recent developments in high-tech areas such as lasers, fusion experiments, and particle beam technology require gas-phase discharge switching devices. The duration of the electron conduction pulse is an important parameter for designing some type of switches, for example, opening switches and high repetition (rep)-rate switches. The duration could be shortened by increasing the electron decay rate, which could in turn be controlled by attaching the conduction electrons with various electron attaching gases. The electron attaching rates for various gas media in discharge conditions are thus needed for developing various discharge switches.

In this paper, we report a method for measuring the electron attachment rates for electrons in high gas pressures at varied E/N. Initial electrons with known concentration are produced by two-photon ionization of trace trimethylamine in N_2 buffer gas using ArF laser photons. The shortening of the electron conduction pulse duration by electron attacher is observed, and the electron attachment rate is measured from the decay rate of electron pulse.

This new method is tested by measuring the electron attachment rates of O_2[1–5] and N_2O[9–14] which were extensively investigated before. The current results are consistent with the published data measured by different methods. We have extended the current measurement to CF_4, whose data are not well known.

In this experiment, it is found that the electron drift velocity increases when O_2 or CF_4 is added to the N_2 buffer gas. Such increase of electron drift velocity makes the initial electron conduction current increase. This is a very desirable characteristic for high-power and high rep-rate discharge switches.

II. EXPERIMENT

The experimental apparatus is depicted in Fig. 1. The gas cell is a six-way aluminum cross of 6 in. diam. The electrodes are two parallel stainless-steel plates of 5 cm diam a few cm apart. The electrodes are uncoated raw metal. The electrons are produced by two-photon ionization of a trace trimethylamine in nitrogen buffer gas of atmospheric pressure with ArF laser photons (Lumonics model 861S). The laser energy is monitored by an energy meter manufactured by Scientech (model 365). The laser cross-section area between the electrodes is about 1.8×0.6 cm^2.

The charges drift under an applied electric field supplied by a negative high voltage on the cathode. The electron conduction current is converted to a transient voltage pulse by a 1-KΩ resistor connecting the anode to ground. The transient voltage pulse is monitored by a 275-MHz storage oscilloscope (Hewlett-Packard model 1727A). The overall time response of the electronics is tested by measuring the electron pulse produced by laser irradiation on the cathode in vacuum. The rise time of the electronics is about 100 ns. Each transient voltage pulse is captured and stored in the oscilloscope, which is later photographed for a permanent record.

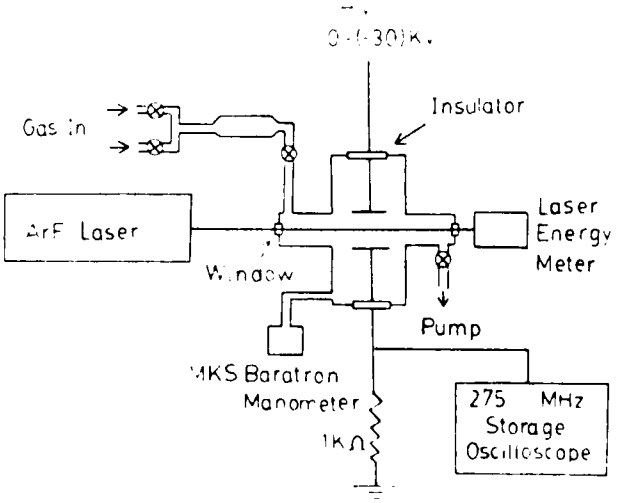

FIG. 1. Schematic diagram for the experimental apparatus.

Diluted trimethylamine (1%) in prepurified nitrogen (manufactured by Matheson) is further diluted by mixing with prepurified nitrogen before admitting into the gas cell. The gas is slowly pumped by a mechanical pump. The gas pressure in the cell is maintained constant by continuously supplying with fresh gas. The flow system will reduce the impurities possibly produced from the photofragmentation of trimethylamine as well as released from walls and electrodes. The gas pressure is measured by an MKS Baratron manometer. The measurements are performed at room temperature.

The N_2, O_2 (both supplied by MG Scientific Gases), N_2O, and CF_4 (both supplied by Matheson) have minimum purities of 99.998%, 99.99%, 99.0%, and 99.7%, respectively. These gases are admitted to the gas cell without further purification.

III. ANALYSIS

When trimethylamine is irradiated by ArF laser photons, an equal amount of electrons and ions are produced by a two-photon-ionization process. The electron density produced is given[15] by

$$n_e = \alpha n \int I^2(t)\,dt/h\nu, \tag{1}$$

where $\alpha = 1.5 \times 10^{-27}$ cm^4/W is the two-photon-ionization coefficient, n is the trimethylamine gas concentration (cm^{-3}), I is the laser intensity (W/cm^2), and $h\nu$ is the photon energy (joules). $\int I^2(t)\,dt$ is integrated over the laser pulse duration.

The electrons produced drift toward the anode under the applied field. The electron drift velocity is much faster than that of the ion, so the ion can be considered as stationary in space during the electron conduction pulse. If the electron density is high, the electric field induced by the space charge may be so large that the applied electric field is seriously disturbed. This subject has been discussed in detail elsewhere.[16] In this experiment, the charge density is limited so low that the applied field is not seriously disturbed by the space-charge-induced field, namely, electrons only move in the direction toward the anode. Thus, the effective electric field is approximately equal to the external applied field.

The current induced by the electron motion is given[17,18] by

$$i(t) = Ae \int_0^D n_e(z,t)W(z,t)\,dz/D, \tag{2}$$

where A is the plasma area in the plane parallel to electrodes, D is the electrode separation, $n_e(z,t)$ is the electron density at a position z from the cathode and at a time t after the laser pulse, and $W(z,t)$ is the electron drift velocity at z and t. $n_e(z,0) = n_e$ is the initial electron density produced by the laser ionization of trimethylamine.

If n_e/E is limited to a low value such that the space-charge effect is not important, $W(z,t)$ will approach the equilibrium electron drift velocity W in a short time after the laser pulse. Thus, the electron conduction current is equal to

$$i(t) = eN_e(t)W/D, \tag{3}$$

where $N_e(t) = A\int_0^D n_e(z,t)\,dz$ is the total number of electrons between electrodes. When t is much greater than the rise time of electronics (~ 100 ns), the current is measured[18] by the transient voltage as

$$V(t) = i(t)R, \tag{4}$$

where R is the resistor connecting the anode to ground.

When an electron attaching gas is added, the conduction electrons will be attached. The electron conduction current thus becomes

$$i'(t) = eN_e'(t)W'e^{-\eta t}/D, \tag{5}$$

where $N_e'(t) = A\int n_e'(z,t)\,dz$ is the total number of electrons, and η is the electron attachment rate of the electron attacher. The electron drift velocity for the mixture of electron attacher and buffer gas may be different from that of buffer gas alone.

The ratio of the transient voltages with and without the electron attaching gas is

$$\ln(V'/V) = \ln(W'/W) + \ln[N_e'(t)/N_e(t)] - \eta t. \tag{6}$$

For an atmospheric buffer gas, the electron drift velocity will reach the equilibrium state in a very short time, so $\ln(W'/W)$ can be considered as a constant. In the absence of electron attachment, the total number of electrons $N_e(t)$ are

$$N_e(t) = n_e AL \quad \text{for } t < l/W \tag{7a}$$

and

$$N_e(t) = n_e A(L+l)\left(1 - \frac{Wt}{L+l}\right) \quad \text{for } t > l/W, \tag{7b}$$

where L is the laser dimension in the electric field direction, and l (~ 1 cm) is the distance from the plasma front to the anode.

If W' nearly equals W, the ratio of N_e' to N_e will be nearly constant at all times t. In the case where W' is very different from W (as in the case for CF_4 in N_2), we analyze the data only at $t < l/W$, so that $N_e'(t)/N_e(t)$ is nearly constant with time. In any case, the ratio of $N_e'(t)/N_e(t)$ is nearly constant for the time duration we choose to analyze the data. The plot of $\ln(V'/V)$ vs t thus gives the electron attachment rate η.

IV. RESULTS AND DISCUSSION

A. O_2

The electron conduction pulse produced by two-photon ionization of 9 mTorr trimethylamine in 400 Torr N_2 by ArF laser photons is shown in Fig. 2(a). The laser energy is 9.6 mJ/pulse. When 20 Torr O_2 is added, the pulse is shortened, as shown in Fig. 2(b). The laser energy is 7.4 mJ/pulse. The reduced electric field is kept at $E/N = 4$ Td (1 Td = 10^{-17} V cm^2) for both pulses, and the separation of electrodes is kept at 4 cm. The laser energy for the case with O_2 [Fig. 2(b)] is lower than that without O_2 [Fig. 2(a)], but the peak voltage is higher for the former case. We propose that the increase of peak voltage is caused by the increase of electron drift velocity due to O_2 added to N_2. At $E/N = 4$ Td, the electron drift velocity[19] for O_2 is 2.5×10^6 cm/s which is higher than 10^6 cm/s for N_2. Another example would be the drift velocity of electrons in air. At $E/N = 4$ Td the electron drift velocity

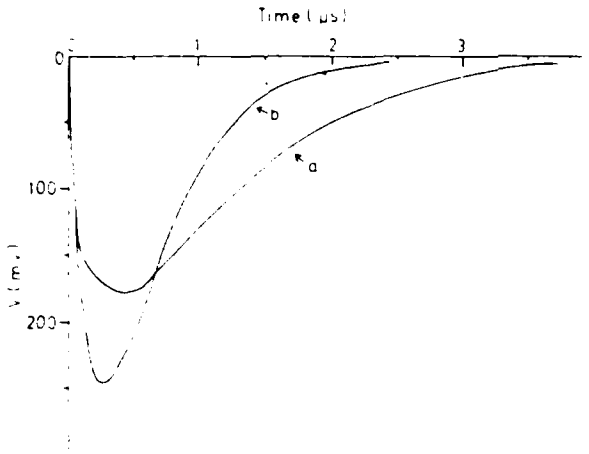

FIG. 2. The electron conduction pulses of (a) without O_2 and (b) with 20 Torr O_2 in 400 Torr N_2, where electrons are produced by two-photon ionization of 9 mTorr trimethylamine with ArF laser energies of 9.6 and 7.4 mJ/pulse, respectively. The E/N is fixed at 4 Td.

is[19] 1.4×10^7 cm/s which is also higher than that in N_2. The increase of electron drift velocity by the addition of O_2 may thus be expected. The half-width of the current pulse is about 0.8 μs which is much larger than the response of electronics (~ 0.1 μs), so the peak current is not seriously affected by the transient response of the experiment.

The ratios of the transient voltages with and without O_2 are plotted in Figs. 3(a), 3(b), and 3(c) for O_2 pressures of 10, 20, and 40 Torr and the E/N of 2, 3, and 4 Td, respectively. The $\ln(V'/V)$ values decrease linearly with t. The decrease is mainly caused by the attachment of electrons by O_2. During the period of $0.1 < t < 1$ μs, the electron density varies slowly with time, so the $\ln[N_e'(t)/N_e(t)]$ term in Eq. (6) is nearly constant and does not contribute significantly to the decrease of $\ln(V'/V)$ with t. Therefore, the decrease is mainly due to electron attachment, and the slope measures the electron attachment rate η.

For the $E/N = 2$–10 Td range studied here, we find that

$$\eta = K_3[O_2]^2 + k_2'[O_2][N_2]. \quad (8)$$

This result is consistent with earlier measurements[1–8] that electrons are attached by O_2 by a three-body attachment process. The three-body attachment rate constants k_3 measured at various E/N are plotted in Fig. 4. The uncertainty is estimated to be within 30% of each given value. The data were taken at various trimethylamine concentrations from 2 to 13 mTorr, while the laser energy was kept nearly constant at a low value. Since the initial electron density is proportional to the trimethylamine concentration, the independence of the rate constants on gas concentration indicates that the charge density is low, and the applied field is not seriously disturbed by the space-charge-induced electric field.[16] When the charge density is high, the applied electric field could be canceled by the space-charge-induced field, so the measured attachment rate constant is equivalent to the value at $E/N \sim 0$.

The data given by McCorkle *et al.*[6] are also plotted in Fig. 4 for comparison. The previous data[6] were measured by a different experimental method, in which the electron attachment rate constants were obtained from the O_2^- ion current. The present data are higher than the values of McCorkle *et al.*,[6] but agree reasonably well with the data of Chanin *et al.*[1] which are also plotted in Fig. 4 for comparison.

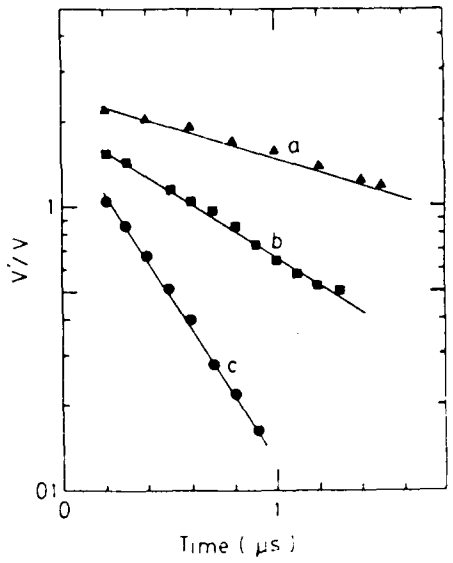

FIG. 3. The plots for the ratios of transient voltages measured with and without O_2, V'/V, at various times after laser pulses. The data was taken at (a) $E/N = 2$ Td, with and without 10 Torr O_2 in 600 Torr N_2, (b) 3 Td, 20 Torr O_2 in 400 Torr N_2, and (c) 4 Td, 40 Torr O_2 in 400 Torr N_2.

The reasonably good agreement between the present data and the earlier measurements indicates that the present method is a useful alternative method for measuring the electron attachment rate coefficient. This good agreement also strengthens the assertion that the pulse shortening is due to the attachment of electrons to O_2.

B. N_2O

The electron conduction pulses with and without 5 Torr N_2O in 440 Torr N_2 are shown in Figs. 5(a) and 5(b), respectively. The E/N is fixed at 10 Td. The separation of electrodes is fixed at 2 cm. (Similar results were obtained with a 4-cm electrode separation.) The trimethylamine pres-

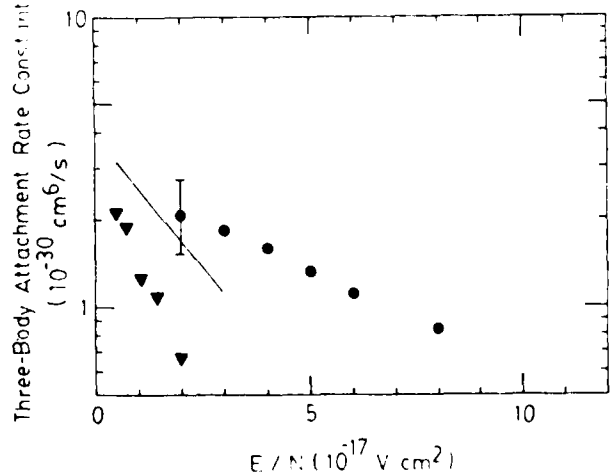

FIG. 4. The three-body attachment rate constants of electrons attached by O_2. The data (solid line) given by Chanin *et al.* (Ref. 1) and (▼) by McCorkle *et al.* (Ref. 6) are plotted for comparison.

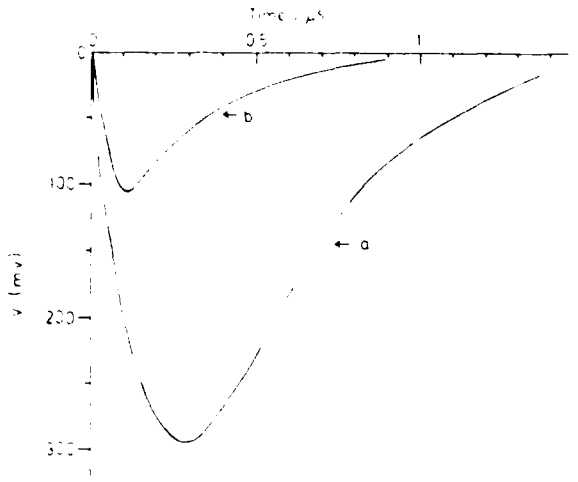

FIG. 5. The electron conduction pulses of (a) without N_2O and (b) with 5 Torr N_2O in 440 Torr N_2. Without N_2O the laser energy is 6.4 mJ/pulse. The trimethylamine pressure is fixed at 8 mTorr. The E/N is at 10 Td.

sure is 8 mTorr. Without N_2O, the laser energy is about 6.4 mJ/pulse in the central region of electrodes. When N_2O is added, the transient voltage decreases as shown in Fig. 5(b). This decrease is probably caused by the absorption of laser intensity by N_2O, as discussed below.

The photoabsorption cross section[20] of N_2O at 193 nm is about 10^{-19} cm^2. For a path length of 25 cm (from the laser entrance window to the central region of electrodes) used in this experiment, the laser intensity attenuated by 5 Torr N_2O will be reduced to 66% of the value without absorption. This means that the initial electron density produced by laser photons will be reduced to 43% when N_2O is added. The peak voltages shown in Figs. 5(a) and 5(b) are consistent with this expectation.

The shortening of the conduction pulse shown in Fig. 5(b) is caused by the attachment of electrons by N_2O. The electron drift velocity does not change significantly when N_2O is added to N_2. The electron drift velocities at 10 Td are 3×10^7 and 8×10^7 cm/s for N_2[19] and N_2O,[21] respectively. It is expected that the electron drift velocity will increase as N_2O is added. However, this expectation is not observed from the peak voltages as shown in Figs. 5(a) and 5(b). Therefore, the electron density is not affected by the electron drift velocity, namely, $\ln[N_e'(t)/N_e(t)]$ is nearly constant and does not contribute significantly to the decay of the electron conduction pulse. The slope of $\ln(V'/V)$ vs t thus gives the electron attachment rate η.

In the E/N region studied, the electron attachment rate results[12] from the two-body attachment of electrons by N_2O as well as the three-body attachment of electrons by N_2O and N_2, namely,

$$\eta = k_a[N_2O] + k_a'[N_2O][N_2]. \tag{9}$$

The results for the $\eta/[N_2O]$ values measured at various N_2O pressures are shown in Figs. 6(a) and 6(b) for $E/N = 2$ and 10 Td, respectively. The attachment rate constant decreases with increasing N_2O pressure. This phenomenon has been observed in previous measurements.[12]

The decrease of $\eta/[N_2O]$ with increasing $[N_2O]$ is probably caused by the decrease of k_a with increasing $[N_2O]$. The mechanism for this decrease is attributed[12] either to the effect of N_2O on the electron energy distribution or by electron detachment of O^- by N_2O. The detachment rate constant caused by the direct associative detachment reaction,

$$O^- + N_2O \rightarrow N_2O_2 + e \tag{10}$$

is ruled out[13] based on its slow reaction rate obtained from the flowing afterglow study.[22] Instead, the detachment is probably caused by the fast processes

$$O^- + N_2O \rightarrow NO + NO^-, \tag{11}$$

$$NO^- + N_2O \rightarrow NO + N_2O + e, \tag{12}$$

with reaction rate constants of 2×10^{-10} and 5.9×10^{-12} cm^3/s for k_{11}[22] and k_{12},[13] respectively.

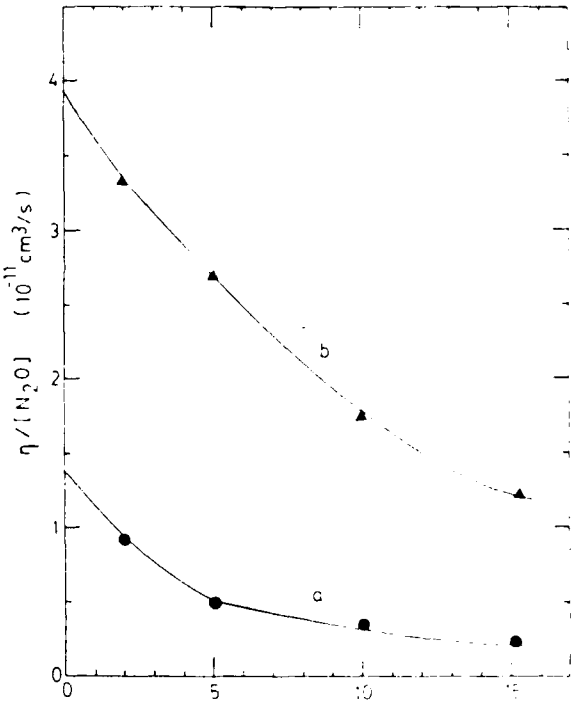

FIG. 6. The $\eta/[N_2O]$ values for varied N_2O pressures in 440 Torr N_2: (a) $E/N = 2$ Td and (b) 10 Td.

The two-body attachment rate constant k_a, measured at various E/N are plotted in Fig. 7. k_a is obtained from the extrapolation of the dependence of $\eta/[N_2O]$ on pressure to $[N_2O] \sim 0$, and then corrected with $k_a'[N_2]$. k_a' is adopted from Ref. 12. The data of Chaney and Christophorou[12] at low E/N are also plotted in Fig. 7 for comparison. The present results are consistent with the previous data that are measured by the swarm method.[12] This good agreement again indicates that the present experiment is a useful method for the electron attachment rate measurement, and the shortening of the electron conduction pulse is indeed caused by the attachment of electrons by N_2O.

C. CF_4

The electron conduction pulses with and without 6.5 Torr CF_4 in 420 Torr N_2 are shown in Figs. 8(a) and 8(b), where the laser energies are 8.4 and 4.2 mJ/pulse, respective-

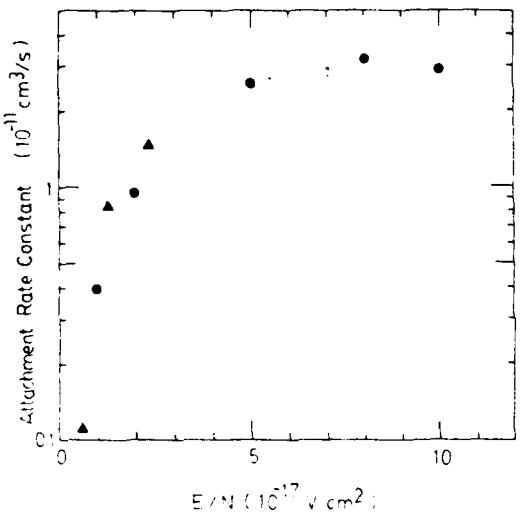

FIG. 7. The two-body attachment rate constants of electrons attached by N_2O at various E/N. The data (▲) given by Chaney and Christophorou (Ref. 12) are plotted for comparison.

ly. The trimethylamine pressure is kept at 9 mTorr. The E/N is fixed at 4 Td. The electrode separation is 4 cm.

When CF_4 is added to N_2, the pulse duration is shortened and the transient voltage increases, as shown in Fig. 8(b). The increase of transient voltage is probably caused by the increase of electron drift velocity. At the same E/N, the electron drift velocity for CF_4 is much higher than that for N_2. For example, at $E/N = 4$ Td, the electron drift velocities are 1.1×10^7 and 10^6 cm/s for CF_4[23] and N_2,[19] respectively. CF_4 may thus significantly affect the electron drift velocity for pure N_2. It has been observed[23] that the electron drift velocity increases more than one order of magnitude when a small amount of CF_4 is added to Ar.

The two-body electron attachment rate constants $\eta/[CF_4]$ are measured for various E/N at several CF_4 pressures. The electron attachment rate constants increase with increasing E/N. At a fixed E/N, the attachment rate constants decrease with increasing CF_4 pressure similar to the case of N_2O. The two-body electron attachment rate constants obtained by an extrapolation to $[CF_4] = 0$ are shown in Fig. 9. Similar to the case of N_2O, this decrease may be

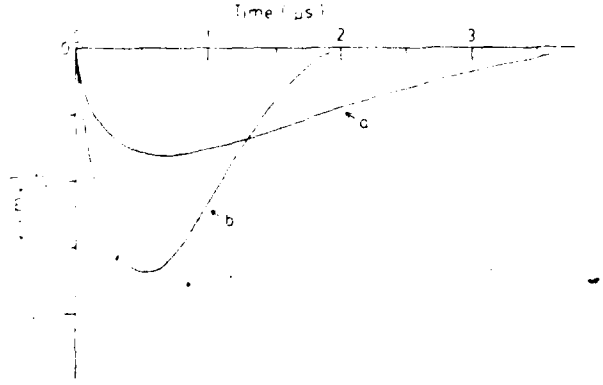

FIG. 8. The electron conduction pulses of (a) without CF_4 and (b) with 6.5 Torr CF_4 in 420 Torr N_2, where the laser energies are 8.4 and 4.2 mJ/pulse, respectively. The trimethylamine pressure is fixed at 9 mTorr, and the E/N is 4 Td.

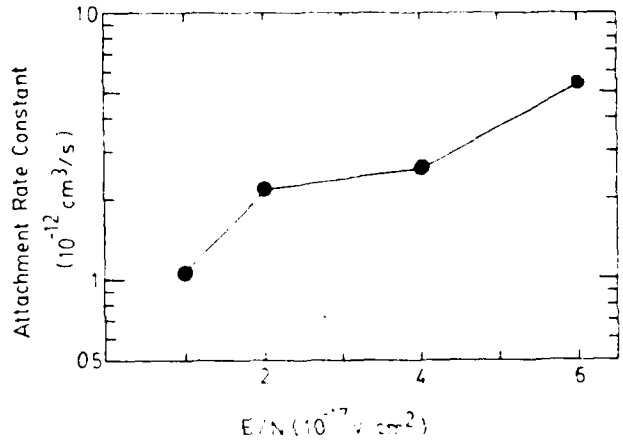

FIG. 9. The two-body attachment rate constants of electrons attached by CF_4 in 420 Torr N_2 at various E/N. The data represent the values extrapolated to the zero CF_4 pressure.

caused either by the electron detachment process or by the effect of CF_4 on the electron energy distribution.

CF_4 has a high rate constant[24,25] for the dissociative electron attachment process at $E/N > 50$ Td. At low E/N, the electron attachment rate constant for the thermal electron has been measured as 7×10^{-13} cm^3/s in an early time[26] and later changed[27] to $< 10^{-16}$ cm^3/s. At $E/N = 40$ Td, the electron attachment rate constant is estimated to be 3×10^{-11} cm^3/s, using the electron attachment cross section[24,27] of 6×10^{-19} cm^2 and the electron drift velocity[24] of 5×10^7 cm/s. The electron attachment rate constants measured here (see Fig. 9) are between the value for the thermal electrons and the value at $E/N = 40$ Td.

For the E/N region studied, electrons do not have enough energy for the dissociative electron attachment process. It is likely that the attachment is due to the formation of CF_4^-. Verhaart *et al.*[28] have suggested that there is a relatively stable state for CF_4^- with an electron in a Rydberg orbital. Since this experiment measures the electron transient pulse, the attachment process for a short-lived species could be observed. If the lifetime of CF_4^- is longer than the transient pulse duration (~ 2 μs), then the electron attachment rate due to CF_4 can be measured. Although the electron attachment is probably due mainly to CF_4, we do not rule out the possibility that the attachment may be partly caused by impurity. The electron attachment rate constants measured at 380 and 200 Torr N_2 are the same. This indicates that the impurity, if it exists at all, is not related to the N_2 gas used, but possibly inherent with the CF_4 gas used. It was observed[27] that the electron attachment rate for thermal electrons by the purified CF_4 sample was much smaller than that for the unpurified one. Because of the uncertainty in impurities, we regard the measured attachment rate constants as the apparent values.

V. CONCLUDING REMARKS

The transient current due to the conduction electrons is observed in this experiment, which is different from the previous swarm method that detects the negative ions. Although the measurement methods are different, the electron

attachment rate constants measured here are generally consistent with other published values. The good agreement demonstrates that this measurement is a useful alternative method for measuring the electron attachment rates.

This new method has an additional advantage in that it can measure the electron attachment rate due to the formation of short-lived negative ions. For example, the electron attachment due to CF_4 is observed in this experiment, which may not be detectable by the swarm method because of the short lifetime of CF_4 . The transient electron pulse is usually in the time duration of ns–μs range, and the ion current pulse is in the ms range. Thus, the lifetime for the negative ions that can be detected by this experiment is much shorter than the case for the swarm method.

The current technique of having a short-time scale is comparable with the method recently developed by Verhaart and van der Laan,[29] which employs a N_2 laser of 0.6 ns duration to produce primary electrons from the irradiation of the cathode. The electrons produced by their method are distributed in a small volume and require the electron-gas ionization to obtain a measurable pulse current. This method is thus limited to measure the swarm parameters in the high E/N region where electrons can gain sufficient energy to ionize gas, in contrast to the present method that can measure the attachment rate constants over a wide E/N range. The present method produces a large number of electrons uniformly distributed in a large volume that gives a measurable current signal without electron-gas ionization, so it can measure the attachment rate constants in the low E/N range as well as the high one.

This method is relatively simple so that it can be easily applied to measure the electron attachment rates for other molecules in various high-pressure buffer gases such as air, SF_6, and hydrocarbons. These buffer gases are usually used in high-energy and high-rep-rate discharge switches. To extend the measurement to high E/N is also of interest. At high E/N, the electron detachment rate is usually large, so the liftime of a negative ion is expected to be short. The present method can be applied for this type of measurement, but the previous method that measures the negative ion current may encounter some difficulties.

The increase of the electron drift velocity by adding attachers (such as CF_4) to a buffer gas is of interest, because the attachers could simultaneously shorten the conduction pulse and also increase the electron conduction current. These are important characteristics required for high-energy and high-rep-rate discharge switches as well as opening switches.

ACKNOWLEDGMENTS

The authors wish to thank Dr. Martin Gundersen at the University of Southern California and Dr. Arthur H. Guenther at the Air Force Weapons Laboratory for useful comments. The authors also thank Dr. E. R. Manzanares, Dr. J. B. Nee, Dr. M. Suto, and Dr. W. C. Wang in our laboratory for useful suggestions and discussion. The technical assistance received from Mr. F. C. Clark is appreciated. This research is sponsored by the Air Force Office of Scientific Research, Air Force Systems Command, USAF, under Grant No. AFOSR-82-0314.

[1] L. M. Chanin, A. V. Phelps, and M. A. Biondi, Phys. Rev. **128**, 219 (1962).
[2] J. L. Pack and A. V. Phelps, J. Chem. Phys. **44**, 1870 (1966).
[3] N. Sukhum, A. N. Prasad, and J. D. Craggs, Br. J. Appl. Phys. **18**, 785 (1967).
[4] M. N. Hirsh, P. N. Eisner, and J. A. Slevin, Phys. Rev. **178**, 175 (1969).
[5] D. Spence and G. J. Schulz, Phys. Rev. A **5**, 724 (1972).
[6] D. L. McCorkle, L. G. Christophorou, and V. E. Andersen, J. Phys. B **5**, 1211 (1972).
[7] F. K. Truby, Phys. Rev. A **6**, 671 (1972).
[8] R. E. Goans and L. G. Christophorou, J. Chem. Phys. **60**, 1036 (1974).
[9] A. V. Phelps and R. E. Voshall, J. Chem. Phys. **49**, 3246 (1968).
[10] J. M. Warman and R. W. Fessenden, J. Chem. Phys. **49**, 4718 (1968).
[11] J. L. Moruzzi and J. T. Dakin, J. Chem. Phys. **49**, 5000 (1968).
[12] E. L. Chaney and L. G. Christophorou, J. Chem. Phys. **51**, 883 (1969).
[13] J. M. Warman, R. W. Fessenden, and G. Bakale, J. Chem. Phys. **57**, 2702 (1972).
[14] H. Shimamori and R. W. Fessenden, J. Chem. Phys. **68**, 2757 (1978); **71**, 3009 (1979).
[15] L. C. Lee and W. K. Bischel, J. Appl. Phys. **53**, 203 (1982).
[16] F. Li and L. C. Lee (unpublished).
[17] L. G. H. Huxley and R. W. Crompton, *The Diffusion and Drift of Electrons in Gases*, (Wiley, New York, 1974), pp. 297–304.
[18] H. Raether, *Electron Avalanches and Breakdown in Gases*, (Butterworth, Washington, 1964), pp. 13–27.
[19] J. Dutton, J. Phys. Chem. Ref. Data **4**, 577 (1975).
[20] M. Zelikoff, K. Watanabe, and E. C. Y. Inn, J. Chem. Phys. **21**, 1643 (1953).
[21] R. A. Nielsen and N. E. Bradbury, Phys. Rev. **51**, 69 (1937).
[22] E. E. Ferguson, Adv. Electron. Electron Phys. **24**, 23 (1968).
[23] L. G. Christophorou, D. V. Maxey, D. L. McCorkle, and J. G. Carter, Nucl. Instrum. Methods **163**, 141 (1979); **171**, 491 (1980).
[24] J. W. Gallagher, E. C. Beaty, J. Dutton, and L. C. Pitchford, JILA Information Center Report No. 22 (1982); J. Phys. Chem. Ref. Data **12**, 109 (1983).
[25] S. M. Spyrou, I. Sauers, and L. G. Christophorou, J. Chem. Phys. **78**, 7200 (1983).
[26] T. G. Lee, J. Phys. Chem. **67**, 360 (1963).
[27] R. W. Fessenden and K. M. Bansal, J. Chem. Phys. **53**, 3468 (1970).
[28] G. J. Verhaart, W. J. van der Hart, and H. H. Brongersma, Chem. Phys. **34**, 161 (1978).
[29] H. F. A. Verhaat and P. C. T. van der Laan, J. Appl. Phys. **53**, 1430 (1982).

APPENDIX C

Space Charge Effect on Electron Conduction Current

SPACE CHARGE EFFECT ON ELECTRON CONDUCTION CURRENT

L. C. Lee and F. Li
Department of Electrical and Computer Engineering
San Diego State University
San Diego, California 92182

ABSTRACT

The electron conduction current due to electron motion between parallel plates is studied at various charge densities and applied fields. Uniform charges of known concentrations are produced by two-photon-ionization of trace trimethylamine in high pressure buffer gas (N_2 or Ar) using ArF laser photons. The space charge can induce large electric field to suppress the applied field so that the duration of the electron conduction current is greatly shortened. The experimental data are analyzed in accord with the theoretical calculation of Morrow and Lowke. The probability for electron leakage from the plasma and the plasma decay time are measured as a function of the ratio of the initial charge density to the applied field. Both the electron leakage probability and the plasma decay time decrease with the increase of the charge to field ratio. The electron leakage probabilities estimated from the theoretical calculation agree very well with the present measurements.

I. INTRODUCTION

Current development of lasers, fusion, and particle beam technology requires various electrical switching devices; in particular, radiation-controlled and electron-beam-controlled gas discharge devices, which operate at high currents, voltages and repetition frequencies, are needed. To improve these devices, the physics of high current discharges and the associated initiation and recovery phenomena needs to be well understood, and is the subject of the present study.

In a gaseous medium of high charge density, the field produced by space charge can be so large that the total electric field is disturbed, and the electron transport parameters need to be modified. The space charge effect on gaseous discharges has been extensively investigated theoretically by the Swansea group [1-4], Kline [5], and Morrow and Lowke [6] as well as experimentally by Doran [7], Waters et al., [8], and Chalmers et al., [9]. These investigations establish that the electric field induced by space charge plays a significant role in the discharge. For example, the time lag and spatial profile of discharge growth are strongly affected by space charge. Here, we study the space-charge effect on the electron conduction current using an experimental method that produces known space charge density. It is found that the electron pulse duration and the electron conduction current are greatly affected by the space charge density.

High power excimer lasers can produce pulses of high charge density by multiphoton-ionization of an organic gas in a high

pressure buffer gas. For example, an electron density of 10^{15} electrons/cm^3 can be produced by two-photon-ionization of 1 torr trimethylamine [$(CH_3)_3N$] with a typical KrF laser pulse of 100 mJ[10]. The coefficients for the two-photon-ionization process have been measured for several organic molecules [10], so the electron density can be determined from the gas density and the laser intensity. This known electron density allows us to study the effects of space charge on the decay of plasma and the electron leakage from the plasma ball.

This experiment provides data to compare with the theoretical calculation of space-charge effect by Morrow and Lowke [6], in which initial conditions set for their calculation are very close to the present experiment. The information obtained from this experiment could also be useful for understanding the pre-breakdown [11] and breakdown [12] processes of gaseous discharges as well as for developing laser-triggered switching devices [13-15].

II. EXPERIMENTAL

In the experiment, intial electron densities are produced by two-photon-ionization of a small amount of trimethylamine mixed in high pressure of nitrogen or argon using ArF laser photons. The transient current pulses voltages associated with electron conduction are measured as a function of the laser intensity, the trimethylamine concentration, the laser beam size, the applied field, and the buffer gas pressure. The dependences of electron pulse duration and electron leakage current on the ratio of the initial charge density

to the applied field are obtained.

The experimental apparatus is depicted in Figure 1. The gas cell is a six-inch diameter 6-way aluminium cross. The electrodes are two parallel uncoated stainless steel plates of 5 cm diameter 4 cm apart. The energy of the ArF laser (Lumonics model 861S) is monitored by an energy meter manufactured by Scientech (model 365).

The charges drift in an applied field produced by a negative high voltage on the cathode. The electron conduction current induces a transient voltage across a 1 KΩ resistor connecting the anode to the ground, which is monitored by a 275 MHz storage oscilloscope (Hewlett-Packard model 1727A). The time response of the electronics is tested by measuring the electron pulse produced by laser irradiation on the cathode in vacuum, which is about 100 ns. Each single transient voltage signal is captured and stored in the oscilloscope, which is later photographied for a permanent record.

Diluted trimethylamine (1%) in prepurified nitrogen (manufactured by Matheson) is further diluted by mixing with prepurified nitrogen before admitting into the gas cell. Gas pressure in the cell is maintained constant by continuously supplying fresh gas as it is slowly removed by a mechanical pump. This flowing system reduces impurities that may be produced from the photo-fragmentation of trimethylamine or released from the walls and electrodes. The gas pressure is measured by an MKS Baratron manometer.

When trimethylamine is irradiated by ArF laser photons, equal amount of electrons and ions are produced by the two-photon-ionization process. The resulting electron density is given by [10],

$$n_e = \alpha n \int I^2(t)dt/h\nu \qquad (1)$$

where $\alpha = 1.5\times10^{-27}$ cm^4/watt is the two-photon-ionization coefficient, n is the trimethylamine gas concentration (cm^{-3}), I is the laser intensity (watt/cm^2), and $h\nu$ is the photon energy (joule). The square of the light intensity is integrated over the laser pulse duration, which is about 10 ns.

Because the laser intensity is uniform over its cross-sectional area, the initial charges produced by the laser ionization of trimethylamine presumably distribute uniformly over the laser path between the parallel plates. The charges later drift out the plasma region by the applied field. Since the mobility of ion is much slower than that of electron, the ion can be considered as stationary in relative to the electron motion. Thus, the conduction current is essentially due to the electron motion only.

The current induced by the electron motion is given by [16],

$$i(t) = Ae \int_{Z_0}^{Z_0+D} n_e(z,t)W(z,t)dz/D \qquad (2)$$

where A is the plasma area in a plane parallel to the electrodes, D is the separation of electrodes. $n_e(z,t)$ is the electron density at a position z from the cathode and a time t after the laser pulse, and W(z,t) is the electron drift velocity at z and t. The Eq. (2) is derived under the assumptions that the charges are distributed uniformly over the A plane, as justified by the facts that the charges are uniformly produced over the laser volume.

The measured transient voltage is approximately expressed by

$$V(t) = i(t)R \qquad (3)$$

where the external current is assumed equal to the electron conduction current i(t). This assumption is justified by the facts that the capacitance between electrodes is small (~ 0.5 pF) and the cathode potential is held constant by the power supply. The transient voltage is a function of the trimethylamine concentration, the laser power, the applied external electric field, and the N_2 gas pressure. In this experiment, we study the transient voltage by varying one parameter a time while other parameters are fixed.

III. RESULTS

A. Trimethylamine Pressure Dependence

Figures 2 a and b show the electron conduction pulses taken at trimethylamine pressures of 4 and 30 mtorr, respectively. The applied field is fixed at 69 V/cm and the nitrogen pressure is 420 torr. The laser energy for each pulse is about 10 mJ. The beam dimension at the center of the electrodes is 1.8 cm along the electric field and 0.6 cm in the perpendicular direction. This perpendicular dimension is fixed throughout the whole experiment.

At low trimethylamine pressure, the electrons usually move in a direction toward the anode only (similar to Figure 3a). For 4 mtorr of trimethylamine the transient voltage has two maxima as shown in Figure 2a. The relative magnitudes of these maxima vary with laser energy, gas density, and applied field. As the trimethylamine pressure increases, the voltage pulse duration becomes shorter as

shown in Figure 2b. At later times the electron motion can even change direction, that is, the electrons move toward the cathode. The reason for the pulse shortening and reverse electron motion is further studied below.

For a laser energy of 10 mJ/pulse and a trimethylamine density of 4 mtorr, the initial electron density produced is about 1.2×10^{9} cm^{-3}. If we take the charge recombination rate constant as 5×10^{-6} cm^{3}/s [17,18], the recombination rate is 6×10^{3} s^{-1}. For pulse durations of a few μs (shown in Figure 2), the fraction of electrons lost by recombination with positive ions is less than 1%. The quick drop in current from maximum to zero within 1 μs (as shown in Figures 2a and b) is apparently not caused by the charge recombination.

The second pulse shown in Figure 2a and the reversed pulsse shown in Figures 2b are also not explainable by the electron attachment processes. This process will make the electrons disappear, so the conduction current would decrease to zero, namely, the later current peaks would not occur. Thus, the second pulse and the reverse current observed are definitely not caused by the electron attachment process.

The observed phenomena are, however, explainable by the space charge effect. The leakage electrons in the plasma front (near the anode) and the ions left in the plasma tail (near the cathode) can induce an electric field to cancel out the electric field in the plasma region. The effective electric field could be reduced to zero if the space charges (the leakage electrons and the ions left behind the plasma tail) are large enough as expected by the calculation of Morrow and Lowke [6]. When the effective electric field is reduced,

the drift velocity for the electrons in the plasma region will decrease. This contributes to the quick decrease of electron conduction current as shown in Figure 2a after the first peak.

At a later time, the first group of electrons leaving the plasma front reach the anode and are absorbed. Then the induced electric field is reduced, and the applied field becomes dominant again. The electrons locked in the central portion of the plasma are again accelerated by the applied field, producing the second pulse as shown in Figure 2a. This explanation is consistent with the observation that the second peak occurs at about 2.2 μs after the laser pulse, which corresponds the drift time of electrons from the plasma front to the anode. The electron drift velocity at E/N = 0.5 Td (as used for taking the pulse of Figure 2a) is about 4×10^5 cm/s [19]. For a drift distance of about 1 cm, the electron drift time is about 2.5 μs, which is consistent with the drift time observed.

It is suprised that the current is reversed at a later time as shown in Figure 2b. This is a common phenomenon observed at high initial charge density. One possible explanation for this phenomenon is that the electric field induced by the charges at the plasma front and tail may be so large that it overcomes the applied field. Thus, the electrons in the plasma region move toward the cathode in opposition to the applied field. Both the pulse intensity and the pulse duration depend strongly on the charge density and the applied field. We will further discuss this phenomenon after more experimental observations are presented.

B. Laser Energy Dependence

The electron conduction pulse depends strongly on the laser energy. Figures 3a and b show the pulses observed at the laser energies of 7.8 and 15 mJ/pulse, respectively. The laser beam cross section in the central region of the electrodes is 1.8x0.6 cm^2. The applied field is fixed at 686 V/cm. The nitrogen pressure is 418 torr, and the trimethylamine pressure is 18 mtorr.

At a low laser energy, the electrons move only in the direction toward the anode as shown in Figure 3a. When the laser energy increases, the pulse duration is shortened, and the electron motion can reverse (toward the cathode) at a later time as shown in Figure 3b.

The shortening of the pulse duration at high laser energy is explainable in terms of space charge effect. High laser energies result in both high charge densities and high induced electric fields, so the drift velocities of electrons in the plasma region are reduced or even reversed as explained above.

C. Laser Beam Size Dependence

The space charge effect depends on the plasma dimensions. Figures 4a and b show the electron conduction pulses produced by beam areas of 0.75x0.6 and 1.2x0.6 cm^2 with laser energies of 9.4 and 17 mJ/pulse respectively. The electric field is fixed at 686 V/cm. The trimethylamine pressure is 10 mtorr and the nitrogen pressure is 417 torr.

In both experiments (Figures 4a and b), the laser fluxes (energy/cm^2) are about the same, so the initial charge densities are nearly equal. However, the electron conduction pulse produced by the

small laser beam lasts longer in the reverse direction than the one produced by the large beam, indicating that the former one is affected longer by the space-charge effect than the latter one. This may be caused by the fact that the leakage electrons last longer for the small laser beam case, because the distance between the plasma front and the anode is larger, and the reverse electric field induced by the space charges thus lasts longer. Again, this result is consistent with the previous assertion that the reverse current is caused by the space charge effect.

D. Applied Field Dependence

The electron conduction pulses depend on the applied field shown in Figures 5a and b for field strengths of 143 and 286 V/cm, respectively. The laser energy and beam area are fixed at 6.2 mJ and 1.8x0.6 cm^2, respectively. The trimethylamine pressure is 18 mtorr, and the nitrogen pressure is 433 torr.

At a small applied field, the pulse duration is short and the direction of electron motion can reverse as shown in Figure 5a. When the applied field is large, the pulse duration becomes longer, and the electrons move only in the direction of the applied field. These results are explainable by the space-charge-effect model. The leakage electrons for the small applied field are smaller than the large one, as indicated by the fact that the pulse peak in Figure 5a is smaller than Figure 5b. However, the small applied field is easily overcome by the space-charge-induced field, so the space charge effect may in fact become more prominently. Thus, the pulse duration, at the small applied field, is shortened by the space-

charge-induced fields and the electron conduction current is even forced to reverse as shown in Figure 5a.

When the applied field is high, the fraction suppressed by the space-charge-induced field becomes small, so the electron conduction pulse is less affected by the space charge. This expectation is consistent with the pulse shown in Figure 5b, in which the electrons only move in the direction toward the anode, namely, the applied field is not overcome by the space-charge-induced field. These results suggest that the electron conduction current is not dependent on either charge density or the applied field alone, but on the ratio of them. This point will be further discussed later.

E. Buffer Gas Dependence

The magnitude of the space charge effect on the electron conduction current depends on the buffer gas used. Figures 6a and b show the electron conduction pulses for the buffer gases N_2 and Ar, respectively. The experimental parameters for Fig. 6a are a laser energy of 8.8 mJ/pulse, a beam size of 3x0.6 cm^2, an applied field of 134 V/cm, a trimethylamine pressure of 18 mtorr, and a nitrogen pressure of 408 torr. The experimental parameters for Fig. 6b are similar to Fig. 6a except that the trimethylamine pressure is 30 mtorr and the buffer gas is changed to Ar at 400 torr.

In general, the space charge effect is more prominent in Ar than in N_2. This may somehow relate to the electron kinetic energy. At the same E/N, the electron kinetic energy in Ar is higher than that in N_2 [19], so more electrons may leak out from the plasma ball in Ar.

IV. DISCUSSION

The present experimental conditions are very similar to the ones used for the theoretical calculation of Morrow and Lowke [6], in which the separation of parallel plates is 3 cm, the applied field is 5.58×10^3 V/cm, and the initial charges of equal ions and electrons are distributed uniformly over the central region between the parallel plates. The plasma ball was approximately a cube of a diameter of 0.5 cm on the plane perpendicular to the applied field and a Gaussian profile of 0.35 cm half-width along the applied field. The densities of electrons and ions were described by the continuity equations in one-dimensional conservative form, in coupling with the three-dimensional solution of Poisson's equation. The electron densities and the space-charge-induced fields were calculated as a function of time for three initial plasma charge densities of 5×10^6, 2.5×10^{10}, and 5×10^{11} cm^{-3}. For the initial charge density of 5×10^6 cm^{-3}, the space-charge-induced field is small, so the electrons drift toward the anode under the applied field without serious distortion. When the initial charge density increases, the space-charge-induced field becomes large and seriously distorts the electric field. For the initial charge density of 5×10^{11} cm^{-3}, the space-charge-induced field can cancel out the applied field in the plasma region, so the drift velocity for the electrons locked inside the plasma region is essentailly reduced to zero. These theoretical expectations are consistent with our experimental observations. We analyze the observed transient pulses in accord with the thoretical calculation [6] as below.

Equal densities of ions and electrons are initially produced by the laser ionization of trimethylamine that distributes uniformly over space. The charge densities can be calculated by Equation (1). In the beginning, the electrons drift toward the anode by the applied field. Since the electron drift velocity is much faster than ion drift, the ions can be considered stationary for a short time period after the charges are produced. As soon as the electrons move, electrons appear at the plasma front and positive ions are left behind the plasma tail as shown in Figure 7a. Accordingly, the resulting space-charge induced fields are added to the applied field (Figure 7b). The induced electric field E_i (produced by space charge alone) as a function of distance from the cathode is sketched in Figure 7c. The effective total electric field $E_e = E + E_i$ at some time after the laser pulse is shown in Figure 7d.

For a high charge density, the theoretical calculation [6] predicts that the total electric field in the plasma region can be reduced to zero. However, in order to interpret the observed reverse current as shown in Figures 2b, 3a, 4ab, 5a and 6ab, it requires $|E_i| > E$, namely, the effective total field is against the applied field so that the electrons in the plasma region move toward the cathode. The current reverse may couple with the external circuit. To understand this phenomenon, it requires more theoretical and experimental analysis which will be pursued in the near future.

The magnitude of the electron conduction current gives information for the electrons leaked from the plasma. And, the pulse duration indicates the decay time of plasma in an external field. We derive these information from our observed data below.

A. Dependence of Leakage Electrons on n_e/E

For a low charge density, the space charge effect is negligible, and the electron drift velocity is a constant. Thus, the electron conduction current can be derived from Equation (2) as

$$i = e N_e W/D \tag{4}$$

where N_e is the total electrons initially produced by laser ionization. For a high charge density, the electrons inside the plasma ball are motionless as soon as the space-charge-induced field cancels out the applied fields. Only the leakage electrons between the plasma front and the anode contribute to the conduction current. Thus, the electron conduction current reduces to

$$i(t) = e N_q(t) W/D \tag{5}$$

where $N_q(t)$ is the number of leakage electrons as a function of time.

We determine the number of electrons from the measured electron conduction current using Equation (4) or (5). For a low initial electron density, the N_e determined from the electron conduction current agrees with the value calculated from the two-photon-ionization formula (Equation (1)) using the laser energy and the trimethylamine concentration measured. This good agreement ensures that we can certainly determine the initial electrons of high density from the calculation, although the space charge effect may prevent us from measuring it experimentally.

For a high charge density, the electron drift velocity W is less

defined, because the electric field is greatly distorted by the space-charge-induced field. As shown in Figure 7d, the effective electric field in the region from the plasma front to the anode is higher than the applied field, so the effective W value is expected to be higher than the one measured at the applied field. However, for the region of E/N studied, the electron drift velocity is not so sensitive to the variation of E/N [19]. Thus, for a first approximation, we take the W value measured at the applied E/N for the calculation of $N_q(t)$ from Equation (5). The ratios of N_q/N_e are plotted as a function of n_e/E in Figure 8 where N_q is measured at the pulse peak and N_e is calculated from the laser energy and the trimethylamine concentration. The N_q value represents the total number of conduction electrons leaking out from the plasma. At a low charge density, N_q will equal to N_e, so the ratio will approach to 1. At a high charage density, the electrons inside the plasma are locked, so N_q represents the maximum electrons leaking from the plasma, namely, N_q/N_e represents the fraction of leakage electrons.

The data shown in Figure 8 were measured at three nitrogen pressures of 208.4, 432.5 and 647.5 torr. The laser size was fixed at 1.8x0.6 cm^2 passing the central region of the plates separated at 4 cm. The trimethylamine was fixed at 18 mtorr. The laser energies varied in the range of 4.4 - 9.4 mJ/pulse, corresponding to the initial charge densities of (1 - 4.4) x 10^9 cm^{-3}. The applied field varied in the range of 7 - 720 V/cm.

It is of interest to compare the measured data with the theoretical calculation of Morrow and Lowke [6]. At $n_e/E = 9x10^2$ e/V $\cdot$ cm^2, the calculated electron motion is free from the space charge

effect, so the N_q/N_e ratio is equal to 1. At $n_e/E = 4.5 \times 10^6$ e/V • cm^2, the space charge effect takes place, the calculated N_q/N_e value estimated from Fig. 2c of Reference 6 at 60 ns after the charges being produced is 0.26. This 60 ns corresponds the electron conduction current reaching the peak which is used for determining our data shown in Fig. 8. At $n_e/E = 9 \times 10^7$ e/V • cm^2, the space charge effect is very large so that the electrons inside the plasma become motionless. The calculated N_q/N_e value estimated from Figure 2e of Reference 6 at 40 ns after the charges being produced is 0.07. These calculated values are also plotted in Figure 8 for comparison. The agreement is suprisingly good, although the uncertainties inherent in both experimental measurements and theoretical calculations are high.

The applied fields and charge densities used in the theoretical calculation are two or three orders of magnitude higher than the values used in this experiment. However, the N_q/N_e values in terms of n_e/E agree very well, indicating that the n_e/E is a good parameter for describing the electron leakage from plasma under an applied field. The N_q/N_e data measured at different N_2 pressures are about the same for each n_e/E value (within experimental uncertainty) as shown in Figure 8. These results suggest that the electron leakage probability is a single function of n_e/E. This assertion could be reasoned below.

The electron leakage from the plasma will stop if the effective electric field inside the plasma is reduced to zero, namely, the applied field E is cancelled out by the space-charge-induced field E_i. The E_i is proportional to the leakage electons, i.e.,

$$E_i(z,t) = g(z,t)\, N_q(t) \qquad (6)$$

where $g(z,t)$ is a geometric function that converts the space charges into electric field, for example, $g(z,t) \sim \frac{1}{\epsilon A}$ if $N_q(t)$ distributes uniformly over a large plane of area A.

At the time of pulse peak, the E_i almost reaches the level of E so that

$$N_q = E/g \qquad (7)$$

and thus,

$$N_q/N_e \sim (n_e/E)^{-1} \qquad (8)$$

This expectation is consistent with the data that at $n_e/E > 10^8$ e/V • cm^2 the slope of $\ln(N_q/N_e)$ versus $\ln(n_e/E)$ approaches -1. This good agreement in turn further supports that the n_e/E is a useful parameter for the characterization of the electron leakage from plasma under an external electric field.

B. Dependence of Pulse Duration on n_e/E

As shown in Figures 2-6, the electron conduction current may reduce to zero. The time duration, Δt, from the laser pulse to the first zero current is much shorter than the electron drift time from the plasma front to the anode. The zero current is not caused by electron loss to the anode, but by the zero average electron drift velocity, namely, the electron drift velocity in the plasma front to

anode region is cancelled out by the electron drift velocity in the plasma region. As soon as the electron drift velocity is reduced to zero or reversed, the plasma will decay out, thus the pulse duration of the electron conduction current is a measure for the plasma decay time. The pulse duration decreases as n_e/E increases as shown in Figure 9. These data are obtained from the same set of data used for determining the N_q/N_e ratios. The pulse duration is likely a function of n_e/E, which is reasoned below.

When the charges are initially produced by the laser ionization, all the electrons will drift by the applied field. The motion of electrons in the plasma region will start to stop when the effective electric field falls to zero, i.e., when $E_i = -E$. At this time, the electrons that move away from the plasma are approximated by

$$q = Aen_eW \quad \Delta t \tag{9}$$

thus combining with Equation (6), we have

$$E = |E_i| = gAen_eW \quad \Delta t \tag{10}$$

or

$$\Delta t \propto \left(\frac{n_e}{E}\right)^{-1} \tag{11}$$

This equation suggests that the plasma decay time is a function of n_e/E, and the decay time will decrease with increasing n_e/E. This expectation agrees qualitatively with the data shown in Figure 9, in

which the observed pulse duration decreases with increasing n_e/E. The Δt value of 200 ns in the high n_e/E region is the limit of the electronics response time. The observed slope of ln (Δt) versus ln (n_e/E) is much smaller than the value of -1 as expected from Equation (11). This indicates that the effect of the pulse duration by space charge may be more complicated than this simple model described. Another reason for the small slope may be caused by the long electronics response time, because the pulse durations in the high n_e/E region may in fact be shorter than the Δt measured. More studies on the plasma decay time are desirable.

The plasma frequencies for the initial charge densities are in the range of $(1-3)\times10^8$ s^{-1}. These frequencies are too fast to be observed by the slow electronics response of the present experiment. At this moment the contribution of the plasma oscillation to the observed current behavior is not known.

V. CONCLUSION

The electron motion in an applied field is studied by monitoring the electron conduction current with an external circuit. The electron conduction current pulses are observed at various laser energies, trimethylamine concentrations, applied fields, N_2 and Ar pressures. It is observed that the electron motion is seriously affected by the space charge. The space-charge-induced field can be so large that it may totally cancel out or even be higher than the applied field in the plasma region. The electron conduction current may thus be stopped or even forced to reverse its direction by the

space-charge-induced field.

Taking the advantage of the initial charges of ions and electrons being uniformly distributed, the probability for the electron leakage from plasma and the plasma decay time are studied in this experiment. The theoretical calculation of the space charge effect by Morrow and Lowke [6], who use similar initial conditions as the present experiment, is adopted as a basis for the analysis of the data observed.

It is found that the ratio of n_e/E is a good parameter for the characterization of the electron leakage current and the plasma decay time. For high n_e/E, the electron leakage probability is inversely proportional to n_e/E as expected from a simple model. The observed electron leakage probabilities are consistent with the theoretical calculation of Morrow and Lowke [6].

The plasma decay time is measured by the pulse duration of electron conduction current. It is found that the decay time decreases with increasing n_e/E. However, the decrease rate is much slower than that expected from a simple model. The discrepancy may be in part caused by the slow electronics response, from which the true pulse duration may not be obtaiend. Further investigation on this subject is interested.

The duration of electron conduction is one of the important parameters required for designing some discharge switches with specified characteristics, such as high repetition rate switches and opening switches. The pulse duration could be shortened by the space charge effect observed in this experiment. The data shown in Figure 9 could be used for estimating the pulse duration affected by the

space charge in various discharge switches.

ACKNOWLEDGEMENT

One of the authors (LCL) wishes to thank Dr. Martin Gunderson of the University of Southern California for useful discussions. The critical comment received from Dr. Gail A. Massey of San Diego State University is appreciated. The authors also thank Dr. E. R. Manzanares, Dr. J. B. Nee, Dr. M. Suto, and Dr. W. C. Wang of our laboratory for useful suggeestions and discussions. The technical assistance received from Mr. F. C. Clark and Mr. J. S. Lai is appreciated. This research is sponsored by the Air Force Office of Scientific Research, Air Force Systems Command, USAF, under Grant No. AFOSR-82-0314.

REFERENCES

[1] A. J. Davies, C. J. Evans and F. L. Jones, "Electrical Breakdown of Gases: the Spatio-Temporal Growth of Ionization in Fields Distorted by Space Charge", Proc. Roy. Soc., Vol. A281, p. 164-183, 1964.

[2] A. J. Davies, C. S. Davies, and C. J. Evans, "Computer Simulation of Rapidly Developing Gaseous Discharges", Proc. IEE, Vol, 118, p. 816-823, June 1971.

[3] A. J. Davies, C. J. Evans and P. M. Woodison, "Computation of Ionization Growth at High Current Densities", Proc IEE, Vol. 122, p. 765-768, July 1975.

[4] A. J. Davies, C. J. Evans, P. Townsend and P. M. Woodison, "Computation of Axial and Radial Development of Discharges Between Plane Parallel Electrodes", Proc IEE, Vol. 124, p. 179-182, Feb. 1977.

[5] L. E. Kline, "Calculations of Discharge Initiation in Overvolted Parallel-Plane Gaps", J. Appl. Phys. Vol. 45, p. 2046-2054, 1974.

[6] R. Morrow and J. J. Lowke, "Space-Charge Effects on Drift Dominated Electron and Plasma Motion", J. Phys. D: Appl. Phys., Vol. 14, p. 2027-2034, 1981.

[7] A. A. Doran, "The Development of a Townsend Discharge in N_2 up to Breakdown Investigated by Image Converter, Intensifier and Photomultiplier Techniques", Z. Physik. Vol. 208, p. 427-440, 1968.

[8] R. T. Waters, T. E. S. Rickard and W. B. Stark, "The Structure of the Impulse Corona in a Rod/Plane Gap I. The Positive Corona", Proc. Roy. Soc. Lond. Vol. A315, p. 1-25, 1970.

[9] I. D. Chalmers, H. Duffy and D. J. Tedford, "The Mechanism of Spark Breakdown in Nitrogen, Oxygen and Sulphur Hexafluoride", Proc. R. Soc. Lond. Vol. A329, p. 171-191, 1972

[10] L. C. Lee and W. K. Bischel, "Two-Photon-Ionization Coefficients of Propane, 1-Butene, and Methylamines", J. Appl. Phys. Vol. 53, p. 203-207, January 1982.

[11] E. E. Kunhardt, "Electrical Breakdown of Gases: the Prebreakdown Stage", IEEE Trans. Plasma Sci., Vol. PS-8, p. 130-138, Spet. 1980.

[12] E. E. Kunhardt and W. W. Byszewski, "Development of Overvoltage Breakdown at High Gas Pressure", Phys. Rev. A, Vol. 21, p. 2069-2077, June 1980.

[13] A. H. Guenther and J. R. Bettis, "A Review of Laser-Triggered Switching", Proc. IEEE, Vol. 59, p. 689-697, April 1971.

[14] A. H. Guenther and J. R. Bettis, "The Laser Triggering of High-Voltage Switches", J. Phys. D: Appl. Phys. Vol. 11, p. 1577-1613, 1978.

[15] M. Gundersen, private communication, 1984.

[16] L. G. H. Huxley and T. W. Crompton, "The Diffusion and Drift of Electrons in Gases", John Wiley, New York, p. 301, 1974.

[17] J. M. Meek and J. D. Craggs, Ed., "Electrical Breakdown of Gases", John Wiley, Chichester, p. 80, 1978.

[18] L. G. Christophorou, "Atomic and Molecular Radiation Physics", Wiley-Interscience, London, p. 431, 1971.

[19] J. Dutton, "A Survey of Electron Swarm Data", J. Phys. Chem. Ref. Data, Vol. 4, p. 577-856, 1975.

FIGURE CAPTIONS

FIGURE 1 Schematic diagram for the experimental apparatus.

FIGURE 2 The electron conduction pulses produced by two-photon-ionization of (a) 4 mtorr and (b) 30 mtorr of trimethylamine in 420 torr N_2. The laser energy is about 9.8 mJ/pulse and the laser beam cross section at the central region of electrodes is 1.8x0.6 cm^2. The applied field is 69 V/cm.

FIGURE 3 The electron conduction pulses produced at laser energies of (a) 7.8 mJ/pulse and (b) 15 mJ/pulse. The laser beam size is 1.8x0.6 cm^2 at the central region of electrodes. The trimethylamine pressure is 18 mtorr and the N_2 pressure is 418 torr. The applied field is 686 V/cm.

FIGURE 4 The electron conduction pulses produced at beam sizes of (a)1.1x0.6 cm^2 and (b) 1.8x0.6 cm^2. The laser energy per unit area is nearly the same for both cases (14.2 mJ/cm^2 and 16.1 mJ/cm^2 for (a) and (b), respectively). The trimethylamine presssure is 10 mtorr and the N_2 pressure is 417 torr. The applied field is 686 V/cm.

FIGURE 5 Electron conduction pulses at applied fields of (a) 143 V/cm and (b) 286 V/cm. The laser energy is fixed at 6.2 mJ/pulse and the beam size is 1.8x0.6 cm^2. The trimethylamine pressure is 18 mtorr and the N_2 pressure is 433 torr.

FIGURE 6 The electron conduction pulses using buffer gases of (a) N_2 and (b) Ar. The laser energy is fixed at 8.8 mJ/pulse, and the beam size is 3x0.6 cm^2. The trimethylamine pressure is 18 mtorr and the nitrogen pressure is 408 torr. The applied field is 134 V/cm.

FIGURE 7 The effective electric field acting on the plasma. (a) electrons and ions produced by two-photon-ionization of trimethylamine with ArF laser photons. (b) the applied electric field. (c) the space-charge-induced field at the plasma front and tail. (d) the total effective electric field.

FIGURE 8 The ratios of the leakage electrons, N_q, to the initial electrons, N_e, versus n_e/E. The data are taken at the N_2 pressures of 208.4 torr (●), 432.5 torr (▲), and 647.5 torr (▼). The theoretical results (0) of Morrow and Lowke are plotted for comparison.

FIGURE 9 The time durations Δt of electron conduction pulses at various n_e/E values. The pulse duration is measured from the laser pulse to the first zero of the conduction current. The data are taken at the N_2 pressures of 208.4 torr (●), 432.5 torr (▲) and 647.5 torr (▼). The original data are the same for both Figures 8 and 9.

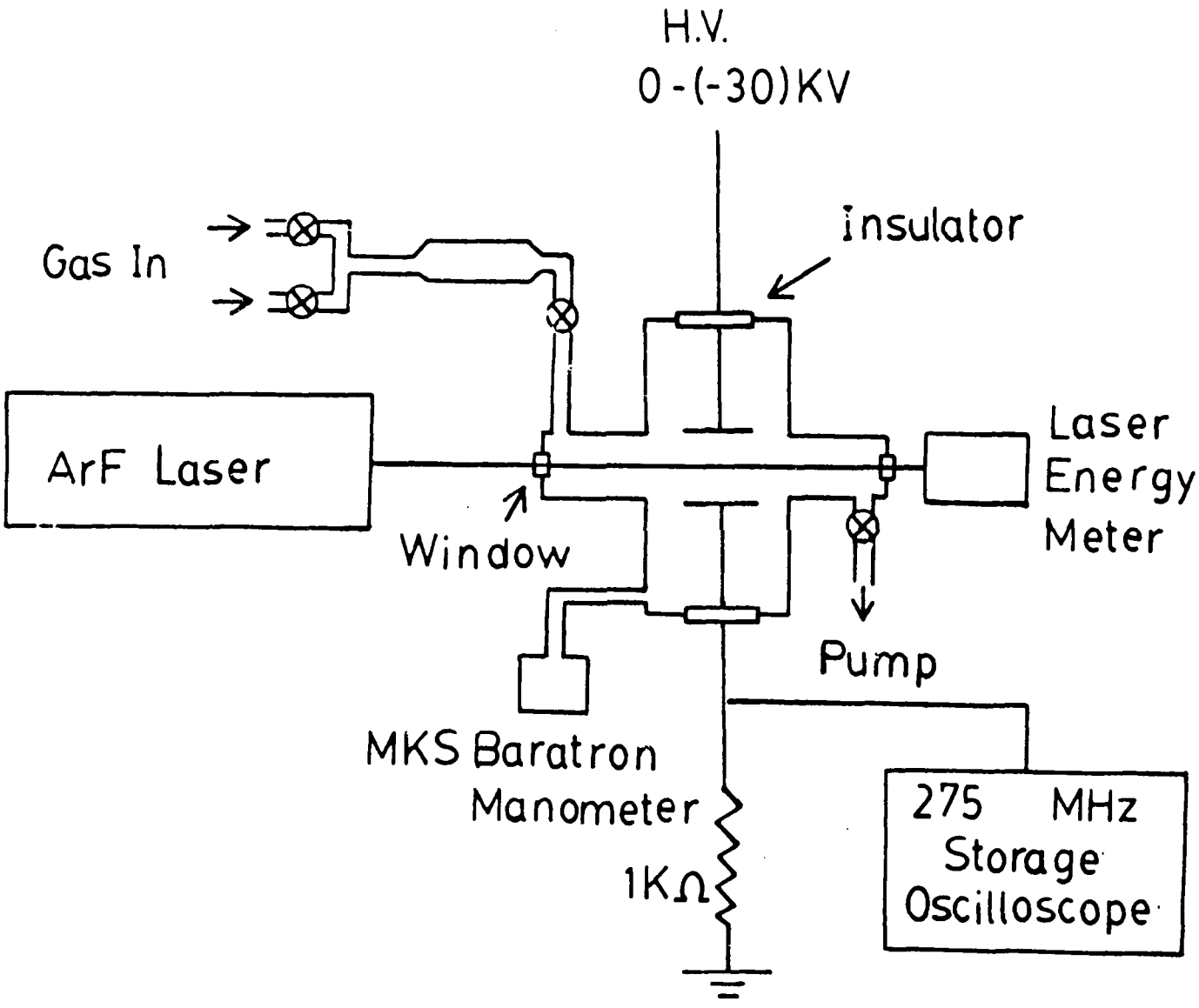
H.V.
0-(-30)KV
Gas In
Insulator
ArF Laser
Laser
Energy
Meter
Window
Pump
MKS Baratron
Manometer
1KΩ
275 MHz
Storage
Oscilloscope

Fig. 1

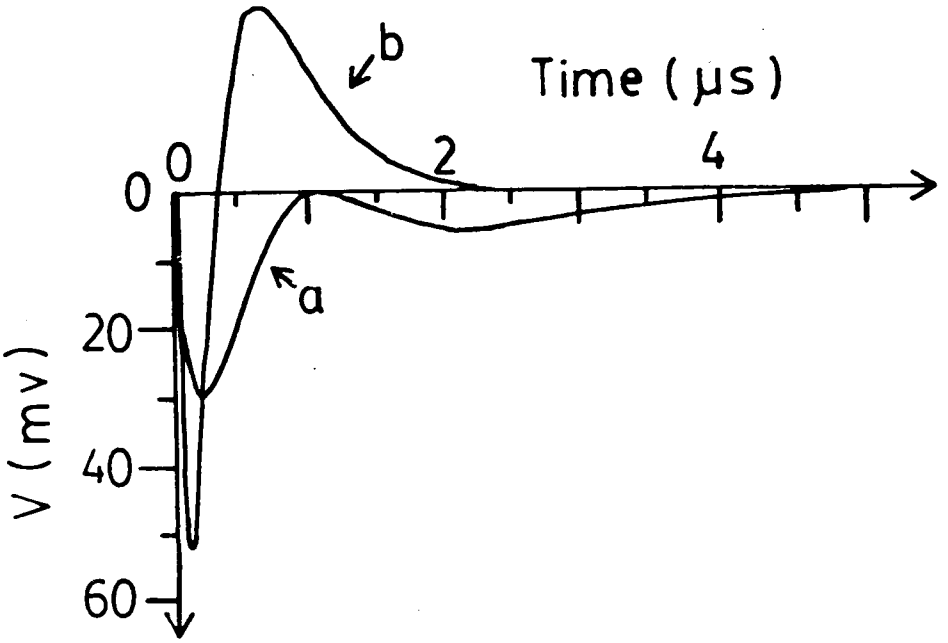

Fig. 2

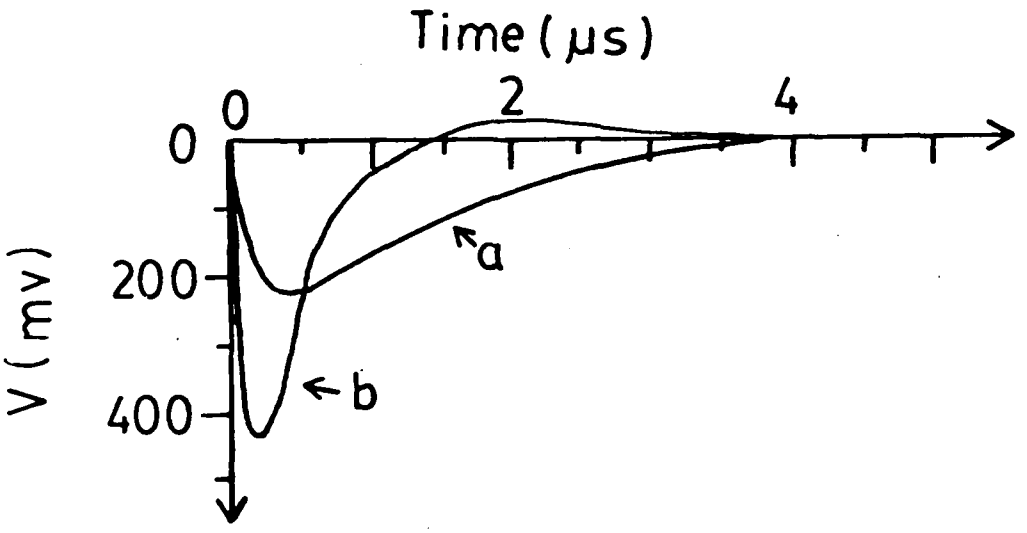

Fig. 3

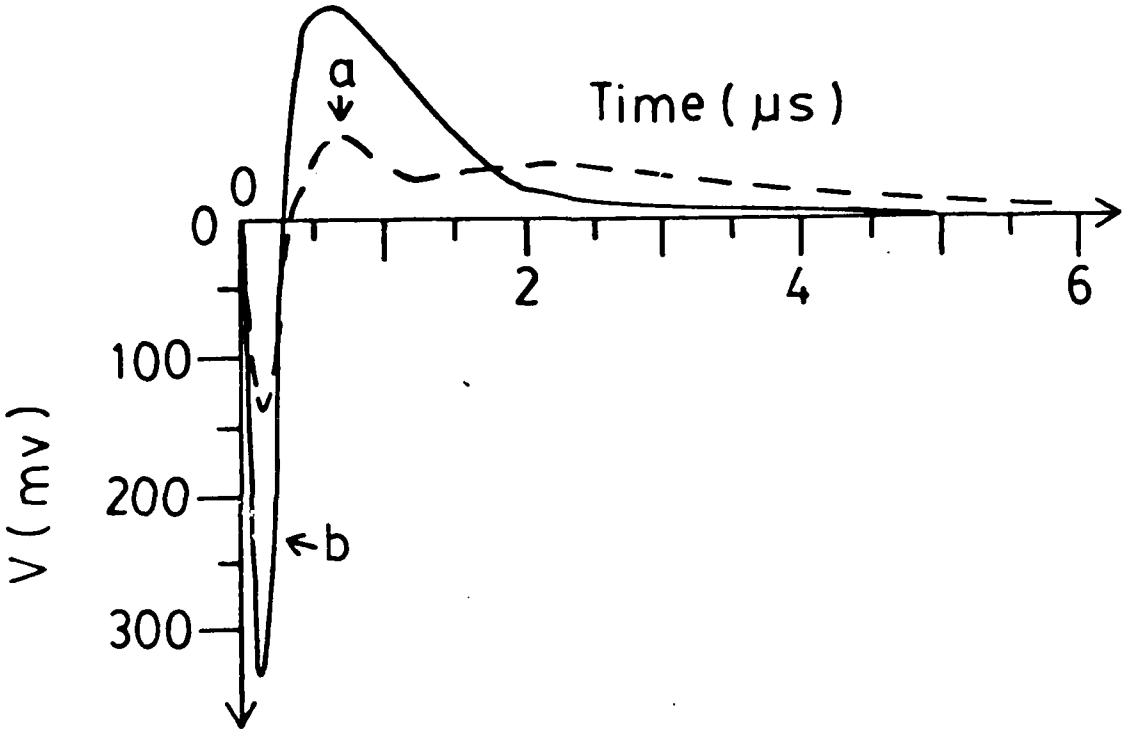

Fig. 4

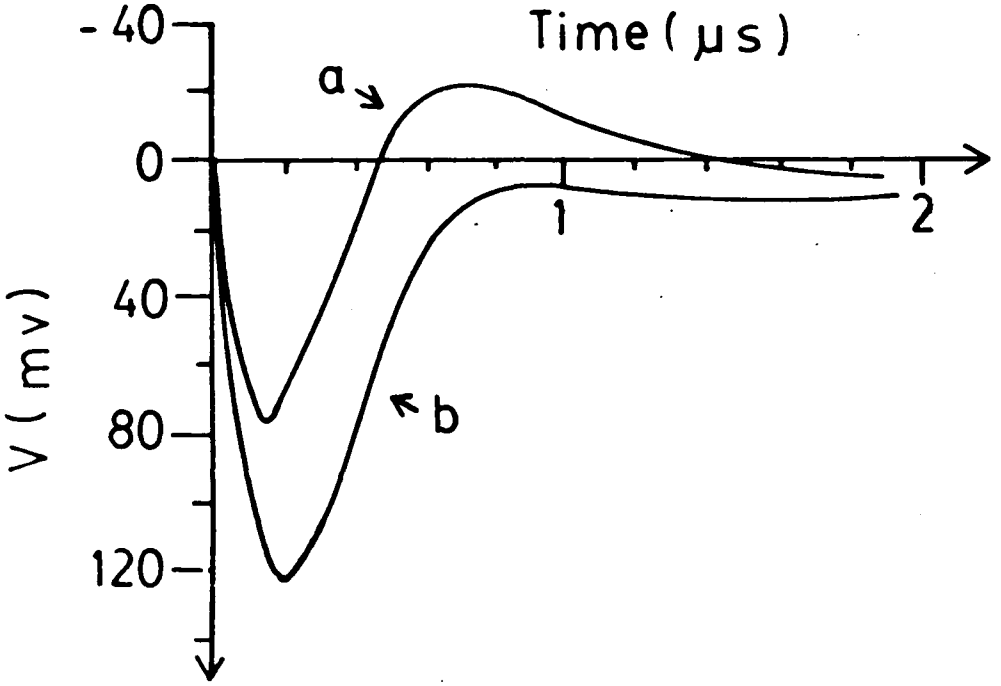

Fig. 5

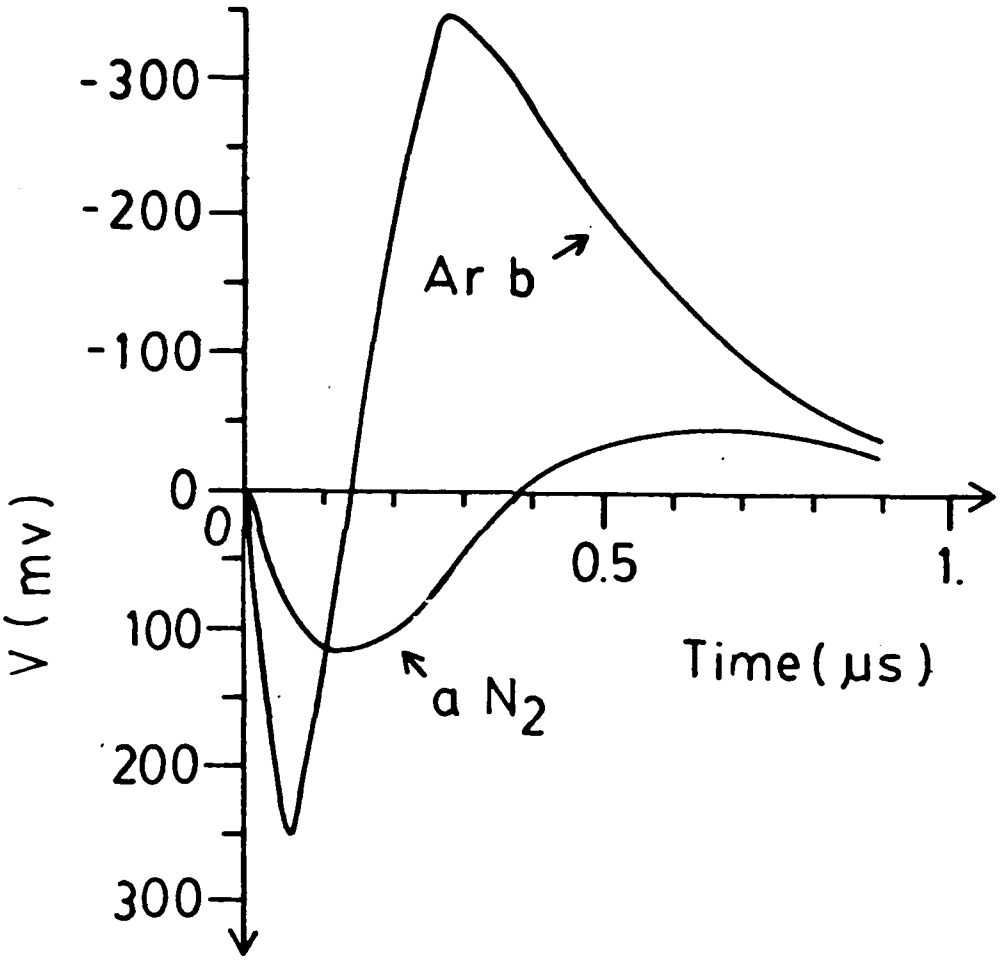

Fig. 6

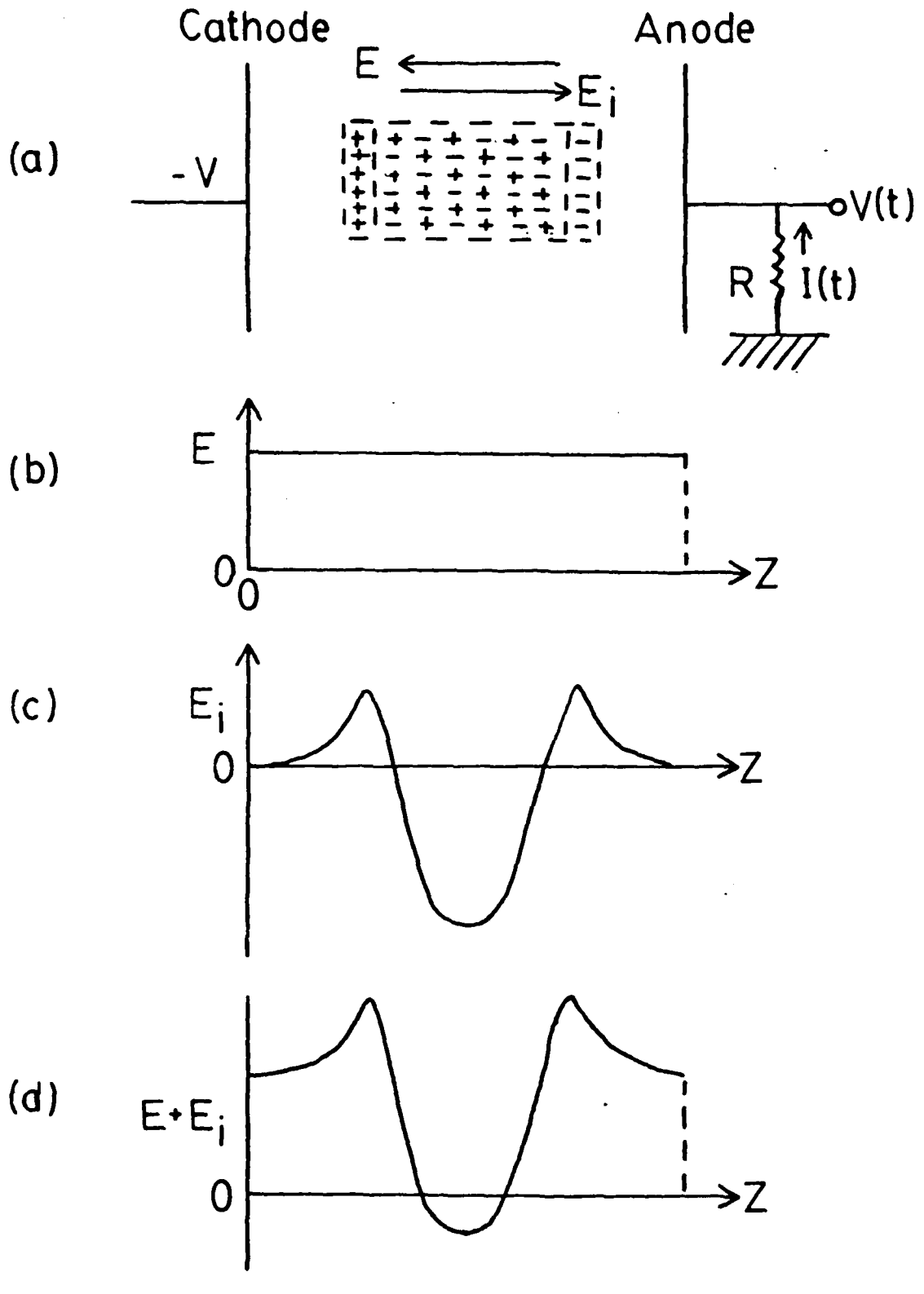

Fig. 7

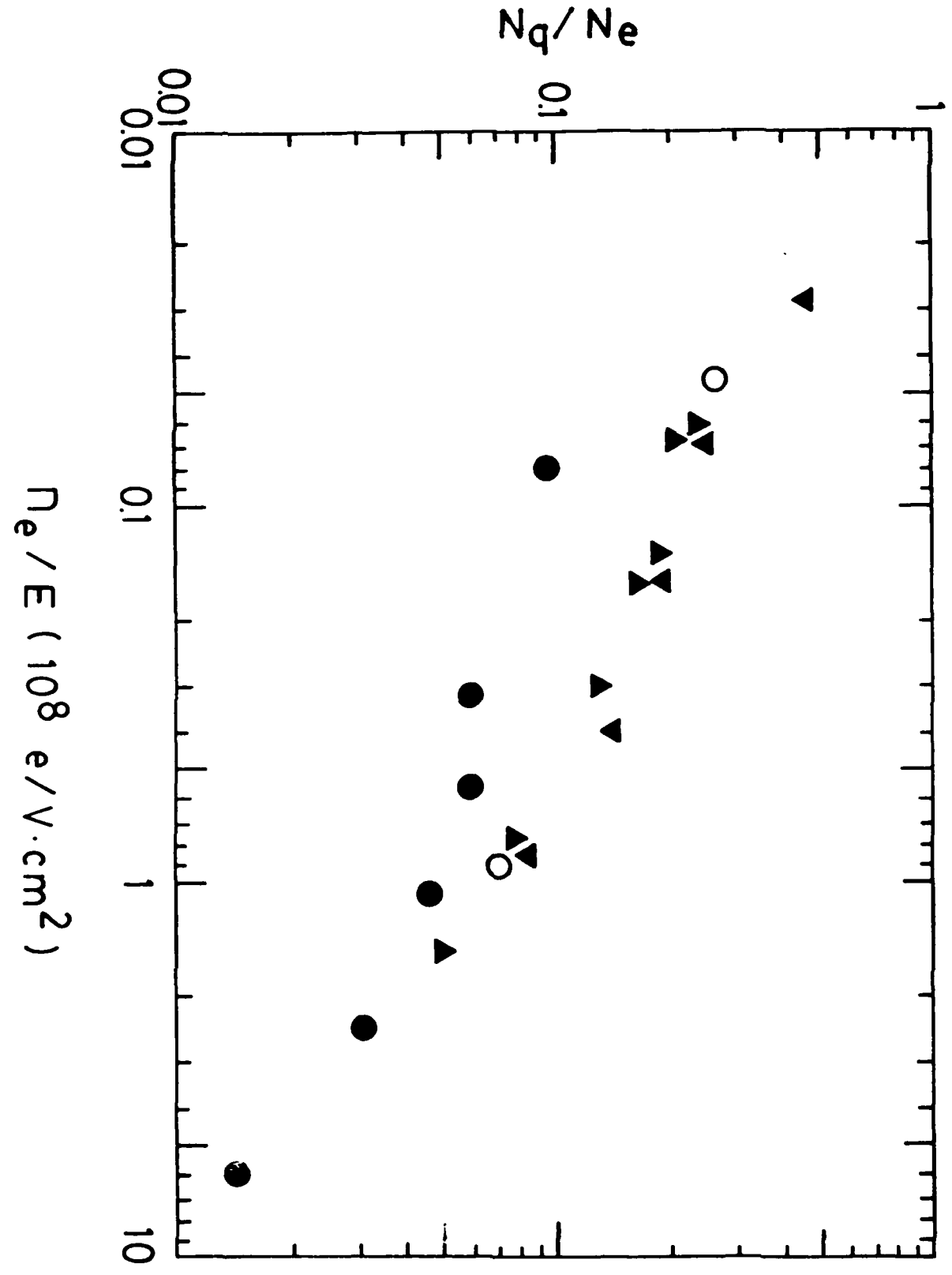

Fig 8

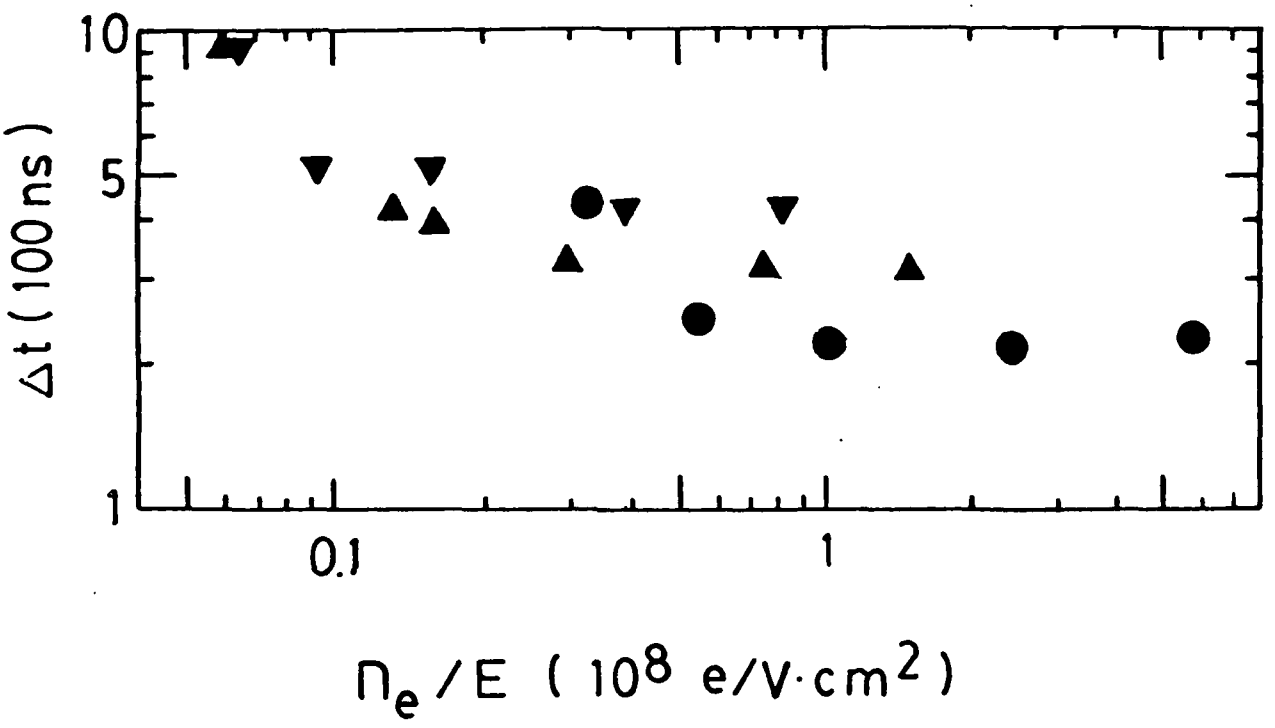

Fig. 9

APPENDIX D

Longitudinal Diffusion Coefficients of Electrons in Ar at High E/N

LONGITUDINAL DIFFUSION COEFFICIENTS OF ELECTRONS IN Ar AT HIGH E/N

F. Li and L. C. Lee
Department of Electrical and Computer Engineering
San Diego State University
San Diego, CA. 92182-0190

ABSTRACT

The parameters for the diffusion of electron swarm in Ar were measured using a parallel-plate drift-tube apparatus. Electron swarms were produced by irradiation on cathode plate using an ArF laser. The electron motion between electrodes was monitored by the transient anode current. Swarm parameters were obtained from the transient waveform analyzed with the Boltzmann transport equation. The electron drift velocity and the electron ionization coefficient obtained from this experiment are comparable with the values measured by other techniques. The longitudinal diffusion coefficients measured in this experiment for E/N in the 30-300 Td region agree with theoretical calculation. At E/N = 100 Td, the product of the Ar density and the longitudinal electron diffusion coefficient is 3×10^{22} $cm^{-1}s^{-1}$.

PACS Index: 52.25 Fi, 52.20 Fs, 34.80 Bm, and 51.50 + V

I. INTRODUCTION

The importance of knowing the electron swarm parameters of various gases has been emphasized in several recent papers (Kücükarpaci et al 1981, Fletcher 1981, Christophorou et al 1982a, and Schoenbach et al 1983). The information could be used for modeling modern electronic devices such as glow discharges, gas laser discharges, and laser-controlled discharge switches.

The electron motion in a gas is characterized by the electron drift velocity and the coefficients of electron diffusion, attachment, detachment, excitation, ionization, and recombination. The collective coupling between these parameters is so complicated that our understanding of this subject is far from complete. The electron motion in inert gases is relatively well studied, because it is somewhat easier to analyze than the case of other complex molecules. Ar is the kind of gas whose electron swarm parameters are extensively studied in both experiments (Nielsen 1936, Engelhardt and Phelps 1964, Pack and Phelps 1961, Kruithof 1940, and Wagner et al 1967), and theorectical calculations (Lowke and Park, Jr. 1969, Ismail and Gaiamoon 1979, Sakai et al 1977, and Tagashira et al 1977).

Among all electron swarm parameters of Ar, the electron drift velocity is most well studied. In contrast, the electron diffusion coefficient is little known. Wagner et al (1967) have measured the longitudinal diffusion coefficient D_L at E/N lower than 4 Td using the time of flight technique. However, there are no experimental data at high E/N. Sakai et al (1977) and Tagashira et al (1977) have

calculated some D_L values at high E/N employing Monte Carlo techniques as well as numerical solutions of the Boltzmann equation. The calculated D_L values are compared with our measurements in the E/N = 30-300 Td region.

There are several experimental methods (Huxley and Crompton 1974) used for measuring electron swarm parameters, such as the steady-state and the pulsed Townsend experiments as well as the time of flight technique. The measured electron swarm parameters may depend upon the type of experiments as suggested by Sakai et al (1977) and Tagashira et al (1977). Our experiment is in principle similar to the pulsed Townsend experiment. Electron swarms were produced by irradiating cathode with ArF laser photons. The electron swarm motion between electrodes was monitored by a transient voltage signal that was analyzed to obtain electron swarm parameters.

II. EXPERIMENT

The experimental setup for a parallel-plate drift tube apparatus is shown in Figure 1. The electrodes were made from stainless steel plates of 5 cm in diameter and their separation could be varied in the 0-10 cm range. A negative high voltage was applied to the cathode. A resistor of R = 50 Ω connected the anode to the ground. The voltage across the resistor was monitored by a 275 MHz storage oscilloscope (Hewlett-Packard model 1727A). A 100 pF capacitor across the resistor was used to attenuate high frequency RF noise produced by the spark gap discharge of excimer laser. The circuit RC time constant of ~10 ns is much shorter than the electron drift time

from the cathode to the anode. The RF noise was further reduced using an oscilloscope bandwidth of a rise time about 17 ns.

The Ar gas of purity better than 99.998% was introduced into the gas cell without further purification. The gas in the cell was slowly pumped out by a Roots blower pump, and the gas pressure was kept constant by supplying with fresh gas. The flow system will reduce the impurity that may release from walls and electrodes. An MKS Baratron was used to measure the gas pressure. The transient signal was taken at a stable pressure that fluctuated less than $\pm$1% of its average value in one minute.

The initial electron swarm was produced by irradiating the cathode with ArF excimer laser photons (Lumonics Model 816S). A similar electron production method was used by Christophorou et al (1982b) to study the electron motion in NH_3. In their case, the photocathode was coated with palladium to increase electron emission. However, in the present measurements the steel cathode produces sufficient electrons to give measureable signals, so it is not coated.

The laser pulse width was about 10 ns, which was smaller than the typical transient voltage signal of about 200 ns. The initial electrons were drifted toward the anode under an applied electric field. The overall pulse width of the laser pulse and the system response was about 20 ns, as checked by the laser irradiation on the cathode in vacuum. Each single transient voltage signal was captured and stored in the oscilloscope. The transient signal was later taken by photography for a permanent record.

AD-A149 535 ELECTRON PRODUCTION ELECTRON ATTACHMENT AND CHARGE RECOMBINATION PROCESS I.. (U) SAN DIEGO STATE UNIV CA DEPT OF ELECTRICAL AND COMPUTER ENGIN.. L C LEE

2/2

UNCLASSIFIED 17 SEP 84 AFOSR-82-0314 F/G 7/4 NL

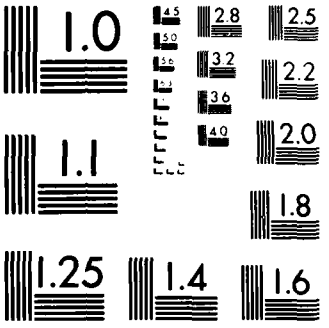

III. RESULTS AND DISCUSSION

A. Data Analysis

The transient voltage signals at various E/N and pressures for an electrode separation of h = 2.3 cm are shown in Figure 2. At low E/N, the voltage signals last several hundred ns, and then gradually decrease to zero. As E/N increases, a hump develops at the later time. The higher the E/N, the earlier the hump occurs. The transient voltage is fitted by a theoretical modeling as follows.

The electron density, n, between electrodes can be described by the Boltzmann transport equation (Huxley and Crompton 1974) as,

$$-\frac{\partial n}{\partial t} + D\left(\frac{\partial^2 n}{\partial x^2} + \frac{\partial^2 n}{\partial y^2}\right) + D_L \frac{\partial^2 n}{\partial z^2} - W \frac{\partial n}{\partial z} + \alpha_i n = 0 \qquad (1)$$

where z is in the direction of the electric field, D and D_L are the transverse and longitudinal diffusion coefficients, W is the electron drift velocity, and α_i is the ionization rate for electron impact on Ar. α_i is related to the Townsend primary ionization coefficient, α, by

$$\alpha_i = \alpha\,(W - \alpha D_L) \qquad (2)$$

This relation takes into account the diffusion effect for the mean electron drift (Hurst and Liley 1965, Crompton 1967).

Since the sizes of electrodes are much larger than the electrode separation h, we may consider that the electric field between

electrodes is nearly uniform. The solution for the electron density, (Huxley and Crompton 1974) which satisfies the boundary conditions of n=0 at z=h and n≈0 at z=0, is

$$n = \frac{N_0 \exp(-\rho^2/4Dt)}{(4\pi Dt)(4\pi D_L t)^{\frac{1}{2}} Wt} \left\{ z \exp\left[-\frac{(z - Wt)^2}{4D_L t}\right] + (z - 2h) \exp\left[-\frac{(z - Wt)^2 + 4h(h - z)}{4D_L t}\right] \right\} e^{\alpha_i t} \quad (3)$$

where $\rho^2 = x^2 + y^2$, and N_0 is the initial electrons produced by excimer laser photons. This formula has been used to analyze the electron density for the type of pulsed Townsend experiment. This experiment is very similar to the pulsed Townsend experiment, except for the initial electron pulse being shorter and the E/N being higher in the present measurement.

The electron motion will induce an anode current equal to (Raether 1964),

$$i(t) = \frac{1}{h} \int_0^h eW dz \int_0^\infty n \, 2\pi\rho d\rho \quad (4)$$

where the electrode sizes are assumed to be very large.

The transient voltage is thus given by

$$V(t) = i(t)R = \frac{N_0 eR}{2ht(\pi D_L t)^{\frac{1}{2}}} \left\{ \int_0^h z \exp\left[- \frac{(z - Wt)^2}{4D_L t} \right] dz + \int_0^h (z - 2h) \exp\left[\frac{hW}{D_L} - \frac{(z - 2h - Wt)^2}{4D_L t} \right] dz \right\} e^{\alpha_i t} \quad (5)$$

There are four parameters involved in Eq. (5), namely, N_0, W, D_L, and α_i. These parameters are obtained by a best least square fit of the transient voltage waveform with Eq. (5). The fitting procedure starts with arbitrary values of W and D_L, and the N_0 and α_i are simultaneously adjusted to best fit the waveform with Eq. (5). The standard deviation of the best fit values from the experimental data is calculated for each set of W and D_L. The W and D_L values are then varied in a pre-selected but arbitrary range. For all sets of W and D_L, the standard deviations are calculated and compared. It is found that for the smallest standard deviation the W and α values are generally consistent with the published data within 20% (see Section B and C).

An example for the comparison of experimental data with the best fit calculation is shown in Figure 3. The data were taken at E/N = 89.9 Td (1 Td = 10^{-17} V cm^2), h = 2.3 cm and Ar pressure of 2.04 torr. Note that the initial spike of Figure 3 is a property of the integral function of Eq. (5). The initial electrons back diffusion to the

cathode will enhance the spike. This spike has been observed long ago by Hornbeck (1951) in the pulsed Townsend experiment. This spike also serves as an indication of the initial time, t = 0, when laser pulse strikes on the cathode.

Whealton et al (1977) have developed a new model to describe the electron motion in parallel-plate drift-tube experiments. We have also used the simplified equation [Eq. (3.5) in Whealton et al (1977)] to analyze the transient voltage waveform. The parameters obtained from this new model are consistent with the results obtaied from Eq. (5). However, the sensitivity of fitting the waveform by varying D_L from the best fit value is low, indicating that the simplified equation is not adequate. It is expected that the more elaborated equation [Eq. (3.3) in Whealton et al (1977)] will fit our data better. The electron transient current calculated by the Monte Carlo technique as illustrated in Figure 9 of Whealton et al (1977) is very similar to the transient pulses observed in this experiment. However, some of the parameters used in the theoretical model are not clearly defined in our experiment. It will introduce more uncertainties if we freely adjust the parameters. Thus, we adopt Eq. (5) for analyzing the transient voltage waveform. The results for the swarm parameters obtained are described below.

B. Electron Drift Velocity

The electron drift velocity is extensively studied in electron swarm experiments. The data of the electron drift velocity are more reliable than other electron swarm parameters. In this experiment, the W values are obtained from the best least square fit of transient

waveforms with an arbitrary choice of initial W and D_L values. The W values obtained are in general consistent with 20% of the published data of Jager and Otto (1962) and Brambring (1964) as shown in Figure 4.

C. Ionization Coefficient

The α_i values are determined from the best least square fit of transient waveforms. They are used to calculate the Townsend primary ionization coefficients, α, using Eq. (2). The α/N values obtained at Ar pressures of 1, 2, and 4 torr are plotted in Figure 5 for various E/N. The previous data of Kruithof (1940) are plotted in Figure 5 for comparison. The current results are in general consistent with Kruithof's data.

D. Longitudinal Diffusion Coefficient

The longitudinal diffusion coefficient of electrons in Ar at high E/N are very little known. In order to ensure the reliability of the electron diffusion coefficient, we fix the electron drift velocity and the ionization coefficient in the waveform analysis as the averaged values shown on the solid lines of Figures 4 and 5, respectively. The longitudinal diffusion coefficients are obtained from the best least square fit of transient voltage waveforms with D_L as variable. In this case, the N_0 values are obtained from normalizing the computed transient waveform with the experimental data. The variation of D_L is sensitive to the fitting similar to that of the W values. On the other hand, the variation of α_i is less sensitive to the fitting. The uncertainties for the D_L values caused by the

analysis are estimated to be within $\pm$ 30% of the given values.

The D_L values for various Ar pressures at E/N = 70 Td are shown in Figure 6, where the electrode separations are h = 1.1 and 2.3 cm. The error bar represents the standard deviation of several D_L values measured. The D_L values for h = 2.3 cm (Figure 6a) are higher than that of h = 1.1 cm (Figure 6b). Nevertheless, the dependences of D_L on Ar pressure are similar for both electrode separations. The D_L values decrease with increasing Ar pressure. For pressures larger than 3 torr, the D_L values are nearly constant. The data for each electrode separation can be approximately represented by

$$D_L = \frac{\beta}{N} + \gamma \qquad (6)$$

where β and γ are constants.

The measured D_L does not approach to zero at high Ar pressure, so it is not the true electron diffusion coefficient. We may define the measured D_L value as an apparent diffusion coefficient. The first term in Eq. (6) is inversely proportional to the Ar density. This is likely caused by the collision of electron with Ar, which is the true electron longitudinal diffusion coefficient. The β data obtained at varioius E/N are shown in Figure 7, where the experimental data were taken at h = 1.1 cm. The error bar shown in figure 7 represents the fluctuation of D_L measured at different experiments. The true uncertainty of D_L may be as large as a factor of 2. There are no experimental data for the β values in the current E/N region. However, theoretical calculations are available as discussed below.

Tagashira et al (1977) have calculated the longitudinal electron diffusion coefficients of Ar at high E/N using both the Monte Carlo techniques and the numerical solutions of the Boltzmann equation. The swarm parameters for the pulsed Townsend experiment were calculated (Sakai et al 1977 and Tagashira et al 1977). Since the present experiment is in principle similar to the pulsed Townsend experiment, the present data are comparable with the calculated results. The diffusion coefficient calculated for the PT experiment (Tagashira 1977) plotted in Figure 7 for comparison. In their calculation only the diffusion caused by electron and Ar collision was considered. Their calculated ND_L values are equivalent with the β values measured in this experiment. As shown in Figure 7, the measurements agree with the theoretical calculations within experimental uncertainty. Considering the difficulties inherent in both experiments and theoretical calculations, this agreement is surprisingly good. These results indicate that the analysis method used here has a certain merit, although this analysis is only an approximate one. The data measured by Wagner et al (1967) at low E/N are also plotted in Figure 7 for reference.

At high Ar pressure, the first term in Eq. (6) becomes small, so the apparent diffusion coefficient D_L approaches constant, γ. The γ values shown in Fig. 6 are 5.6×10^5 and 1.2×10^6 cm^2/s for h = 1.1 and 2.3 cm, respectively. The constant may be somehow related to the width of the initial electron swarm. The work function for a clean iron film is about 4.5 eV (Cardwell 1953, Kobayashi and Kato 1959, Eastman 1970, Ueda and Shimizu 1972). The work function for the steel electrode used in this experiment is expected lower than that of clean iron, possibly in the range of 4 eV. The photoelectrons

produced by the 193 nm laser photons (6.4 eV) thus carry kinetic energy in the range of 0-2.4 eV. The electrons could have an initial velocity up to 10^8 cm/s that is one order of magnitude higher than the electron drift velocity. Ejection of these high energy photo-electrons into space may cause the initial width of the electron swarm larger than $W\Delta t$, where Δt is the laser pulse duration. Because of high electron kinetic energy, the initial width of electron swarm may not depend on the gas pressure. This initial width will result the γ term that does not depend on Ar pressure. The initial electron ejection process may be equivalent to the diffusive process, so its contribution to the total diffusion coefficient is additive.

Braglia and Lowke (1979) have concluded from their calculation that the diffusion coefficient will depend on the electrode position. The electrode effect is very complicated and difficult to estimate. This effect may have some contribution to the γ term. Furthermore, the ions produced by the electron ionization of Ar could modify the electric field and affect the swarm parameters near the anode. Although the space charge effect is estimated to be not serious in this experiment (discussed below), its effect on the diffusion coefficient is, however, difficult to assess.

E. Space Charge Effect

At high E/N, the effect of space charge on the measured parameters deserves a special concern. The magnitude of this effect can be estimated from the electron density between electrodes that can be determined from the transient voltage pulses shown in Figure

2. The electron densities estimated are about 10^7 cm^{-3} for low E/N and 10^8 cm^{-3} for high E/N. These electron densities are smaller than the limit of charge density (Raether 1964) of 10^9 cm^{-3} that may induce significant space charge effect. Thus, the space charge effect is not expected to play a significant role in this experiment.

To further show the D_L values being not affected by space charge, the transient voltage waveforms were observed at various laser intensities. The electron density increases with the laser intensity, so the space charge effect may appear at high laser intensity. The longitudinal diffusion coefficients obtained from the transient voltage waveforms at various laser intensities are shown in Figure 8. The data were taken at E/N = 70 Td, h = 2.3 cm, and Ar pressures of 3.7 and 5.4 torr. The laser intensity changes nearly an order of magnitude, but the D_L values do not avry more than the experimental uncertainty. The measred D_L values are thus not affected by the space charge.

At high gas pressure and high E/N, the charge density produced by an electron ionization of Ar may be so large that the space charge effect may play a significant role, and electron swarm parameters may be affected by the large space charge density. This problem will be further investigated.

F. Initial Electrons Produced by Excimer Laser

The number of electrons initially produced by laser irradiation on the cathode will be a function of the laser intensity, the natuare of cathode material, and the electric field. During the time of laser irradiation, the electrons ejected earlier from the cathode

will exert a repulsive force on those ejected later (Penning 1957). Also, the ejected electrons are pulled back by the image force of electrode. These forces will decrease the number of initial photo-electrons entering the space. These forces can be overcome by increasing the applied electric field. At high electric field, the electrons may gain enough energy to ionize Ar to produce slow moving positive ions that will neutralize electron charges near the cathode. Thus, the electrons will leave the cathode region more easily at high electric field. The initial electrons ejected into space are expected to increase greatly with increasing electric field.

The initial electron density $N_o e$ measured at various E/N for Ar pressures of 1 and 2 torr are shown in Figure 9. The laser intensity and the electrode separation were kept constant in the experiment. $N_o e$ increases with $(E/N)^{1.5}$. At a fixed E, $N_o e$ is proportional to $N^{1.5}$. The net result is that $N_o e$ is proportional to $E^{1.5}$ only, namely, the number of initial electrons are independent of the gas pressure studied. This result lends some support to previous assertion that the initial width of electron swarm is not affected by gas pressure, so the electron diffusion coefficient has a constant term added on.

ACKNOWLEDGEMENT

This research is sponsored by the Air Force Office of Scientific Research, Air Force Systems Command, USAF, under Grant No. AFOSR-82-0314.

REFERENCES

Braglia, G. L. and Lowke, J. J., 1979, J. Phys. D: Appl. Phys. 12, 1831-38.

Brambring, J., 1964, Z. Phys. 179, 539-43.

Cardwell, A., 1953, Phys. Rev. 92, 554-6.

Christophorou, L. C., Hunter, S. R., Carter, J. G., and Mathis, R. A., 1982 a, Phys. Lett. 41, 147-9.

Christophorou, L. C., Carter J. G., and Maxey, D. V., 1982 b, J. Chem. Phys. 76, 2653-61.

Crompton, R. W., 1967, J. Appl. Phys., 38, 4093-4.

Eastman, D. E., 1970, Phys. Rev., B2, 1-8.

Engelhardt, A. G., and Phelps, A. V., 1964, Phys. Rev., 133, A375-80.

Fletcher, J., 1981, Proc. of Second International Swarm Seminar, (Pergamon Press), pp 1-10.

Hornbeck, J. A., 1951, Phys. Rev., 84, 615-20.

Hurst, R. W., and Liley, B. S., 1965, Aust. J. Phys., 18, 521-40.

Huxley, L. G. H., and Crompton, R. W., 1974. The Diffusion and Drift of Electrons in Gases (New York: John Wiley).

Ismail, I. A., and Garamoon, A. A., 1979, J. Phys. D: Appl. Phys. 10, 1117-23.

Jager, G., and Otto, W., 1962, Z. Phys., 169, 517-25.

Kobayashi, H., and Kato, S., 1969, Surf. Sci. 18, 341-9.

Kruithof, A. A., 1940, Physica 7, 519-40.

Kücükarpaci, H. N., Saelee, H. T., and Lucas, J., 1981, J. Phys. D: Appl. Phys. 14, 9-25.

Lowke, J. J., and Parker, J. H. (Jr.), 1969, Phys. Rev., 181, 302-11.

Nielsen, R. A., 1936, Phys. Rev., 15, 950-4.

Pack, J. L., and Phelp, A. V., 1961, Phys. Rev. 121, 798-805.

Penning, F. M., 1957, Electrical Discharges in Gases (New York: Macmillan).

Raether H., 1964, Electron Avalanches and Breakdown in Gases (Washington: Butterworth).

Sakai, Y., Tagashira, H., and Sakamoto, 1977, J. Phys. D: Appl., Phys. 10, 1035-49.

Schoenbach, K., Schaefer, G., Kristiansen, M., Hatfield, L. H., and Guenther, A. H., 1983, Proc. NATO Advanced Study Institute on Electrical Breakdown and Discharge in Gases (Plenum Press) pp. 415-27.

Tagashira H., Sakai, Y., and Sakamoto, S., 1977, J. Phys. D: Appl. Phys. 10, 1051-63.

Ueda K. and Shimizu R., 1972, Jap. J. Appl. Phys., 11, 916-7.

Wagner, E. B., Davis, F. J., and Hurst, G. S., 1967, J. Chem. Phys., 47, 3138-47.

Whealton, J. H., Burch, D. S., and Phelps, A. V., 1977, Phys. Rev., A15, 1685-95.

FIGURE CAPTIONS

FIGURE 1. Schematic diagram for the experimental apparatus.

FIGURE 2. The transient voltage signals measured at various E/N and Ar pressures. The scales of signal amplitudes are indicated on the right-hand side.

FIGURE 3. Comparison of the transient voltage waveform (solid line) with the best least square fit calculation (●). The data were taken at E/N = 89.8 Td, h = 2.3 cm, and Ar pressure of 2.04 torr. The waveform was fit by Eq. (5) with $N = 6 \times 10^8$ electrons, $W = 6.7 \times 10^6$ cm/s, $\alpha_i = 2.45 \times 10^6$ s^{-1}, and $D_L = 1.28 \times 10^6$ cm^2/s.

FIGURE 4. Electron drift velocity as a function of E/N. The data (■) are obtained from the best least square fit of the transient waveforms, (▼) from Nielsen (1936), (▲) from Jager and Otto (1962), and (●) from Brambring (1964). The solid line is used as the standard drift velocity for calculating the longitudinal electron diffusion coefficient.

FIGURE 5. Townsend primary ionization coefficients as a function of E/N. Data were obtained from the best least square fit of transient voltage signals taken at Ar pressure of 1 (■), 2 (▼), and 4 (▲) torr. The data (●) of Kruithof (1940) are plotted for comparison. The solid line is used as the standard ionizaton coefficient for calculating the longitudinal electron diffusion coefficient.

FIGURE 6. Apparent longitudinal diffusion coefficients, D_L, of electrons in Ar at E/N = 70 Td as a function of Ar pressure. (a) Data (▲) were taken at h = 2.3 cm. (b) Data (●) were taken at h = 1.1 cm.

FIGURE 7. The products of the longitudiinal diffusion coefficient and the Ar density as a function of E/N. Data (●) were the β values from the best least square fit of transient voltage signals. Values of ND_L calculated by (▲) Sakai et al (1977) and by (▼) Tagashira et al (1977) are plotted for comparison. The values at low E/N (■) measured by Wagner et al (1967) are also plotted.

FIGURE 8. Apparent longitudinal diffusion coefficients, D_L, of electrons in Ar measured at various laser intensities. The data were taken at E/N = 70 Td, h = 2.3 cm, and Ar pressure of 3.7 (●) and 5.4 (▲) torr.

FIGURE 9. The space charges initially produced by ArF laser irradiation on cathode as a function of E/N at Ar pressure 1 (■) and 2 (●) torr. A line of slope = 3/2 is shown to compare with present data.

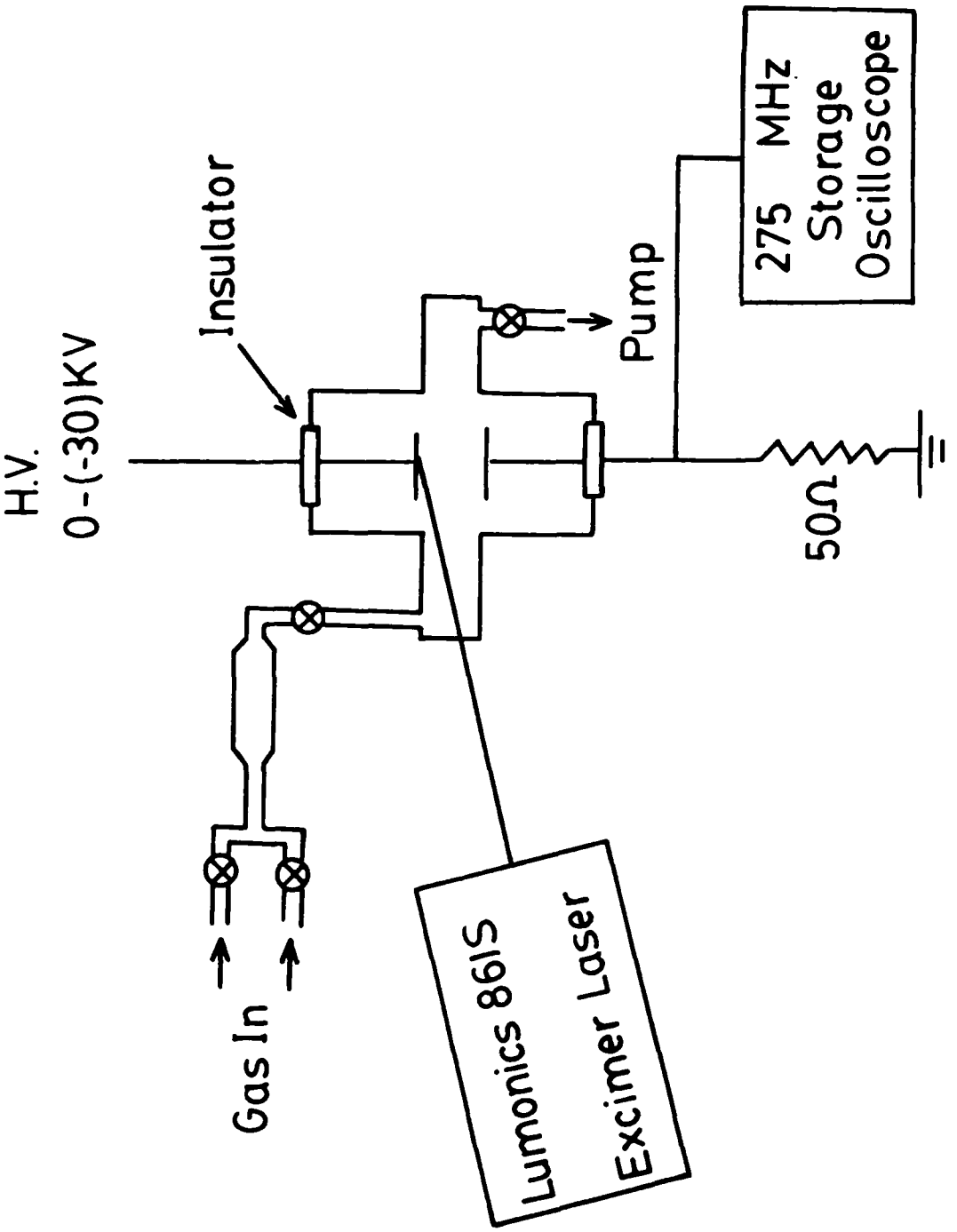
H.V.
0-(-30)KV
Insulator
Pump
275 MHz
Storage
Oscilloscope
50Ω
Gas In
Lumonics 861S
Excimer Laser

FIGURE 1

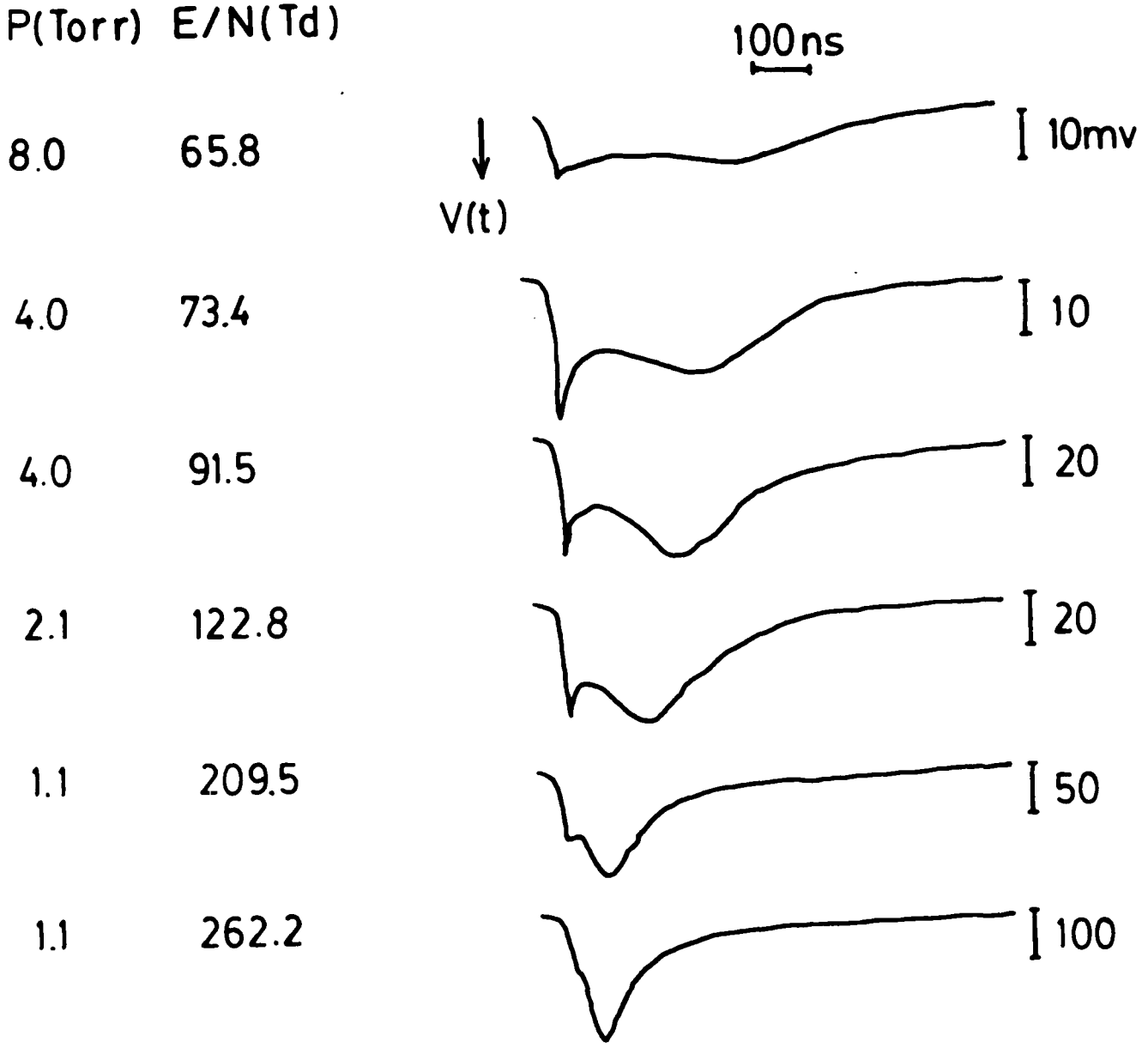
P(Torr) E/N(Td)
100ns
8.0 65.8
V(t)
10mv
4.0 73.4
10
4.0 91.5
20
2.1 122.8
20
1.1 209.5
50
1.1 262.2
100

FIGURE 2

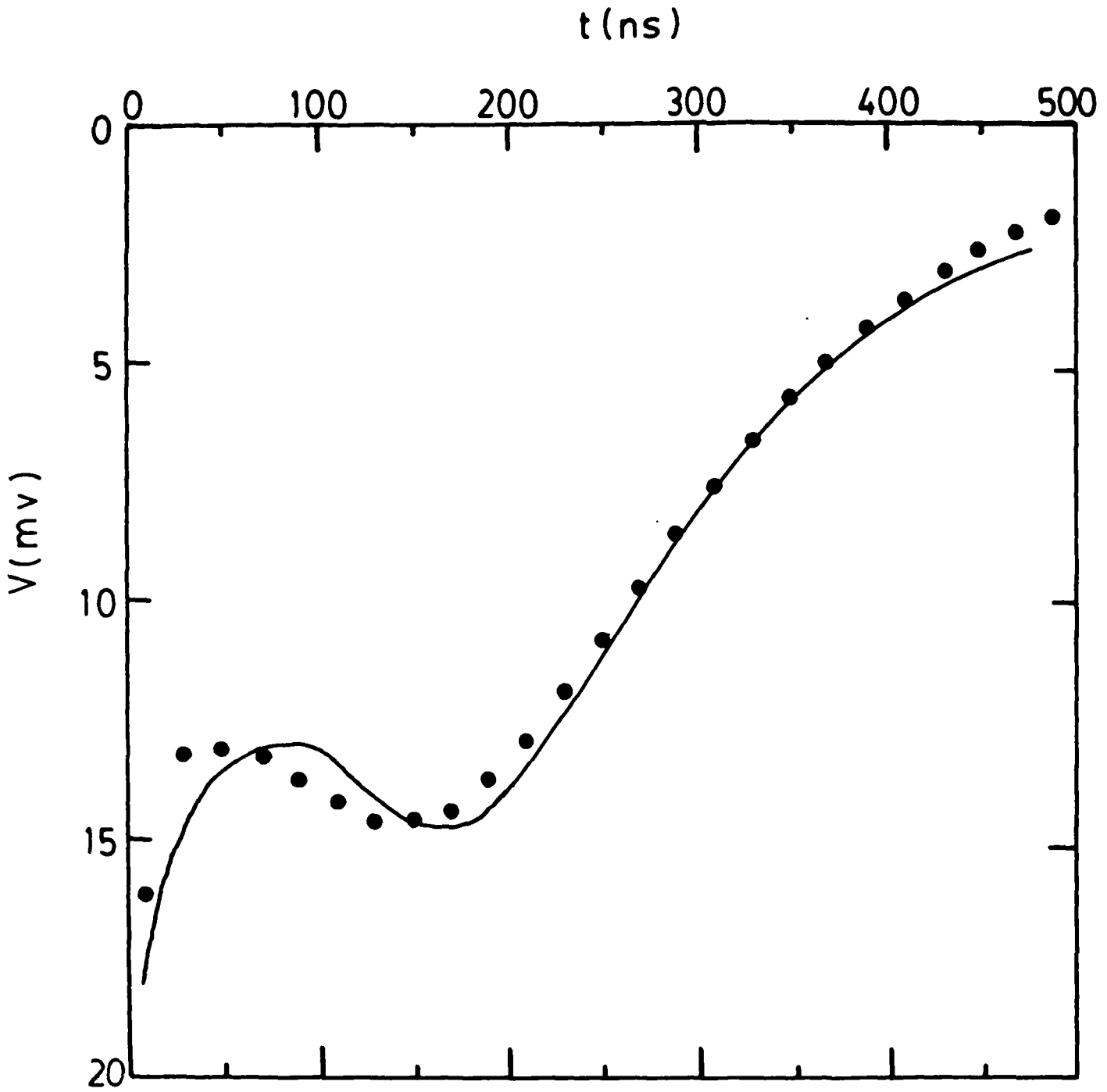

FIGURE 3

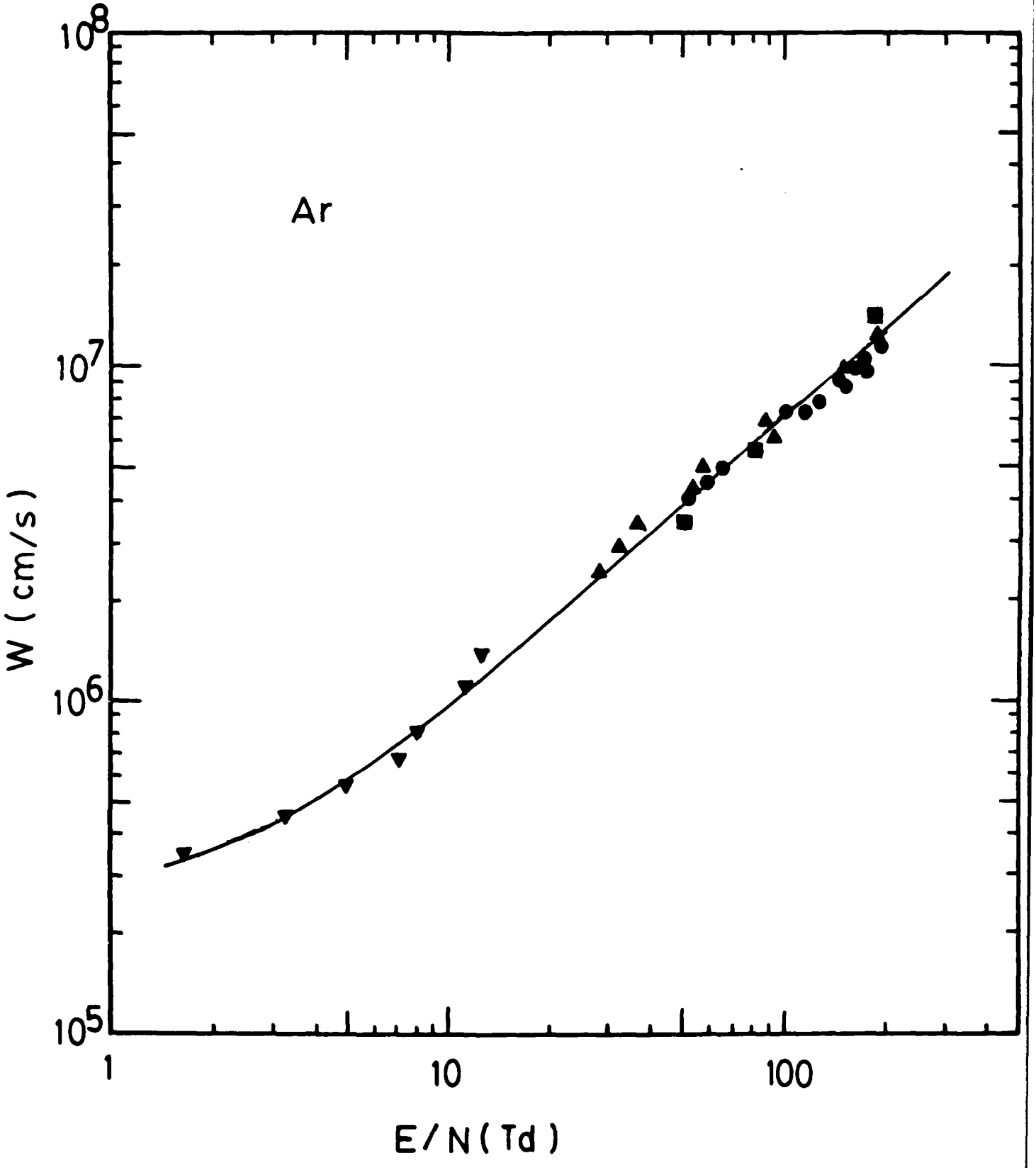

FIGURE 4

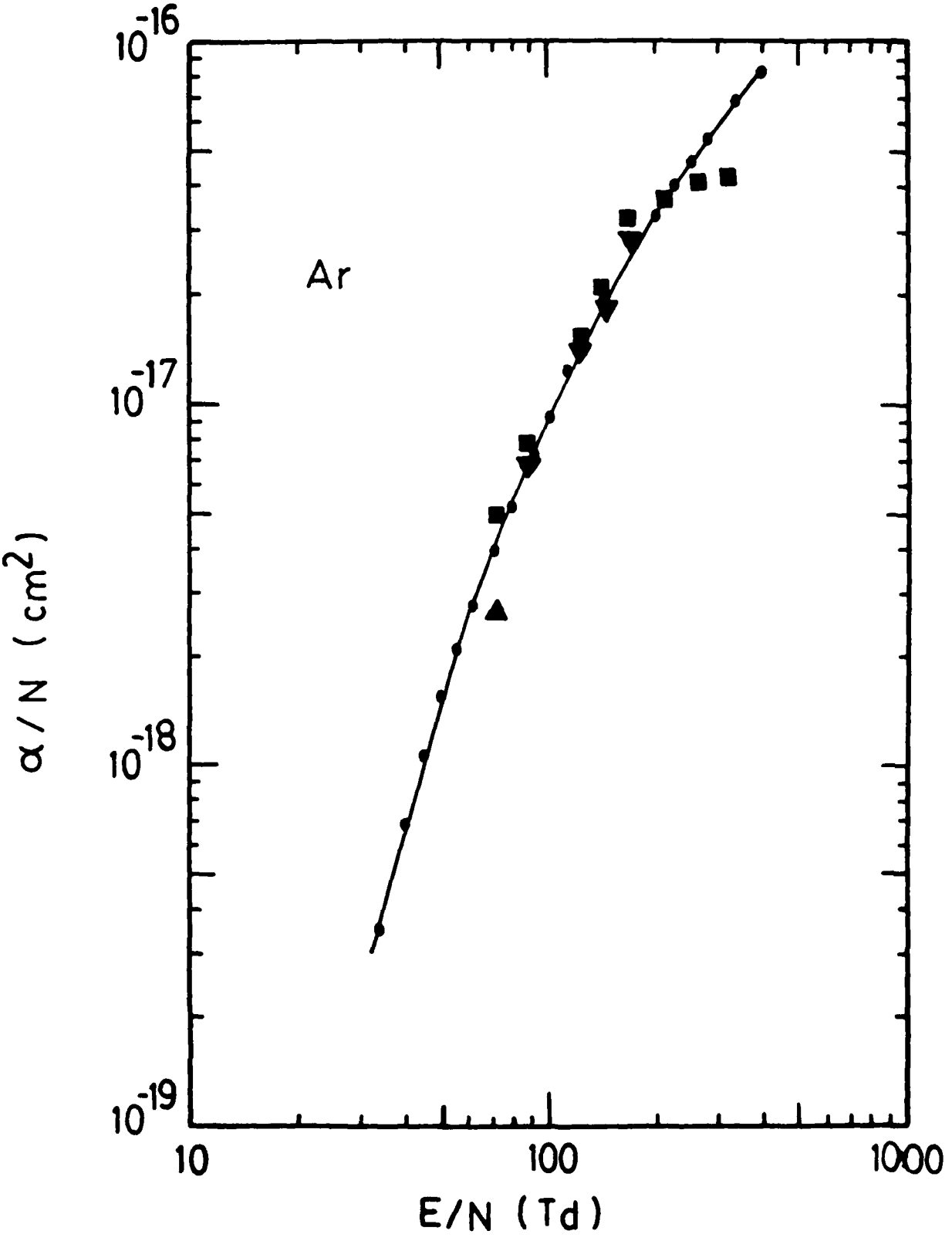

FIGURE 5

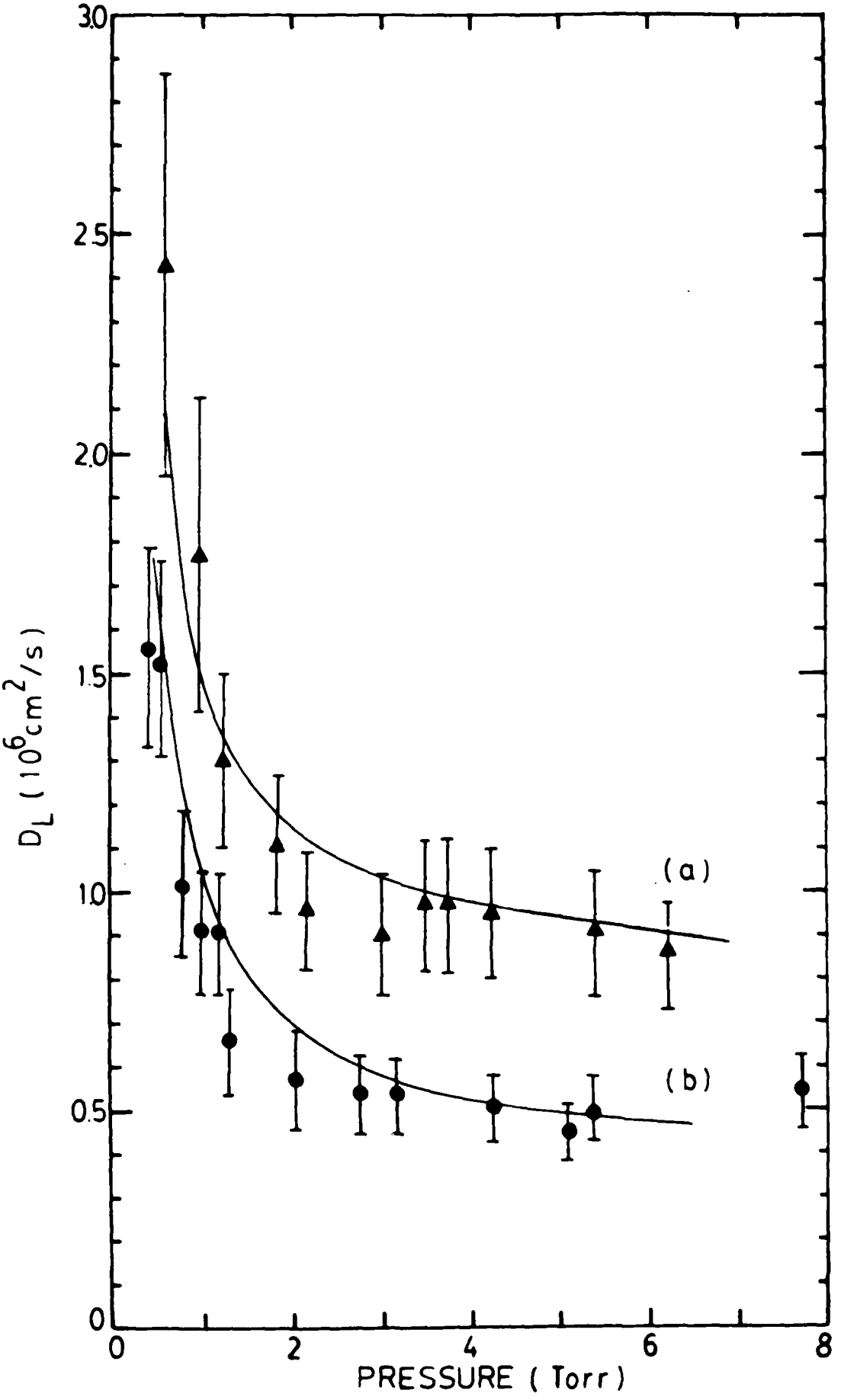

FIGURE 6

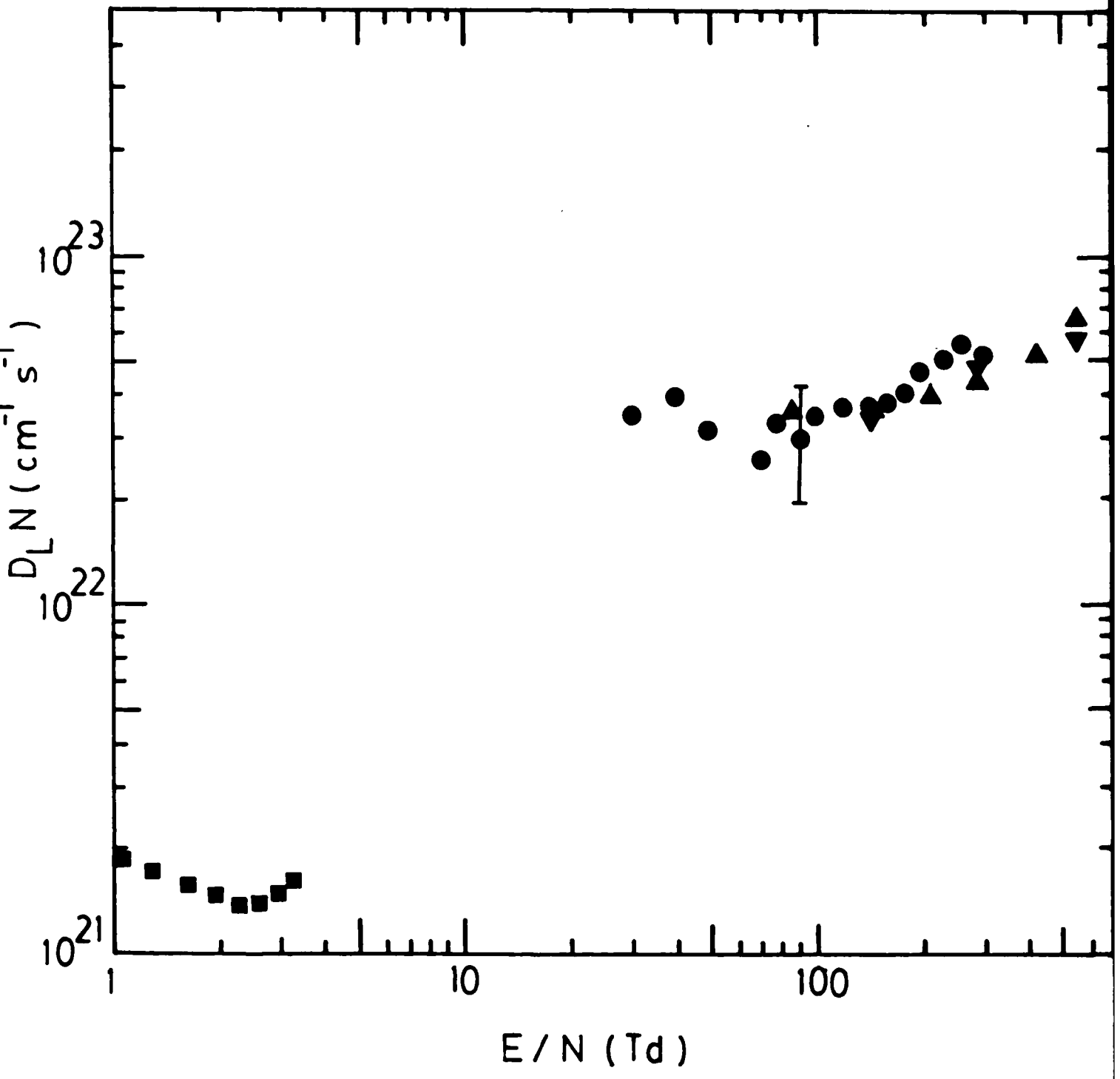

FIGURE 7

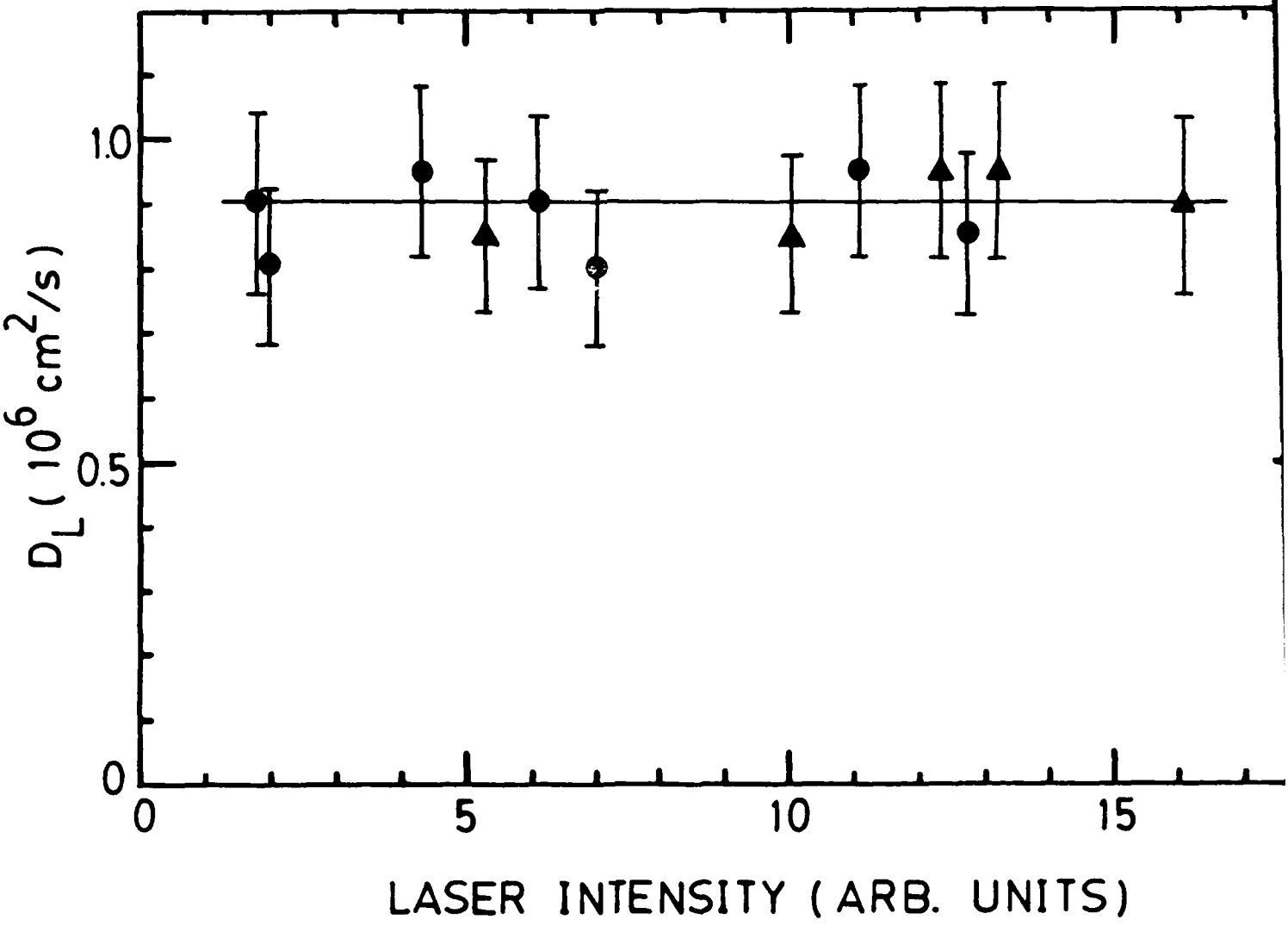

FIGURE 8

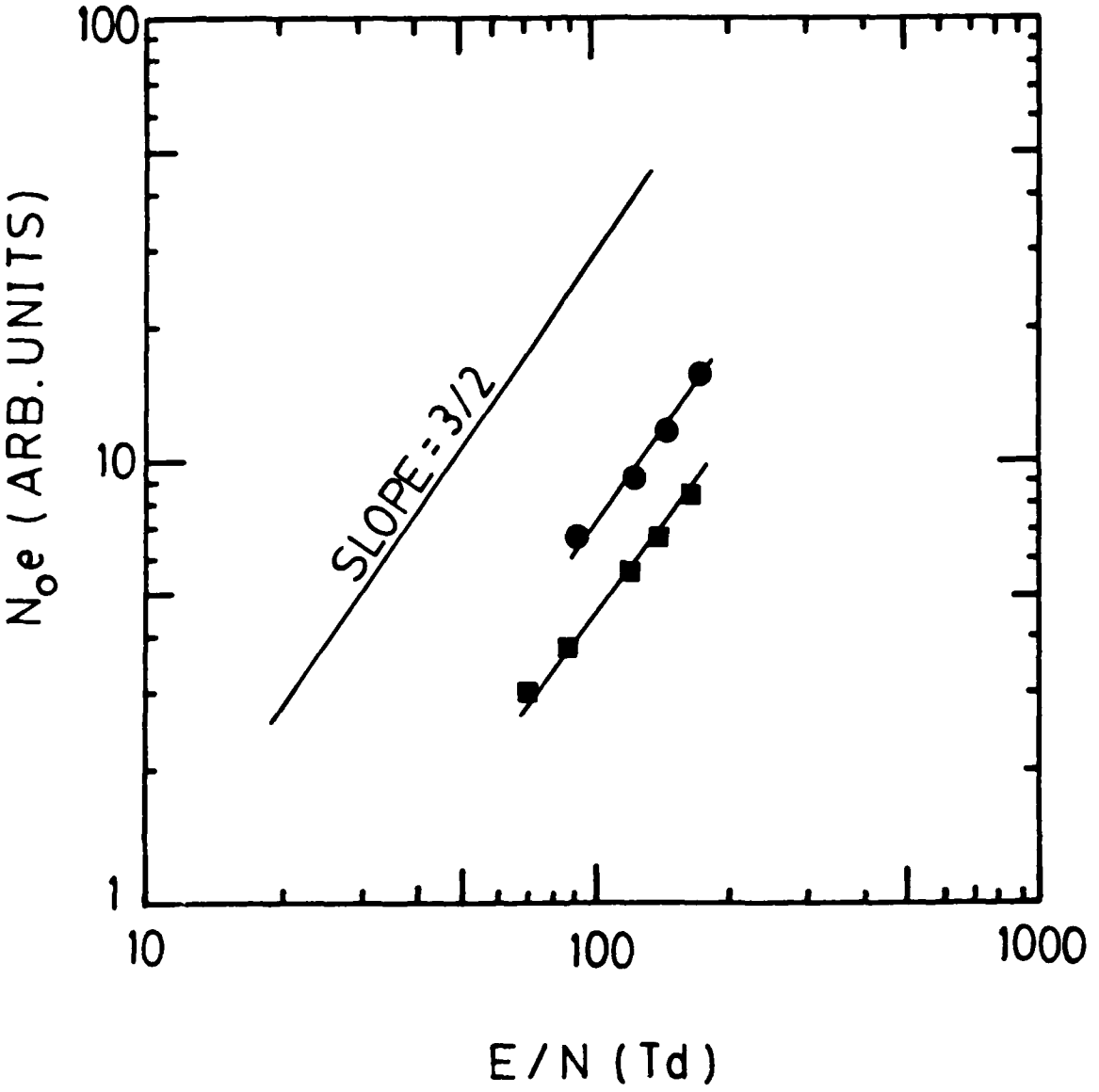

FIGURE 9

END

FILMED

2-85

DTIC